STEADY-STATE ANALYSIS OF CONTINUOUS SUCCINIC ACID FERMENTATIONS BY *ACTINOBACILLUS SUCCINOGENES*

BY

MICHAEL FORD ALEXANDER BRADFIELD

A THESIS SUBMITTED IN PARTIAL FULFILMENT OF THE REQUIREMENTS FOR THE DEGREE

DOCTOR OF PHILOSOPHY IN CHEMICAL ENGINEERING

IN THE

DEPARTMENT OF CHEMICAL ENGINEERING

FACULTY OF ENGINEERING, THE BUILT ENVIRONMENT AND INFORMATION TECHNOLOGY

UNIVERSITY OF PRETORIA

PRETORIA

SOUTH AFRICA

MARCH 2016

STEADY-STATE ANALYSIS OF CONTINUOUS SUCCINIC ACID FERMENTATIONS BY *ACTINOBACILLUS SUCCINOGENES*

Author: Michael Ford Alexander Bradfield

Supervisor: Professor Willie Nicol

Department: Department of Chemical Engineering, University of Pretoria

Degree: Doctor of Philosophy in Chemical Engineering

SYNOPSIS

Succinic acid (SA) is poised to become a significant building-block or platform chemical in the bio-based economy. Of the microbial strains that show promise for biological SA production, the wild-type bacterium *Actinobacillus succinogenes* is one of the top-contenders. While strides have been made towards understanding the behaviour of the organism and developing the fundamentals for an industrial process based on the organism, there is still a large scope of research required and a multitude of challenges to be addressed. In particular, an improved understanding of the metabolism of the organism under favourable biofilm conditions is required and its potential as a microbial host in a biorefinery setting needs to be established. Therefore, the aim of this thesis is to develop a fundamental understanding of the central metabolism of the organism under biofilm conditions on relevant substrates, and to determine its performance as a SA producer on scalable biorefinery streams. Continuous operation is chosen as the processing mode as it allows for both reactor and metabolic steady-state conditions which facilitates more accurate analysis of fermentation data through metabolic flux balancing, and resembles the foreseeable mode of industrial operation. In addition, fermentations are conducted under biofilm conditions in custom reactors since the organism naturally and unavoidably produces biofilm, and unique and process-favourable metabolic behaviour has been observed in biofilms of *A. succinogenes*.

The thesis firstly assesses the performance of the organism on xylose in relation to the model substrate glucose, since both these carbohydrates constitute major fractions of renewable feedstocks, especially lignocellulosic biomass. Continuous biofilm fermentations reveal that *A. succinogenes* is able to effectively ferment xylose to SA. However, although xylose consumption rates are similar to those of glucose at dilution rates of 0.05, 0.10 and 0.30 h^{-1}, lower yields (0.55 – 0.68 g g^{-1}) and SA productivities (1.5 – 3.4 g L^{-1} h^{-1}) are achieved. SA titres of between 10.9 and 29.4 g L^{-1} are attained with SA-to-acetic acid ratios between 3.0 and 5.0 g g^{-1}. In addition, pyruvic

acid formation is found to be substantially greater in xylose fermentations (1.2 – 1.9 g L^{-1}) as detected by means of a modified HPLC method. In agreement with glucose fermentations, increased SA yields on xylose are observed at increasing SA tires indicating increased carbon flux to SA. Mass balance closures on xylose (80.6 to 85.3%) are shown to be lower than those on glucose, and are incomplete for both substrates. Furthermore, redox balances suggest that the central metabolic network, based on measurements of excreted metabolites, is unable to produce the required reduction power (as NADH) to account for the measured SA concentration. A possible source of the reduction power is the oxidative pentose phosphate pathway (OPPP).

Following the findings of the first portion of the thesis, the second section further investigates the metabolic behaviour of *A. succinogenes*. To probe the metabolic flux distributions beyond the limitations of metabolite-based flux balancing and to explore the hypothesis of the OPPP serving as the source of additional reduction power, assays of glucose-6-phosphate dehydrogenase (G6PDH) are performed on cell extracts of biofilm removed *in situ* during fermentations. A kinetic model of the assay data, based on Michaelis-Menten kinetics, is developed *in vitro* to estimate flux into the OPPP from glycolysis at the glucose-6-phosphate node. From the kinetic model it is found that G6PDH rates, normalised to cell concentration and substrate uptake rate, increase with increasing SA titre, corresponding to increasing deviations in the redox balance. Furthermore, metabolic flux models that include OPPP flux show similar trends to those observed through the kinetic models. Therefore, evidence of the OPPP leading to increased SA yields is provided. The OPPP generates reduction power as NADPH which can be converted to NADH by transhydrogenase, thereby facilitating additional flux through the reductive branch of the TCA cycle, wherein SA is produced, and closing the redox balance.

The final portion of the thesis explores the applied potential of *A. succinogenes* as a microbial platform for SA production in a biorefinery context. Fermentations of non-detoxified, deacetylated, dilute acid pretreated, corn stover hydrolysate (DDAP-H) are performed in a continuous reactor fitted with a novel agitator fixture capable of supporting biofilm to increase cell density. *A. succinogenes* is found to achieve competitive yields (0.78 g g^{-1}), titres (39.6 g L^{-1}) and productivities (1.8 g $L^{-1}h^{-1}$) on DDAP-H at dilution rates of 0.02, 0.03, 0.04 and 0.05 h^{-1}. Furthermore, the organism is able to handle putative microbial inhibitors such as furfural and hydroxymethyfurfural (HMF) through conversion to less inhibitory compounds, likely the alcohol counterparts. However, it is found that continuous operation at reasonable productivities is only possible by starting at low dilution rates (~0.01 h^{-1}) after initial batch operation, then gradually increasing the throughput to allow the culture to adapt – even under complete conversion of furfural and HMF. Various lignin-derived, low molecular weight phenolic compounds are shown to be present in the feed and

increase during fermentation suggesting a possible link to the observed inhibition and the need for an acclimatisation phase.

Overall this thesis demonstrates that biofilms of *A. succinogenes* have the potential to produce SA at enhanced yields and productivities on glucose, xylose and process-relevant biorefinery streams under continuous operation. Furthermore, insight is provided into the unique metabolic behaviour of the organism under non-growth conditions where increased OPPP flux generates reduction power capable of sustaining increased flux to SA. In future work, this advantageous behaviour should be leveraged to develop a process capable of homosuccinate production with *A. succinogenes*, particularly employing a biorefinery stream as feedstock.

Keywords: *Actinobacillus succinogenes*, biofilm, continuous fermentation, corn stover hydrolysate, glucose, metabolic flux analysis, pentose phosphate pathway, redox balance, steady-state, succinic acid, xylose

ACKNOWLEDGEMENTS

Firstly, I would like to thank my advisor Professor Willie Nicol for being an exceptional and inspiring mentor over the past four-and-a-bit years. His intuition into what drives a process and his ability to rapidly draw out the crux of a problem has been a guiding light through both my MEng and PhD research. While the workload has been immense, especially over the past two years, he provided a unique environment of freedom, flexibility and independence that is rare yet essential to performing research efficiently. Furthermore, I would like to thank him for the opportunity to pursue both the MEng and PhD degrees and for the funding that he has provided through scholarships and research funds. In addition, I must thank him for the many generous pub lunches – as a veteran student, these are always most welcome to wash down.

The Bioreaction Engineering group at UP is relatively small yet highly productive, I suppose you could say it has an attractive process productivity. This lies in the quality of the people that form the group. To the pioneers, Dr Deon Brink and Carel van Heerden, thank you for providing me with a solid basis to conduct effective lab work and for your eagerness to assist in the lab or engage in meaningful conversation – not always within the theme of engineering, not always constructive and often quite far from the lab, but always stimulating and sincere. Adolf Krige and Andre Naude have walked the treacherous road of continuous fermentations alongside me and I thank them for their friendship and support over the past three years. I am particularly grateful to Andre for his help with SolidWorks and in the development of the bioreactors. I thank the new guy, Charles Mokwatlo, for his assistance during the final stages of my lab work and for lending me his setup to “pump out” the xylose data. Thank you to Cherryl Engelbrecht for all the support and motivation despite the rocky shores. Also, thanks to Jolandi Herselman and Ansie Wiid for being friendly faces around the lab. Not quite a part of the Bioreaction group but almost part of the furniture, I thank Dr Shatish “Stix” Ramjee for the many conversations and multitude of double Jamesons that we dutifully enjoyed at Aandklas and Hatfield Square, before it was rudely demolished, literally. Thanks to my buddy Mathieu Ugrin for the many lunches and for always being a great friend and for almost, but not quite, gassing out the basement lab and electrocuting us.

A substantial portion of the research was conducted in collaboration with the National Renewable Energy Laboratory (NREL) in Golden, Colorado. I would like to thank my colleagues at NREL that made the collaboration possible and undoubtedly successful. In particular I would like to thank Dr Gregg Beckham for co-ordinating and accelerating the project through his inspiring work ethic and passion for impactful science and engineering – and thanks also for the temporary loan of the Prius

and the 18th century bicycle. I would like to thank Ms Nancy Dowe and Dr Davinia Salvachúa for their friendship and support during my stay in the US and for their valuable contribution to the project. Thanks also to Dr Brenna Black, Holly Smith, Deb Hyman, Wes Hjelm, Rich Voss, Rob Nelson and Mike McCausey for the important roles played in the success of the project and the assistance in the lab. Most of all though, I thank Dr Ali Mohagheghi and his wife Manijeh for their mentorship, friendship and endless assistance during my stay in the USA. To the provider of the legendary "Red Pickup", Dr Mike Crowley, I thank you greatly, without those wheels my stay in Golden would have been quite restricted and I would not have mastered snow drifting. During my stay in Colorado I forged solid friendships with a number of people who I am grateful to have met. Thanks especially to Thieny Trinh, Jason Boehm, Brad and Harmony Jones, and Elizabeth Clarke, for the fun and enjoyable times in Steam Boat, Breckenridge, Denver and Boulder. I would also like to thank Jeanette Henry, Sarah Feeney and Carolyn Gaglione for the adventures around Denver, and Smriti Dutta and Bruno Godin for being brief, yet sociable roommates.

A number of staff members in the Department of Chemical Engineering at UP contributed to the success of this research. In particular, I thank Mrs Elmarie Otto for her patience and diligence in dealing with countless orders and for always going the extra mile to ensure that things are in order. I thank Professor Phillip de Vaal for effectively addressing many of my issues and complaints. Thanks also to Gerrie Claasen, Paul Sonnendecker and Shadrack Phosane for assisting with the facilities. Beyond the Department of Chemical Engineering, I am grateful to Professor Lyn-Marie Birkholtz from the Department of Biochemistry for the use of her laboratory and to Professors Megan Bester, Zeno Apostolides and Don Cowan for their initial assistance on the enzyme assay work. In particular, I thank Mrs Sandra van Wyngaardt for her invaluable contribution to developing the assay methodology and for helping me get situated in the Biochemistry Labs.

Finally, I thank my parents, sisters and Eshchar Mizrachi for their love, support and understanding during this busy and often highly frustrating phase.

The financial assistance of the National Research Foundation (NRF) towards this research is hereby acknowledged. Opinions expressed and conclusions arrived at, are those of the author and are not necessarily to be attributed to the NRF.

NOTE ON PDF NAVIGATION

All in-text references of figures, tables, sections and sub-sections, and equations in the PDF version of this thesis are cross-referenced to their respective locations in the document by hyperlinks. The links are not visible (i.e. no blue font, underlined) as this disrupts the visual effect of the document. To determine whether an item is a hyperlink, placing the cursor over the item (or number) will change the cursor to the following pointer symbol: 

Furthermore, when using Adobe Acrobat Reader, it is possible to return to the point from which the link was clicked by pressing the “Alt” and “Left arrow” keys together, or by following View->Page Navigation->Previous View in the menu bar.

CONTENTS

LIST OF FIGURES

LIST OF TABLES

NOMENCLATURE

6PG	6-phosphogluconolactone	
6PGDH	6-phosphogluconate dehydrogenase	
6PGL	6-phosphoglucono-δ-lactone	
AA	acetic acid	
Ac-CoA	acetyl-CoA	
AcP	acetyl-phosphate	
Ald	aldehyde	
ATP	adenosine triphosphate	
C_{AA}	acetic acid titre	(g L^{-1})
C_{FA}	formic acid titre	(g L^{-1})
C_{SA}	succinic acid titre	(g L^{-1})
CSL	corn steep liquor	
C_x	biomass concentration in original assay sample	(g L^{-1})
C^f_x	total biomass concentration in fermenter	(g L^{-1})
D	dilution rate	(h^{-1})
DAP-H	dilute acid pretreated corn stover hydrolysate	
DCW	dry cell weight	(g L^{-1})
DDAP-H	deacetylated, dilute acid pretreated corn stover hydrolysate	
DHAP	dihydroxyacetone phosphate	
E4P	erythrose-4-phosphate	
F1,6BP	fructose-1,6-biphosphate	
F6P	fructose-6-phosphate	
FA	formic acid	
FDH	formate dehydrogenase	
G1P	glucose-1-phosphate	
G3P	glyceraldehyde-3-phosphate	
G6P	glucose-6-phosphate	
G6PDH	glucose-6-phosphate dehydrogenase	
Gal1P	galactose-1-phosphate	
Glc	glucose	
Gt6P	gluconate-6-phosphate	
HMF	hydroxymethylfurfural	

HPLC	high performance liquid chromatography	
K_m	Michaelis constant	(mM)
LAC	lactonase	
MFA	metabolic flux analysis	
NAD^+	nicotinamide adenine dinucleotide (oxidised)	
NADH	nicotinamide adenine dinucleotide	
$NADP^+$	nicotinamide adenine dinucleotide phosphate (oxidised)	
NADPH	nicotinamide adenine dinucleotide phosphate	
OPPP	oxidative pentose phosphate pathway	
PDH	pyruvate dehydrogenase	
PEP	phosphoenolpyruvate	
PFL	pyruvate formate-lyase	
PGI	phosphoglucose isomerase	
PP	polypropylene	
PPP	pentose phosphate pathway	
Pyr	pyruvate or pyruvic acid	
Pyr_{ex}	extracellular pyruvate	
q_{SA}	succinic acid volumetric productivity	($g\ L^{-1}h^{-1}$)
R5P	ribose 5-phosphate	
r_i	measured metabolite rate in flux model	(C-mole s^{-1})
Ribu	ribulose	
r_s	volumetric substrate uptake rate	(mol $L^{-1}\ s^{-1}$)
r'_s	specific substrate uptake rate	(mol $g_{biomass}^{-1}s^{-1}$)
Ru5P	ribulose-5-phosphate	
S7P	sedoheptulose-7-phosphate	
SA	succinic acid	
TCA	tricarboxylic acid	
TSB	tryptone soy broth	
v_i	metabolic pathway flux	(C-mole s^{-1})
V'_{max}	maximum volumetric rate of reaction	(mol $g_{biomass}^{-1}s^{-1}$)
Xu5P	xylulose-5-phosphate	
Xyl	xylose	
Xylu	xylulose	
Y_{AAFA}	formic acid to acetic acid ratio	($g\ g^{-1}$)
Y_{AASA}	succinic acid to acetic acid ratio	($g\ g^{-1}$)

Y_{GlSA}	succinic acid yield on glucose	(g g^{-1})
Y_{sSA}	succinic acid yield on total sugars	(g g^{-1})
Y_{xylSA}	succinic acid yield on xylose	(g g^{-1})

Greek letters

α	OPPP flux-to-substrate uptake flux (metabolic model)	(mol mol^{-1}) or (C-mole C-$mole^{-1}$)
ΔX_m	actual or measured xylose consumed	(g L^{-1})
ΔX_r	xylose consumed to satisfy the product-based redox balance	(g L^{-1})
γ	OPPP flux-to-substrate uptake flux (experimental)	(mol mol^{-1})

1 | INTRODUCTION

Humanity finds itself at a potential tipping point. In addition to the perpetual social and political issues that pervade every era, it now faces a more insidious threat to its prosperity. The threat lies in the dependence of modern civilisation on fuels, power and chemicals that, for the past 100 or so years, have been produced almost exclusively from non-renewable resources such as coal and petroleum [1]. Despite the seemingly plentiful nature of these resources and the unusually low price of Brent Crude, the rate of consumption of these resources is increasing and will continue on this course as populations grow, industrialisation spreads and the demand for energy increases [2]. Furthermore, petroleum sources tend to be uncertain and unstable and current estimates suggest that petroleum production may peak within the next few decades [3], although views and estimates in general tend to be polarised [4]. However, even if non-renewable resources were available in a boundless, unconstrained supply, their processing and consumption leads to the release of various by-products that are undeniably polluting and challenging to the environment, possibly on a global scale and to an irreversible extent [5]. In essence, humanity has (ironically) built its survival "machinery" largely on an unstable, detrimental platform. The logical response and challenge of today, therefore, is to transform this platform and reduce its negative impact by finding and developing replacements for the unsustainable raw materials and processing technologies. Ideally, the replacements should necessitate only mild tweaking of the existing "machinery" and should be compatible with the natural environment. To this end, the burgeoning field of biotechnology provides a wealth of potential.

Biotechnology provides a set of tools with which biology can be purposefully exploited and manipulated to solve unique problems. In the context of fuels and chemicals production, biotechnology enables renewable, bio-based resources to be converted into traditional, substitute or novel chemicals and fuels, thereby serving as a potential replacement for petroleum and similar finite resources with a reduced impact on the environment. Moreover, the catalysts for such transformations are of biological origin and can be fine-tuned for a specific purpose. These catalysts are either individual enzymes or microorganisms; the latter can conveniently be viewed as "microbial cell factories". For example, production of biofuels and value-added chemicals by these microbial cell factories using agriculturally derived carbohydrates has been demonstrated

commercially [6–8] and continues to gain momentum. While there may be suitable alternatives to petroleum fuels and power sources (e.g. electric vehicles, solar and wind power), alternatives for chemical building blocks are somewhat limited, making sustainable production of chemicals vitally important. Bio-based chemicals are attractive not only as end-products in standalone processes, but also as co-products for integration in a biorefinery to bolster the overall economics of biofuels production [9]. Analogous to petroleum refineries, the goal of biorefineries is to produce myriad fuels, chemicals and power at a single, integrated facility, with the main exception being the utilisation of renewable, bio-based feedstocks.

A particular chemical that is increasingly gaining attention within the bio-arena is succinic acid (SA), an aliphatic four carbon dicarboxylic acid. Succinic acid is considered one of the top potential value-added [10] and bulk [11] chemicals derived from biomass. It currently has a variety of specialty applications in the food, pharmaceuticals, coatings and surfactants industries, with potential to serve as a precursor for numerous industrially important chemicals (e.g. adipic acid, 1,4-butanediol, tetrahydrofuran, etc.) [12]. Broader application of SA is currently limited due to the expensive petrochemicals route of its production. Successful bio-production of SA is expected to augment its supply and expand the market size substantially. As such, various microbial strains have been explored for fermentative production of SA with the most notable being wild-type *Actinobacillus succinogenes* [13–16], *Anaerobiospirillum succiniciproducens* [17,18], *Basfia succiniciproducens* [19,20] and *Mannheimia succiniciproducens* [19–23], and engineered strains of *Escherichia coli* [24–27] and *Saccharomyces cerevisiae* [28]. With a demonstrated ability to produce SA at high titres, productivities and yields [13–16], *A. succinogenes* is rapidly becoming one of the most promising candidates for industrial bio-based SA production. In addition, *A. succinogenes* has a comparatively high tolerance to acids [29], is able to consume a broad spread of carbohydrates [30] and sequesters CO_2 in SA production, offering the potential for CO_2 recycling in an integrated biorefinery [31].

As with any industrial chemical process, successful commercialisation of the product is linked to three key reactor design parameters: productivity, yield and titre [32]. To determine the set of these three parameters where the process is most economically attractive, a techno-economic optimisation that includes operating and capital expenses should be performed. Process optimisation and a fundamental understanding of the microbial strain are important to the accuracy of the techno-economic optimisation. To date, bench-scale succinic acid production studies on *A. succinogenes* have been primarily conducted in batch mode where promising performance has been demonstrated (e.g. [33–35]). However, the majority of the batch studies are merely exploratory, or focus on optimising fermentation parameters or investigating potential renewable substrates. Only a

limited number of studies focus on process-relevance and directly target improvements in the three design parameters.

Productivity enhancements have been achieved through high cell density fermentations of *A. succinogenes* using either a membrane reactor system [36] or by immobilisation of cells within a bioreactor [13–15,37–39]. Cell immobilisation is particularly well suited to *A. succinogenes* due to its tendency to naturally and unavoidably form biofilm [15,37,38], therefore fermentations with *A. succinogenes* are necessarily biofilm based. Moreover, these fermentation studies have shown that immobilised biofilms of *A. succinogenes* significantly increase productivity and outperform chemostat counterparts [16]. In addition, repeat fed-batch on an established biofilm of *A. succinogenes* showed improved productivities compared to regular batch operation [14]. Similar to most commercial SA bioproduction processes that use starch-based carbohydrates [28], these studies employed clean or pure sugar feedstreams which are useful in determining limitations of the organism. However, ideal bioproduction of succinic acid will utilise a non-edible, inexpensive and more abundant feedstock – the most promising candidate being lignocellulosic biomass [40].Therefore, it is important to perform similar productivity improvement studies on more industrially relevant feedstock, while also considering titre and yield.

Titre and yield are largely dependent on the microbial strain and can be enhanced by improving the performance of the microorganism through various strain improvement strategies or through appropriate environmental conditions. These improvements require knowledge of potential targets for metabolic engineering and the metabolic behaviour of the organism under different conditions (i.e. phenotypic changes). Despite the availability of the genome of *A. succinogenes* [41], strain improvement studies have been limited to genome shuffling [42], mutant screening strategies [43] and more recently, the development of strains that overexpress glucose-6-phosphate dehydrogenase and/or malate dehydrogenase for increased succinic acid production [44]. Regarding wild-type *A. succinogenes*, most production studies merely report fermentation data and make little, or no attempt to form a fundamental understanding of the organism, especially with regard to its central metabolism wherein succinate is produced.

However, in a limited number of studies on succinate production with *A. succinogenes*, fermentation results have been analysed using metabolic flux analysis. From these analyses, it has been found that *A. succinogenes* displays unique metabolic behaviour under biofilm conditions favouring succinic acid production and leading to enhanced yields and reduced by-product formation [15]. Furthermore, it has been shown that the unique behaviour is linked to an acid titre-dependent transition from a growth to a non-growth state [15,16]. Therefore, wild-type *A. succinogenes* may

have the potential to serve as an efficient SA producer without the need for strain improvement, possibly approaching homosuccinate fermentation under a specific set of process conditions. To achieve this, an improved understanding of the metabolic behaviour that affords favourable succinate production is required. Therefore, in combination with the above, there is a need to expand on current fermentation studies on SA production by *A. succinogenes* in terms of both its industrial processing potential, and the fundamental behaviour of the organism.

Continuous operation of a bioreactor is particularly well suited to exploring both these avenues as it offers two primary advantages: **(1)** improved processing through enhanced productivities and consistent product quality, and **(2)** steady-state operation. Steady-state in a continuous bioreactor is most suitable for proper determination of microbial metabolic fluxes [45] due to the constant environmental conditions of the organism and its consequent constant metabolic state. These conditions allow for a more fundamental understanding and a more accurate analysis of the microorganism, particularly with regard to metabolic network analysis and flux balancing. Continuous processing is, therefore, advantageous not only from an applied or processing perspective, but also from a more theoretical standpoint where an improved understanding of the microorganism and its environment is sought.

In light of the above, the objective of the current research was to investigate fermentative production of succinic acid by the wild-type bacterium, *Actinobacillus succinogenes,* by leveraging the advantages of continuous operation of biofilm systems under steady-state conditions. In particular, the research aimed to **(1)** explore and advance the processing potential of *A. succinogenes* from an applied perspective*,* and **(2)** develop a more fundamental understanding of the metabolic flux distributions of *A. succinogenes*. For the more fundamental aspects of the research, pure carbohydrates were used, namely glucose and xylose, since pure sugar or "clean" feedstreams are more suitable for fundamental studies of an organism. While for the applied or processing aspects of the research, pure sugars were used initially to establish performance baselines followed by acid pretreated, lignocellulosic feedstock to test the bulk processing potential of the organism on a more industrially relevant feedstock.

The research is divided into three main research themes reflected by Chapters 3, 4 and 5, with background provided in Chapter 2. In **Chapter 3**, an understanding of the basic requirements and performance of continuous succinic acid fermentations with *A. succinogenes* biofilms is developed, specifically the metabolic behaviour and limitations on two model substrates - glucose and xylose. Mass and redox balances are used to interpret and assess the completeness of the fermentation data and to provide insight into the active central metabolic network of *A. succinogenes*. Building on

the mass and redox analyses of Chapter 3, **Chapter 4** provides an improved understanding of carbon flux distribution in the central metabolic network of the organism under non-growth conditions. In particular, an increase in pentose phosphate pathway flux relative to substrate uptake flux under non-growth conditions is demonstrated, which affords increased carbon flux to succinic acid. **Chapter 5** provides an applied case study that explores the processing potential of *A. succinogenes* on an industrially relevant feedstream. High yield, titre and productivity of succinic acid are demonstrated on a non-detoxified, bio-based feedstock namely corn stover hydrolysate, thereby advancing the potential of industrial-scale, bio-succinic acid production by *A. succinogenes*. Although of an applied nature, mass and redox balances are also performed on the Chapter 5 results to gain insight into the behaviour of the organism on more representative feedstock and to compare this to the model, pure sugar cases.

2 | LITERATURE

2.1 BIO-SUCCINIC ACID

Organic acids are poised to become important building-block, or platform, chemicals derived from biomass and microbial processes [46]. These molecules, and biomass-derived chemicals in general, have a higher oxygen content compared to petroleum-based compounds and contain existing functional groups that make them attractive as starting materials in chemical synthesis [47]. In the petroleum industry, such functional groups are added to the carbon backbone through costly and often harsh oxidative processes [47]. Most organic acids are products or intermediates of microbial metabolism and therefore can be readily produced through microbial processes. Given economical and cost-competitive bio-production of these acids, new opportunities for their application in the chemicals industry will arise thereby augmenting the market size of each. A particular group of organic acids is the dicarboxylic acids, which includes succinic acid, fumaric acid and malic acid (Figure 2.1) – all C_4 intermediates in the tricarboxylic acid (TCA) cycle and each considered to be a "top value-added chemical from biomass" by the US Department of Energy [48]. These three acids are easily interconverted and therefore all have the potential to replace maleic anhydride – a precursor in the chemicals industry derived from petroleum with a substantial market size of 213,000 tons per year [46]. A diacid of particular interest in the bio-arena is succinic acid (SA), also known as butanedioic acid or "spirit of amber" due to its natural presence in amber resin and its distinct odour observable during the destructive distillation of amber [49].

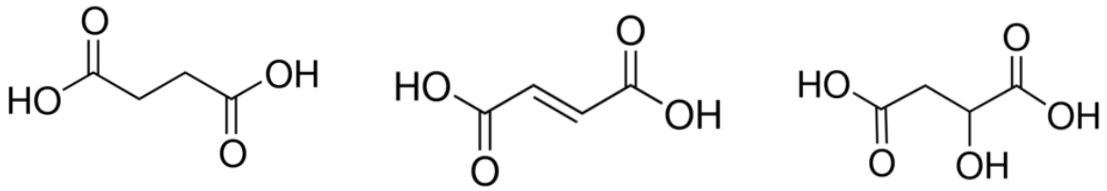

succinic acid – $C_4H_6O_4$ **fumaric acid – $C_4H_4O_4$** **malic acid – $C_4H_6O_5$**

Figure 2.1. **Naturally produced, four-carbon, dicarboxylic acids.** These compounds have potential to serve as building-block chemicals derived from renewable, bio-based resources and microbial conversion processes.

2.1.1 SUCCINIC ACID APPLICATIONS AND MARKETS

Succinic acid currently has five main areas of commercial application: (1) as a surfactant or foaming agent, (2) as an ion chelator to prevent corrosion and pitting during electroplating, (3) as an acidulant, flavouring agent and an anti-microbial agent in the food industry, (4) as an intermediate in health-based and personal care products such as pharmaceuticals, antibiotics, amino acids and vitamins, and (5) in the production of resins, coatings and pigments [50,51]. Besides these markets, succinic acid also finds application in polymer production (e.g. polybutylene succinate and polyester polyols) [51]. Today, the majority of succinic acid is produced petrochemically via the catalytic hydrogenation of maleic anhydride derived from butane [52]. It has been suggested that fermentative production of succinic acid from renewable, bio-based resources (i.e. bio-succinic acid) can compete with the traditional petrochemical process [12]. If this is realised and commercially developed, new opportunities will arise for succinic acid, primarily as a building-block in the synthesis of value-added chemicals such as 1,4-butanediol, γ-butyrolactone, adipic acid, tetrahydrofuran, 2-pyrrolidone, succinamide, maleic anhydride, etc. [12]. In addition, bio-SA could serve as a precursor for various bio-based polymers including polyamides and polyesters (particularly polybutylene succinate) thereby augmenting their production and creating new opportunities for these polymers [53]. As seen in Table 2.1, succinic acid has an established market size that is expected to grow attractively with the advent of successful commercial bio-production.

Table 2.1. Key indicators of the current and projected succinic acid market [51].

Market size (2011)	40 kton
Market value (2011)	$63 million
Projected market size (2020)	600 ktons
Projected market value (2020)	$539 million
Petroleum-based SA price (2011)	$2.4 – 2.6/kg
Bio-based SA price (2011)	$2.9 – 3.0/kg

Today, commercial bio-SA production is underway with a number of facilities coming online in recent years (Table 2.2). These processes either opt for low pH conditions using a yeast as the microbial host where the product remains in the acid form, thereby favouring downstream separation processes and minimising neutralisation requirements, or apply a neutral pH, bacterial process with integrated downstream separation that attempts to recover salt precipitates. In all the current industrial bio-SA processes, starch-derived glucose is used as the carbon substrate with an

indication that the Succinity process is able to use glycerol [54]. Moreover, all these processes utilise genetically engineered microbial strains.

Table 2.2. Prominent commercial bio-succinic acid ventures [28].

Company/Venture	Capacity (kton/year)	Organism	Technology	Start-up year
Myriant	14	*Escherichia coli*	Neutral pH; NH_3 with precipitation	2013
BioAmber, Mitsui	30	*Candida krusei*	Low pH; NaOH and electrodialysis	2014
Succinity (BASF/Corbion-Purac)	10	*Basfia succiniciproducens*	Neutral pH; $Mg(OH)_2$	2013
Reverdia (DSM/Roquette)	10	*Saccharomyces cerevisiae*	Low pH	2012

2.1.2 BIO-PRODUCTION STUDIES AND MICROBIAL HOSTS

An assortment of microbial strains has been studied for the fermentative production of succinic acid using pure carbohydrates (Table 2.3) and biomass feedstocks (Table 2.4). The selection criterion for including studies in these tables (and similar tables that follow) is based on the study attaining comparatively high values of yield, productivity and titre, as these are the most important performance indicators or design parameters of a bulk fermentation process [32]. Yield reflects the efficiency in converting feedstock to the desired product and influences the variable costs of the process. Productivity reflects the efficient utilisation of the production capacity or reactor volume and is related to capital costs of the process, while titre indicates the extent of downstream processing required to separate the desired product from the fermentation broth and also influences variable and capital costs.

Studies using pure carbohydrates generally test the limitations of the organism and seek to understand its physiology, while studies using biomass substrates explore the applied nature of the organism and whether it can serve as a catalyst within an industrial process, using a more cost-effective feedstock. Detailed reviews on the fermentative production of succinic acid, including markets, microbial hosts and fermentation technology are available [12,28,55]. Of the strains investigated for succinic acid production, those showing particularly good performance include *Anaerobiospirillum succiniciproducens, Actinobacillus succinogenes, Corynebacterium glutamicum,*

Enterococcus faecalis, Escherichia coli and *Mannheimia succiniciproducens*. Generally, eukaryotes are not well suited for succinate production due to compartmentalisation where succinate must cross both the mitochondrial and cytoplasmic membranes prior to excretion, whereas other acids (e.g. fumaric acid [56]) do not face this obstacle as they are produced in the cytoplasm. Therefore, the majority of the contending production hosts for succinic acid are bacterial where succinate need only cross the cytoplasmic membrane during excretion. In the case of the industrially applied eukaryotes (Table 2.2), both organisms are genetically modified with the ability to overexpress enzymes in the succinate production pathways [57].

Table 2.3. Representative bio-succinic acid production studies on starch-derived or pure sugars for a variety of wild-type and engineered microbial hosts.

Organism	Feedstock	Mode	Titre[a] ($g\ L^{-1}$)	Yield ($g\ g^{-1}$)	Productivity[b] ($g\ L^{-1}h^{-1}$)	Reference
Actinobacillus succinogenes 130Z	Glucose	Continuous	32.5	0.90	10.8	[13]
Anaerobiospirillum succiniciproducens	Glucose	Continuous	15.5	0.81	14.8	[17]
Corynebacterium glutamicum ΔldhA-pCRA717	Glucose	Fed-batch	146	0.92	3.17	[58]
Enterococcus faecalis RKY1	Fumarate/glycerol	Continuous	72.0	1.0	7.2	[59]
Escherichia coli AFP111-pyc	Glucose	Fed-batch	99.2	1.10	1.31	[24]
Escherichia coli KJ122	Glucose	Continuous	25.0	0.77	3.0	[60]
Mannheimia succiniciproducens MBEL55E	Glucose	Continuous	9.5	0.48	2.85	[36]
Saccharomyces cerevisiae AH22ura3 Δsdh2Δsdh1Δidh1Δidp1	Glucose	Batch	3.62	0.072	0.022	[61]

[a]The values for each performance indicator are not necessarily from the same experiment within each study, but rather the highest value attained for each.

[b]Batch productivity is calculated as the final succinic acid titre divided by the duration of the fermentation

Table 2.4. Representative bio-succinic acid production studies on lignocellulosic and other bio-derived feedstocks for a variety of microbial hosts.

Organism	Feedstock	Mode	Titre ($g\ L^{-1}$)	Yield ($g\ g^{-1}$)	Productivity ($g\ L^{-1}h^{-1}$)	Reference
Actinobacillus succinogenes CGMCC 1593	Corn straw hydrolysate	Fed-batch	53.2	0.82	1.21	[62]
Anaerobiospirillum succiniciproducens	Whey	Continuous	14.3	0.71	3.3	[63]
Basfia succiniciproducens DD1	Crude Glycerol	Continuous	5.21	1.02	0.094	[19]
Escherichia coli AFP111/pTrcC-cscA	Cane molasses	Fed-batch	37.3	0.79	1.04	[64]
Escherichia coli AFP184	Softwood hydrolysate	Batch	42.2	0.72	0.72	[65]
Fibrobacter succinogenes S85	Cellulose	Continuous	3.20	0.94[a]	0.051	[66]
Mannheimia succiniciproducens MBEL55E	Wood hydrolysate	Batch	11.7	0.56	1.17	[67]
Mannheimia succiniciproducens MBEL55E	Whey	Continuous	5.6	0.63	3.8	[22]

[a] g SA/g anhydroglucose

Of the microbial strains mentioned above, there are a number of wild-type bacteria that naturally produce succinate in appreciable amounts. All these strains have associated advantages and disadvantages. For example, *M. succiniciproducens* has a complete TCA cycle and is able to grow well in aerobic and anaerobic conditions [23]. Despite achieving somewhat high productivities, yields on glucose tend to be low and *M. succiniciproducens* has a number of auxotrophies [68]. However, a major advantage of *M. succiniciproducens* is the availability of its full genome sequence, which creates opportunities for efficient metabolic engineering of the organism [69]. *A. succiniciproducens* is strictly anaerobic which makes industrial-scale use impractical due to the complexities involved in cost-effectively maintaining completely anoxic conditions. Furthermore, it is an opportunistic pathogen [70], making it unsuitable for practical industrial use. In the case of *E. faecalis*, high succinic acid productivities and yields were achieved in a coupled fungal-bacterial process where fumarate was produced from rice bran by *Rhizopus* sp., then used directly for succinic acid production by *E. faecalis* [71]. The problem with this approach is that fumarate productivities (0.2 g $L^{-1}h^{-1}$) and yields (0.5 g g^{-1}) are low, essentially moving the process limitations from succinic acid production to fumaric acid production.

The most notable downside of the natural producers is their auxotrophies which necessitates the use of complex, expensive growth media. To overcome this, genetically modified strains have been developed which seek to achieve competitive succinate production on a minimal, or at least cheaper, medium thereby overcoming the costs of rich media. *E. coli* [27,72] and *C. glutamicum* [58] both require genetic modifications of the central carbon metabolism as they do not naturally produce succinic acid at appreciable titres. However, modified strains of these organisms have been unable to achieve the high productivities of natural producers, as hinted at in Table 2.3, although more comprehensive comparative studies are still required. Moreover, genetically modified organisms often do not perform as expected [60] or suffer reversion during prolonged fermentations [73], which adds an element of risk to their commercial application. An advantage of using modified strains, especially *E. coli* (the bacterial “workhorse”) and *S. cerevisiae* (the yeast “workhorse”), is the wealth of genetic tools and information available for their manipulation and an overall deeper understanding of their physiologies due to the extent of research already performed on these organisms. A plausible strategy is to start off with strains that naturally produce the desired product at high titres and rates, then optimise these strains for enhanced performance through metabolic engineering [45]. Of course, this depends on the availability of genetic information on the organism and the ease with which modifications can be successfully achieved, i.e. the genetic accessibility of the organism. In essence, competitive wild-type succinate producers offer the advantage of less

required investment into genetic modifications and a more stable phenotype in prolonged fermentations.

Among the succinate producers, of particular interest is the wild-type bacterium *A. succinogenes.* Despite lacking a complete TCA cycle and glyoxylate shunt [41], the organism is able to achieve high succinic acid yields and productivities partly because of its tolerance to high acid titres [29]. Furthermore, *A. succinogenes* consumes an array of carbohydrate substrates [74], incorporates CO_2 during SA production, is non-pathogenic [41] and is a facultative anaerobe [30] making industrial application practically feasible. Therefore, despite a number of auxotrophies, *A. succinogenes* is a top-contender as a microbial host for industrial succinate production.

To gauge the research interest in *A. succinogenes* versus other microbial hosts, the number of publications dealing with fermentative succinic acid production by each organism was estimated by a combination of keyword search schemes on Scopus aiming to zone in on relevancy (Figure 2.2A). It is clear that interest in *A. succinogenes* is considerable (97 papers) and, based on the estimate, substantially exceeds other strains, except for *E. coli* where a large number of studies (181 papers) have been performed, particularly on genetic engineering of the organism for improved succinic acid production. Succinic acid studies on *S. cerevisiae* are focused primarily on wine and liquor manufacturing instead of bulk, bio-succinate production [75]. Figure 2.2B gives the equivalent search to Figure 2.2A but excludes terms related to genetic engineering or modifications in order to focus more specifically on succinic acid production studies, as opposed to genetic engineering studies. The reason for the greater interest in *A. succinogenes* is likely due to the naturally occurring advantages offered by the organism (as discussed above), the ready availability of the organism and the relative ease with which it can be studied (e.g. no need for genetic modifications, facultative anaerobe, non-pathogenic). Also, it is likely that the initial demonstrations of its potential as a succinic acid producer served as a platform attracting more attention which has led to a domino-effect in the publication rate and interest in the organism.

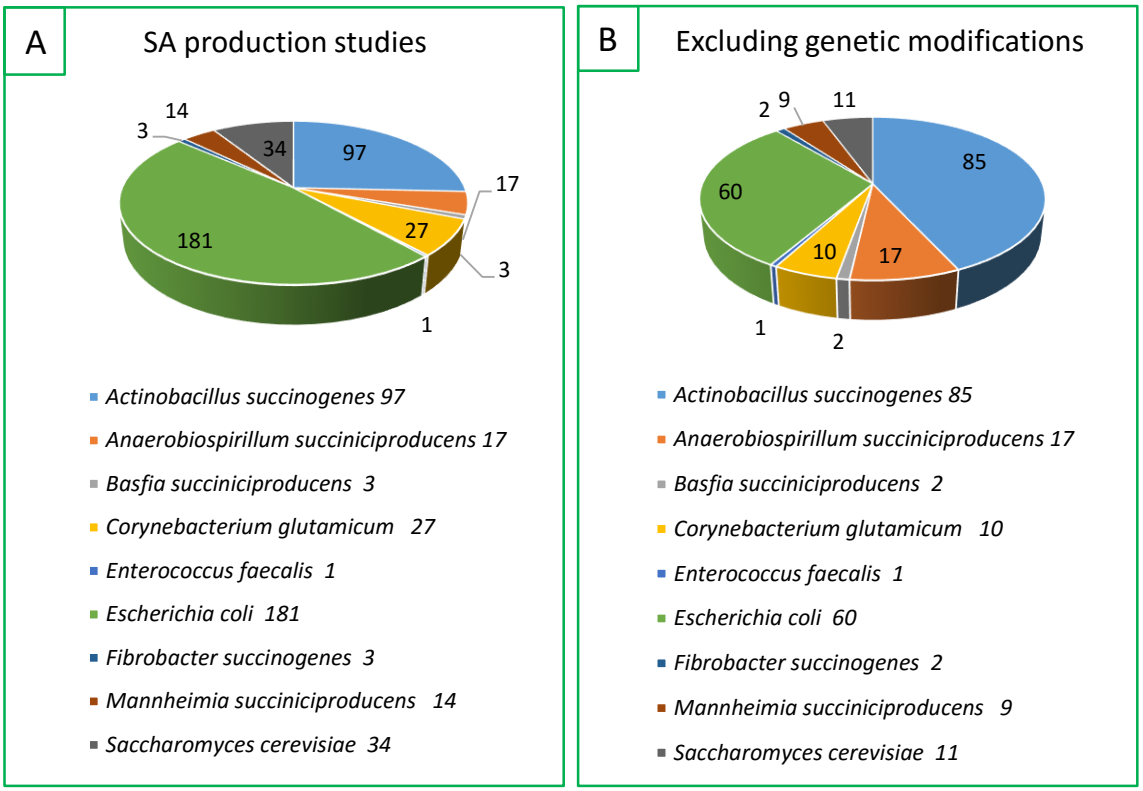

Figure 2.2 Estimated interest in each microorganism as a succinic acid producer based on the total number of publications matching unique search strategies on Scopus. (A) Search results based on all articles (excluding reviews) that include (1) "succinate" or "succinic acid" in the title, (2) the microorganism name in the title or keywords, (3) "production/producing/fermenta*" in the title, abstract or keywords and (4) excluding words unique to certain organisms to further narrow the search (e.g. "bread" and "wine" for *S. cerevisiae*). **(B)** Search results based on all articles (excluding reviews) that include the same parameters as A, but exclude terms relating to genetic modifications of the organism (e.g. "mutant" and "metabolic engineering")

2.2 THE BIOCATALYST: *ACTINOBACILLUS SUCCINOGENES* 130Z

A. succinogenes (ATCC 55618; DSM 22257) is a Gram-negative, facultative anaerobe of the family *Pasteurellaceae* isolated from bovine rumen and first characterised by Guettler et al. [30] in 1999. In nutrient rich fermentations, the bacterium mainly produces succinic acid, acetic acid and formic acid with small amounts of pyruvic acid, oxaloacetic acid and ethanol [30]. Within the rumen, *A. succinogenes* has a commensal relationship with the ruminant where it produces succinic acid, which is then decarboxylated to propionic acid and used by the host in the gluconeogenic pathway. The naturally high CO_2 content and anaerobic conditions in the rumen have likely led to the enhanced growth rate of *A. succinogenes* and the improved succinic acid production seen at high CO_2 levels, making it a capnophilic organism. Furthermore, *A. succinogenes* is a mesophilic neutrophile as it grows well between temperatures of 37 and 39 °C and at pH values between 6.0 and 7.4 [74]. The optimal temperature and pH, at least for CO_2 uptake, are considered to be 37 °C and 6.8, respectively [76].

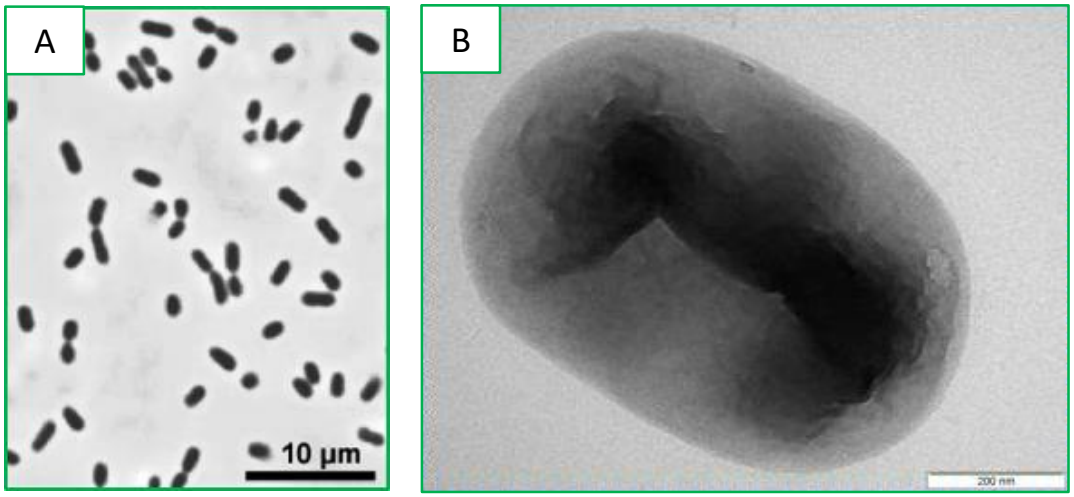

Figure 2.3. Typical cell morphology of *A. succinogenes*. (A) As a pleomorphic organism, *A. succinogenes* cells can occur as either rods or coccobacillus forms, **(B)** A close-up micrograph of a single *A. succinogenes* cell. (Images: (A) James McKinlay, Michigan State University, public domain; (B) Claire Vielle, Michigan State University, on request).

2.2.1 CENTRAL METABOLIC NETWORK

The genome of *A. succinogenes* has been sequenced and largely interpreted by McKinlay et al. [41], which is instrumental in understanding the metabolism of the organism and identifying potential targets for metabolic engineering. In the central carbon metabolism of *A. succinogenes* (catabolism), C_6 sugars are deconstructed via glycolysis, while C_5 sugars are deconstructed via the pentose

phosphate pathway (PPP) initially, then via glycolysis entering the pathway at fructose 6-phosphate (F6P) and glyceraldehyde 3-phosphate (G3P) (Figure 2.4).

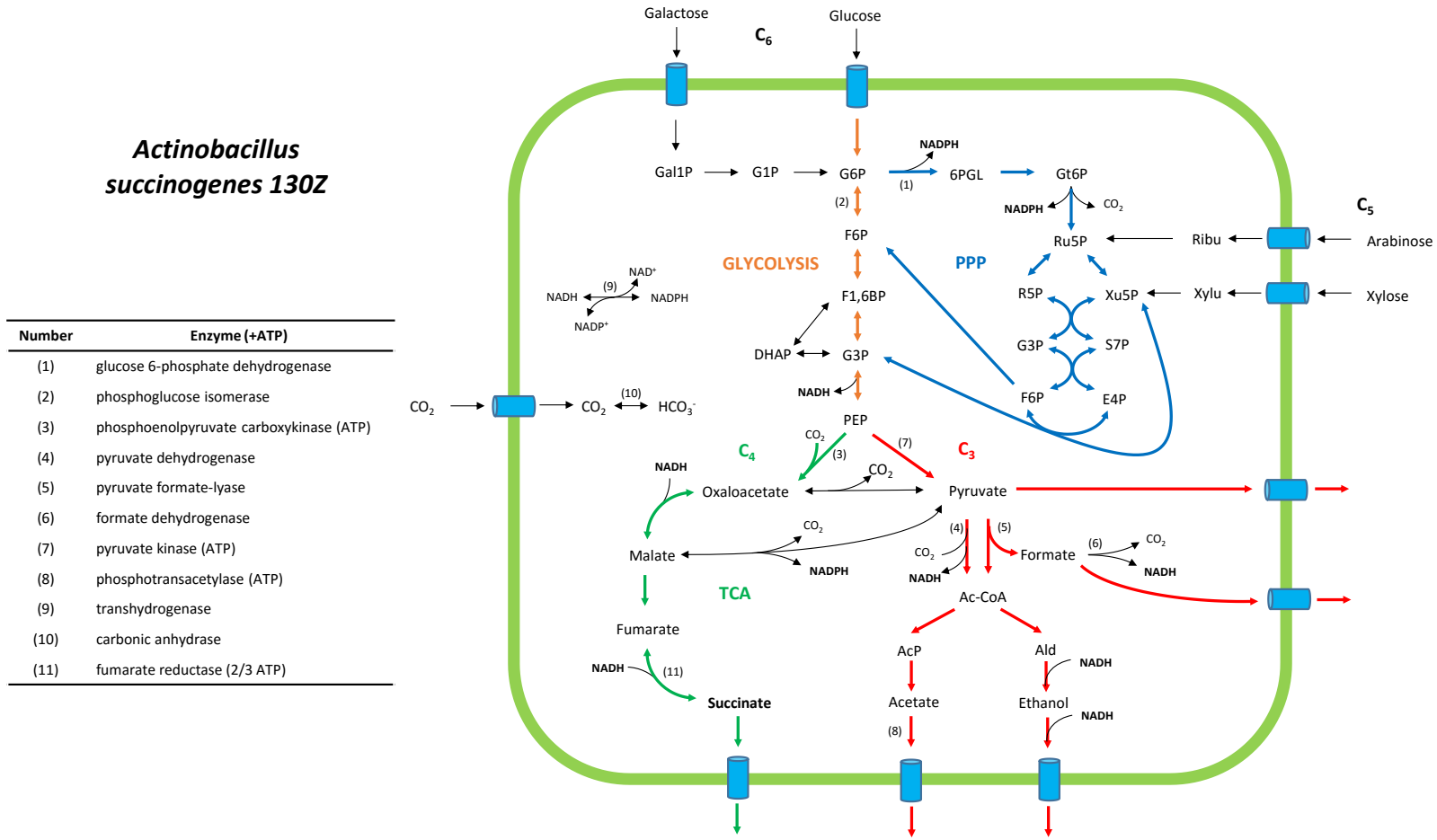

Number	Enzyme (+ATP)
(1)	glucose 6-phosphate dehydrogenase
(2)	phosphoglucose isomerase
(3)	phosphoenolpyruvate carboxykinase (ATP)
(4)	pyruvate dehydrogenase
(5)	pyruvate formate-lyase
(6)	formate dehydrogenase
(7)	pyruvate kinase (ATP)
(8)	phosphotransacetylase (ATP)
(9)	transhydrogenase
(10)	carbonic anhydrase
(11)	fumarate reductase (2/3 ATP)

Figure 2.4. Central metabolic network of *A. succinogenes*. A simplied view of the primary catabolic reactions of *A. succinogenes* with each of the major pathways in a different colour, based on [41,77] and the genome (KEGG). Abbreviations: 6PGL: 6-phosphogluconolactone; Ac-CoA: acetyl-CoA; AcP: acetyl-phosphate; Ald: aldehyde; DHAP: dihydroxyacetone phosphate; E4P: erythrose 4-phosphate; F1,6BP: fructose 1,6-biphosphate; F6P: fructose 6-phosphate; G1P: glucose 1-phosphate; G3P: glyceraldehyde 3-phosphate; G6P: glucose 6-phosphate; Gal1P: galactose 1-phosphate; Gt6P: gluconate 6-phosphate; PEP: phosphoenolpyruvate; PPP: pentose phosphate pathway; R5P: ribose 5-phosphate; Ribu: ribulose; Ru5P: ribulose 5-phosphate; S7P: sedoheptulose 7-phosphate; TCA: tricarboxylic acid cycle; Xu5P: xylulose 5-phosphate; Xylu: xylulose

In anaerobic fermentations, where energy is produced via substrate level phosphorylation, carbon flux can split to either the C_4 or C_3 pathway after glycolysis at the phosphoenolpyruvate (PEP) node. Since *A. succinogenes* does not possess the genes that code for citrate synthase and isocitrate dehydrogenase, the oxidative portion of the TCA cycle is incomplete [41] and carbon flux is restricted to the reductive branch of the TCA cycle, which forms the C_4 pathway. Moreover, *A. succinogenes* lacks a glyoxylate shunt [41] and therefore carbon cannot be channelled from the oxidative portion of the TCA cycle (with acetyl-CoA) to form malate and succinate directly. Alternatively, the C_3 (fermentative) pathway is capable of generating reduction power, or rather does not consume the reduction power generated in glycolysis. Therefore, the C_4 pathway can be viewed as reductive and the C_3 pathway as oxidative.

The C_4 pathway begins with the conversion of PEP to oxaloacetate by means of PEP carboxykinase (PEPCK; EC 4.1.1.49). This enzyme is important as it generates an ATP molecule and sequesters a CO_2 molecule for every PEP molecule converted. In contrast to *A. succinogenes*, not all succinate-producers possess this enzyme; instead a PEP carboxylase (EC 4.1.1.31) is present which does not yield ATP. Also, PEPCK from non-capnophilic organisms may have an affinity for the reaction converting oxaloacetate and ATP into PEP and ADP as part of gluconeogenesis, such as in *E. coli* [78], thereby directing carbon flux away from succinic acid. The efficacy of PEPCK native to *A. succinogenes* in succinic acid production was demonstrated, where overexpression of the enzyme in *E. coli* increased succinic acid production 6.5 times [79]. Besides favouring flux towards succinic acid in *A. succinogenes*, the gain in ATP through PEPCK is advantageous to succinic acid production, since growth and maintenance energy requirements can be partly satisfied by the C_4 route. After PEP conversion to oxaloacetate, carbon flows ultimately to succinate via malate and fumarate as intermediates, consuming two NADH molecules for reduction of the carbon backbone and generating 2/3 ATP molecules [77] through fumarate reductase.

Alternatively, the C_3 pathway begins with the conversion of PEP to pyruvate through pyruvate kinase with the formation of one ATP molecule. Pyruvate then acts as an important node where it can be oxidised by either pyruvate formate-lyase (PFL) or pyruvate dehydrogenase (PDH). In the case of PFL, acetyl-CoA is produced together with formate - a major by-product and inhibitor in *A. succinogenes* fermentations. In the case of PDH, NADH is produced along with CO_2 and acetyl-CoA. Regarding succinic acid production, it is preferred that the conversion takes place via PDH since additional NADH is produced and as a direct consequence, greater C_4 pathway flux at reduced levels of by-product formation occurs. Similarly, formate can be broken down to NADH and CO_2 by formate dehydrogenase, which provides the same boost to C_4 pathway flux as PDH. The additional CO_2

generated by the dehydrogenases is also useful to maintain a sufficient supply for the conversion of PEP to oxaloacetate. Downstream from pyruvate, acetyl-CoA also serves as a node, although seemingly less important, where it can be converted to acetyl-phosphate or acetaldehyde. The acetyl-phosphate route generates one ATP molecule and ends in acetate - the second major by-product of *A. succinogenes* fermentations - while acetaldehyde is converted to ethanol without any ATP gain but at the expense of NADH. Under CO_2-limiting conditions, C_4 pathway flux is constrained, therefore ethanol production is a likely means to balance redox as two NADH molecules are required for its production. Overall, the C_3 pathway forms the by-products acetic acid, formic acid, pyruvic acid and ethanol in succinate fermentations and it is desirable to minimise carbon flux through this pathway.

A potential by-product also within the C_3 route is lactic acid. Despite the presence of a lactate dehydrogenase, lactic acid production has been excluded in two early studies on *A. succinogenes* [41,74] and its presence in fermentations is considered to be from lactic acid-producing contaminants [36]. However, one publication [80] reported high levels of lactic acid production by *A. succinogenes* and suggested a dual-phase scheme for optimised production. This result is likely erroneous as the mass balances are inconsistent and repeatable evidence of lactic acid production by *A. succinogenes* is yet to be provided.

The theoretical maximum yield of succinic acid on glucose is 1.12 g g^{-1}. In the general case of a central metabolic network containing a full TCA cycle and/or a glyoxylate shunt, this theoretical maximum yield can be achieved when no biomass is generated [25]. This implies full conversion of glucose and CO_2 to succinic acid without any by-product formation. Since *A. succinogenes* lacks both a full TCA cycle and a glyoxylate shunt in its catabolic network (i.e. excluding the pentose phosphate pathway which is considered part of the anabolism), redox constraints limit the maximum succinic acid yield on glucose to either 0.66 g g^{-1} or 0.87 g g^{-1} for pyruvate conversion to acetyl-CoA by pyruvate formate-lyase or pyruvate dehydrogenase (Figure 2.4), respectively [15]. When formate is broken down by formate dehydrogenase, the maximum yield is also 0.87 g g^{-1} due to equivalent NADH production to the PDH route. For each of these cases, the maximum selectivity of succinic acid to the major by-product acetic acid is 1.97 g g^{-1} and 3.93 g g^{-1} respectively and the overall selectivity is 1.11 g $g_{by\text{-}products}^{-1}$ and 3.93 g $g_{by\text{-}products}^{-1}$, respectively. Therefore, without an additional source of reducing power to drive carbon flux through the C_4 pathway, homosuccinate fermentation is not possible by *A. succinogenes*.

2.2.2 AUXOTROPHIES

Due to the environmental richness of the rumen and its abundance of vitamins and amino acids, *A. succinogenes* does not possess all biosynthetic routes for their production and is auxotrophic for a number of essential compounds. Regarding amino acids, *A. succinogenes* cannot synthesise glutamate and methionine and is unable to reduce sulphate [81]. Since sulphur is required for cysteine biosynthesis, a non-sulphate sulphur source (e.g. sodium sulphide or sodium thiosulphate) or cysteine should be included in the growth medium together with glutamate and methionine. In addition to these amino acids, *A. succinogenes* requires four vitamins for growth, namely nicotinic acid, pantothenate, pyridoxine, and thiamine [41]. Biotin is not considered essential for growth but provides a stimulatory effect [82] and since *A. succinogenes* is missing several genes involved in biotin synthesis [41], it is advantageous to include biotin in the growth medium along with the four vitamins. These essential amino acids and vitamins can be supplied by a complex nitrogen source such as yeast extract or corn steep liquor, or separately as part of a defined medium. In industrial scale fermentations, it will likely be more cost effective to use a complex nitrogen source and current pricing estimates favour corn steep liquor ($0.0753/kg in 2014$ [83]) over yeast extract ($3.5/kg in 2000$ [84]). However, it is necessary to determine whether corn steep liquor can provide all the essential compounds at adequate concentrations and whether fermentation performance is maintained. Auxotrophies such as these are common disadvantages of wild-type succinate producers.

2.2.3 BATCH FERMENTATION STUDIES

To date, the majority of the succinic acid fermentation studies on *A. succinogenes* were performed in batch mode. Various pure and starch-based carbohydrates have been explored for batch and fed-batch production of succinic acid (Table 2.5) as well as a variety of lignocellulosic and other biomass feedstocks (Table 2.6). Similar to the general succinate production studies in Table 2.3 and Table 2.4, pure sugar substrates are used for a more fundamental understanding of the organism, while biomass feedstocks offer a more industrial or biorefinery-based perspective on the potential of the organism. The most notable batch studies on wild-type *A. succinogenes* using pure carbohydrates achieved yields, productivities and titres of up to 0.87 g g^{-1}, 2.16 g $L^{-1}h^{-1}$ and 60.5 g L^{-1} (Table 2.5) respectively, while those on bio-derived feedstocks achieved 1.02 g g^{-1}, 1.50 g $L^{-1}h^{-1}$ and 64.3 g L^{-1} (Table 2.6). Therefore, while titres and yields are comparable between the two groups of feedstocks, work still needs to be done in improving productivities on industrially relevant feedstock for *A. succinogenes* to compete cost-effectively on an industrial scale.

Greater focus has been placed on batch fermentations, the "traditional" and more popular mode used in microbiology, largely because bench-scale operation of batch fermenters is easier than continuous operation and multiple batches can be run simultaneously with minimal supervision. Batch studies tend to focus on the physiology or potential of the organism and for screening of suitable feedstocks. For example, numerous batch studies have been performed on *A. succinogenes* that explore and optimise process parameters including redox [85,86], temperature and pH [76,87], fermentation medium [33,88,89], neutralising agents [90], cell immobilisation [91] and CO_2 [76,92]. In addition, Corona-Gonzalez et al. [35] investigated the growth kinetics of *A. succinogenes* and determined the maximum specific growth rate to be 0.41 h^{-1}. Investigation of product inhibition on *A. succinogenes* growth and productivity found that of the major excreted catabolites, formic acid is the most inhibitory followed by ethanol, acetic-, pyruvic- then succinic acid [29]. In addition, it was found that at total acid concentrations near 20 g L^{-1} (formic-, acetic- and succinic acids), formation of biomass terminated [35]. Inhibition by glucose appears to be limited as *A. succinogenes* is able to tolerate concentrations of up to 143 g L^{-1}, while cell growth terminates above 158 g L^{-1} [29] and optimal growth occurs below glucose concentrations of 55 g L^{-1} [35].

Also commonly explored in batch reactors is the performance of genetically modified or improved strains. Only a limited number of studies have been performed on genetically modified strains of *A. succinogenes* and tools for genetic engineering of the organism. Kim et al. [93] constructed a shuttle vector for expression of recombinant proteins in *A. succinogenes* and used electroporation to introduce plasmids into the cells. The mutant CCTCC M2012036 was developed by genome shuffling of the parent strain CGMCC1593 and showed enhanced succinic acid production [42]. Guettler et al. [43] developed a number of fluoroacetate-tolerant variants (e.g. FZ 6, FZ 53) from the parent strain 130Z, which showed increased succinic acid and decreased acetic acid production. Finally, Joshi et al. [94] developed a markerless knockout method for *A. succinogenes* 130Z using natural transformation or electroporation, where single-knockout mutants of the fumarate reductase and of the pyruvate-formate lyase-encoding genes were obtained. General considerations and strategies for improving succinic acid production by metabolic engineering and metabolically engineered succinate producers have been reviewed by Cheng et al. [95]. So while there may be potential for genetic improvement of *A. succinogenes*, currently the focus has mainly been on the wild strain.

Table 2.5. Representative batch bio-succinic acid production studies with *A. succinogenes* on starch-derived or pure carbohydrates. Studies achieving high yields, productivities and/or titres are included.

Feedstock	Strain	Mode	Titre[a]	Yield	Productivity	Reference
Cellobiose	NJ113	Batch	38.9	0.66	1.08	[96]
Fructose	CGMCC 1593	Batch	38.4	0.79	0.64	[97]
Glucose	130Z	Batch	39.0	0.79	0.49	[34]
Glucose	130Z	Repeat batch	35.1	0.87	0.88	[33]
Glucose	CCTCC M2012036	Repeat batch	39.0	0.85	3.61	[14]
Glucose	CCTCC M2012036	Fed-batch	98.7	0.89	2.77	[14]
Glucose	FZ 6	Batch	63.7	0.94	1.01	[43]
Glucose	FZ 53	Batch	105.8	0.82	1.36	[43]
Glycerol	130Z	Fed-batch	49.6	0.64	0.96	[98]
Lactose	CGMCC 1593	Batch	40.1	0.81	0.67	[97]
Maltose	CGMCC 1593	Batch	38.8	0.80	0.65	[97]
Sucrose	NJ113	Fed-batch	60.5	0.83	2.16	[99]
Sucrose	CGMCC 1593	Batch	40.3	0.81	0.67	[97]
Xylose	CGMCC 1593	Batch	32.6	0.77	0.54	[97]

[a]The values for each performance indicator are not necessarily from the same experiment within each study, but rather the highest value attained in the study.

Table 2.6 Bio-succinic acid production studies with *A. succinogenes* on lignocellulosic and other biomass feedstocks. Studies with the highest productivities for each feedstock type were included.

Feedstock	Strain	Main sugars	Mode	Titre ($g\ L^{-1}$)	Yield ($g\ g^{-1}$)	Productivity ($g\ L^{-1}h^{-1}$)	Reference
Bread hydrolysate	130Z	Glucose	Batch	47.3	1.16[a]	1.12	[100]
Cane molasses	GXAS 137	Sucrose, glucose, fructose, other	Fed-batch	64.3	0.76	1.07	[101]
Cheese whey	130Z	Lactose (galactose and glucose)	Batch	22.2	0.57	0.44	[102]
Corn fibre hydrolysate	NJ113	Glucose, xylose, arabinose	Batch	35.4	0.73	0.98	[103]
Corn stalk hydrolysate	BE-1	Glucose, xylose, cellobiose	Batch	17.8	0.66	0.56	[104]
Corn straw hydrolysate	CGMCC 1593	Glucose, xylose, arabinose, cellobiose	Fed-batch	53.2	0.82	1.21	[62]
Corncob hydrolysate		Xylose, arabinose, cellobiose, glucose	Batch	23.6	0.58	0.49	[105]
Cotton stalk hydrolysate		Glucose, xylose	Batch	63.0	0.64	1.17	[106]
Macroalgal hydrolysate		Glucose, mannitol	Batch	33.8	0.63	1.50	[107]
Rapeseed meal	130Z	Sucrose, glucose, fructose, arabinose	Fed-batch	23.4	0.60	0.33	[108]
Sake less hydrolysate		Glucose (reported)	Batch	36.3	0.59	1.21	[109]
Sugarcane bagasse hydrolysate		Xylose	Batch	22.5	0.43	1.01	[110]
Wheat hydrolysate		Glucose	Batch	62.1	1.02	0.91	[111]

[a]The yield is greater than the theoretical maximum ($1.12\ g\ g^{-1}$).

2.3 CONTINUOUS SUCCINIC ACID PRODUCTION

Industrial-scale reactors operate in one of two principal modes, batch or continuous. Batch (and fed-batch) processes are traditionally used for high-value, low-volume products (e.g. pharmaceuticals) or biological processes (e.g. beer and wine), while continuous processes are traditionally used for high-volume, low-value products (e.g. chemicals and petroleum products). These differences stem from the reactor performance under each condition, product requirements and the associated operational costs of each mode. Each of these modes has pros and cons (Figure 2.5) and while bioprocesses have traditionally been operated in batch mode, a trend towards continuous operation is emerging and is likely to gain popularity in the future [112].

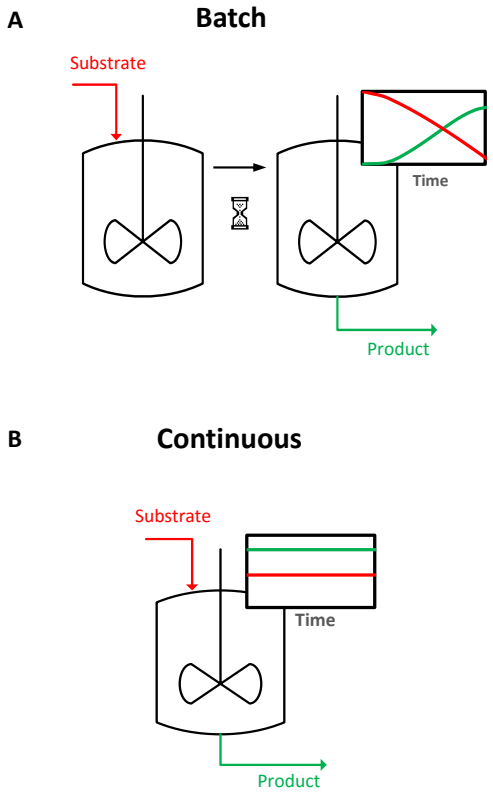

Advantages	Disadvantages
Versatile and easily modified	Time-dependent behaviour
Easily sterilisable and easier to maintain sterility	Mass and redox balances are difficult and less accurate
Complete substrate conversion possible	High labour cost
	Significant idle time for sterilisation, cleaning, inoculum outgrowth, etc.

Advantages	Disadvantages
Constant product quality	Higher risk in sterility failure
More accurate mass and redox balances	Genetic instability over prolonged operation
High productivity due to autocatalytic bioreactions	Inflexible
Steady-state operation	Difficulties in operating downstream equipment continuously
Low capital and labour costs	

Figure 2.5. The advantages and disadvantages of (A) batch and (B) continuous bioreactors. Partly derived from [32].

For commodity or bulk chemicals, it is important that the process is able to generate sufficiently high volumes of product, making a high product output rate (productivity) essential. Considering the demonstrably high productivities achieved under continuous operation of some bioprocesses (e.g. 536 g $L^{-1}h^{-1}$ ethanol [113], 20.1 g $L^{-1}h^{-1}$ lactic acid [114], 10.8 g $L^{-1}h^{-1}$ succinic acid [13]), the reduced

labour and capital costs, and the consistent product quality compared to batch mode, continuous mode is likely the best option for bulk bio-production of succinic acid. However, continuous production poses challenges of its own including incomplete substrate conversion, a potential increase in purification costs due to lower product titres and increased risk of contamination as the process is an open system. Therefore, these factors need to be considered when developing bulk continuous processes. Since feedstock preparation and downstream processing are costly and play a crucial role in overall process economics [115], it is also essential to achieve high yields and titres in bulk bioprocesses as discussed in 2.1.2. In essence, the optimal combination of all three parameters – yield, productivity and titre – must be determined when assessing the economic feasibility of a bulk, continuous process.

As discussed in 2.2.3, most fermentation studies on *A. succinogenes* have been performed in batch mode, largely due to its familiarity and ease of operation on the bench-scale. However, strides have been made in continuous succinate fermentations with *A. succinogenes* (Table 2.7). The first of these fermentations were performed by Urbance et al. in 2004 [37], where cells self-adhered to a plastic composite support leading to enhanced productivities, titres and yields compared to suspended cell fermentations. Following this, Kim et al. [36] attempted to increase cell density through an external membrane, cell recycle system but encountered extensive fouling of the membrane which led to inoperability of the reactor, most likely caused by biofilm formation or cell accumulation. Van Heerden and Nicol [38] extended the continuous work on *A. succinogenes* by considering the transient behaviour of the system, by-product distributions and the advantages of cell immobilisation in an externally recycled reactor packed with Genulite™ Groperl. It was found that the SA yield on glucose remained constant at 0.69 g g^{-1} across all dilution rates while growth appeared to be higher at higher dilution rates, slowing substantially above a succinic acid titre of 10 g L^{-1}.

In all these pioneering studies, it was found that *A. succinogenes* has the ability to readily self-adhere to surfaces and unavoidably, and extensively, produce biofilm [61, 62]. Biofilm consists of microbial cells held together by a self-produced, extracellular matrix comprising polymeric substances that adhere to surfaces and provide a form of natural cell immobilisation [116]. Since rates of product formation can be improved by increasing the cell density in a fermenter [117], and biofilm leads to increased cell density, biofilm can serve as a natural means for enhancing fermentation productivity. To this end, and the tendency of *A. succinogenes* to unavoidably produce biofilm, subsequent continuous production studies on *A. succinogenes* targeted high cell density fermentations, focusing particularly on biofilm behaviour, formation and stability [13–15,39].

Using an externally recycled reactor with stainless steel wool as biofilm support, Bradfield and Nicol [15] found that at increasing acid titre (or amount of substrate consumed), biofilms of *A. succinogenes* exhibit unique metabolic behaviour where carbon flux to succinic acid is favoured, leading to an improvement in yield and reduced by-product formation (Figure 2.6). A yield of succinic acid on glucose of up to 0.91 g g^{-1} was achieved with the succinic acid-to-acetic acid ratio increasing from 2.4 g g^{-1} to 5.7 g g^{-1}. Therefore, compared to suspended cells, biofilms of *A. succinogenes* afford unique yield improvements in addition to the productivity bonus. Similarly, Maharaj et al. [13] showed that the increase in yield with increasing acid titre is repeatable across various dilution rates, where higher titres (32.5 g L^{-1}), thus yields (0.90 g g^{-1}), are attained at lower dilution rates. In the study, the reactor was packed with Poraver® beads instead of stainless steel wool, thereby excluding the type of biofilm support material as the cause of the shift in the metabolism. In addition, it was shown that specific cell productivities (based on the total biomass content in the fermenter) decreased with decreasing dilution rate and increasing acid titre. Moreover, the study exemplified the productivity advantages of continuous operation of a high cell density system by achieving a productivity of 10.8 g $L^{-1}h^{-1}$ and operating at a dilution rate of 0.72 h^{-1}, which is substantially greater than the reported maximum growth rate of 0.41 h^{-1} [35]. Such high dilution rates are only possible in an immobilised-cell fermenter as complete cell washout at high dilution rates is overcome.

To compare the productivity and yield of chemostat and immobilised-cell reactors, Brink & Nicol [16] achieved regular chemostat operation (i.e. without biofilm present) with *A. succinogenes* under high shear conditions in a tubular reactor. It was demonstrated that the biofilm reactor clearly outperformed the chemostat in terms of succinic acid productivity (> 9 times), yield (59% at D=0.5 h^{-1}) and selectivity (i.e. reduced by-product formation). Furthermore, it was found that specific growth rates of *A. succinogenes* and specific succinic acid productivities are severely inhibited by the presence of organic acids (Figure 2.7) which dovetails with the observations of Maharaj et al. [13]. In addition, it was found that cell growth terminates at SA titres between 8 g L^{-1} and 14 g L^{-1} (Figure 2.7A), which corresponds approximately to 13 g L^{-1} and 22 g L^{-1} total acids, similar to the inhibition value suggested by Corona-Gonzalez et al. [35] under batch conditions. As a result of the termination of growth, maintenance production of succinic acid becomes more prominent with increasing succinic acid titre and dominates at titres above 12 g L^{-1} (Figure 2.7B), within the range where the shift in the metabolic flux distribution is triggered (Figure 2.6). Therefore, the transition from growth to non-growth metabolism is controlled by overall acid titre and is accompanied by a shift in metabolic flux distribution which favours succinic acid production. Also, since growth is minimal (or absent) at SA titres greater than 14 g L^{-1}, cell content in the reactor outlet is minimal, allowing for

simplified downstream separation processes. Consequently, it is desirable to operate a continuous biofilm reactor with *A. succinogenes* at succinic acid titres sufficiently high (>14 g L^{-1}) to benefit from the shift in metabolic flux. However, sufficiently high titres are only possible at low dilution rates where overall reactor productivity is low. Therefore, a trade-off exists between achieving high productivities at low titres (high dilution rates) without capitalising on the yield and selectivity benefits, or achieving lower productivities at high titres (low dilution rates) but with associated improvements in yield and at reduced levels of by-product formation. The production "sweet spot" will depend on the economic constraints of the overall process.

An approach with the potential to balance these trade-offs is to operate in repeat-batch mode once stable biofilm has been established. In the initial stages of each batch, specific and volumetric productivities would be high due to low acid titres which do not substantially inhibit specific productivity. Thereafter, as acid titres increased, the shift in metabolic flux would be initiated leading to an increase in succinic acid yield and selectivity, but at lower specific and volumetric productivities. The overall effect would then be a period of high productivity with lower yields, followed by a period of lower productivity at high yields. The net result may afford optimisation of all three design parameters. The process can then be repeated over the lifetime of the biofilm. Yan et al. [14] hinted at the potential success of this approach where titres, yields and productivities of 98.7 g L^{-1}, 0.87 g g^{-1} and 2.77 g $L^{-1}h^{-1}$ respectively, were achieved in repeated fed-batch fermentations with *A. succinogenes* cells immobilised on a stirred fibrous bed.

Despite attractive fermentation performance with biofilm reactors, stability challenges continue to be a limitation due to the tendency of biofilm to "shed" and detach unpredictably [13], thereby making it difficult to control the total active biomass content in the reactor [15]. Biofilm overgrowth and removal of inactive biofilm tend to be paramount processing challenges, however a critical amount of biofilm is required in order to achieve sufficiently high productivities and titres. Therefore, a second trade-off arises in continuous fermentations with *A. succinogenes* – achieving sufficiently high cell density without compromising on reactor operability. Prolonged, stable continuous operation has been demonstrated by Yan et al. [39] using the same stirred, fibrous bed bioreactor as in [14], while Maharaj et al. [13] showed repeatability of steady-states at various dilution rates with different fermentation histories. Therefore, while progress has been made towards developing a robust biofilm process for succinic acid production, opportunities still exist to develop effective attachment schemes that allow for high cell densities and streamlined reactor operation with the potential for scale-up.

A further major consideration for commercialisation and scale-up, is the use of industrially relevant feedstock. While the continuous studies on succinate production by *A. succinogenes* (Table 2.7) clearly outperform the batch studies (Table 2.5) in terms of productivity at similar yields but generally lower titres, all these studies utilise clean, pure sugar feedstreams. Therefore, there is no continuous equivalent of Table 2.6, where lignocellulosic or other bio-derived feedstocks are used. Achieving truly sustainable succinic acid production, especially in the context of a biorefinery, hinges on the performance of the microbial host on more process relevant feedstreams making this an important avenue of research.

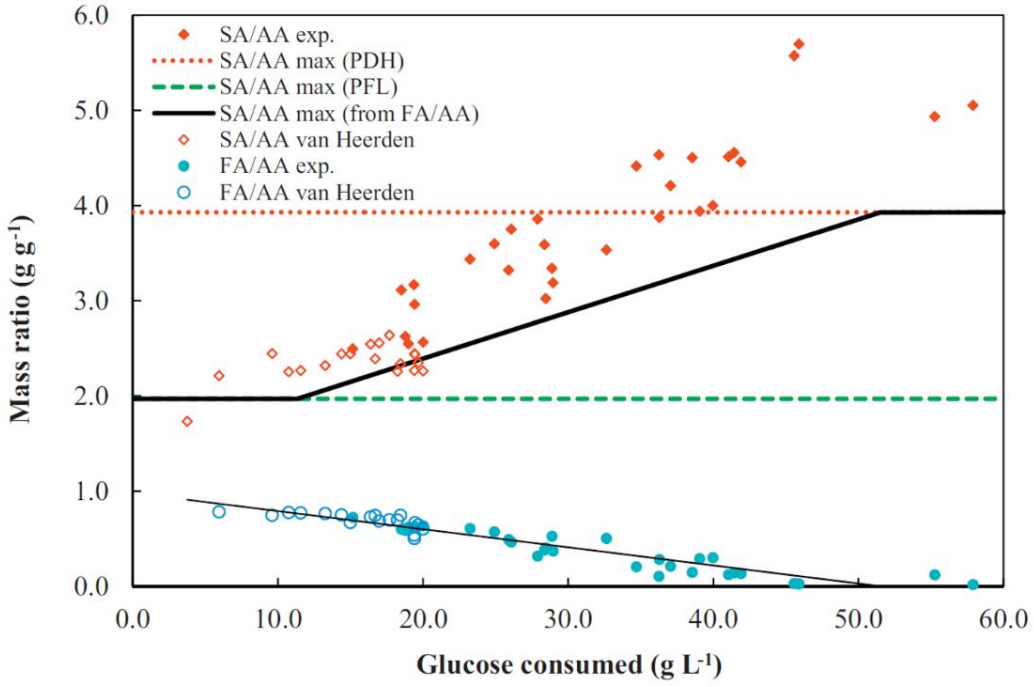

Bradfield MFA, Nicol W *Biochem Eng J* 2014, 85:1-7

Figure 2.6. Carbon flux to succinic acid increases with increasing acid titre (or glucose consumed) [15]**.** SA/AA = succinic acid to acetic acid mass ratio (C_4 vs. C_3 pathway split); FA/AA = formic acid to acetic acid mass ratio; PDH = pyruvate dehydrogenase pathway; PFL = pyruvate formate lyase pathway. van Heerden = [38].

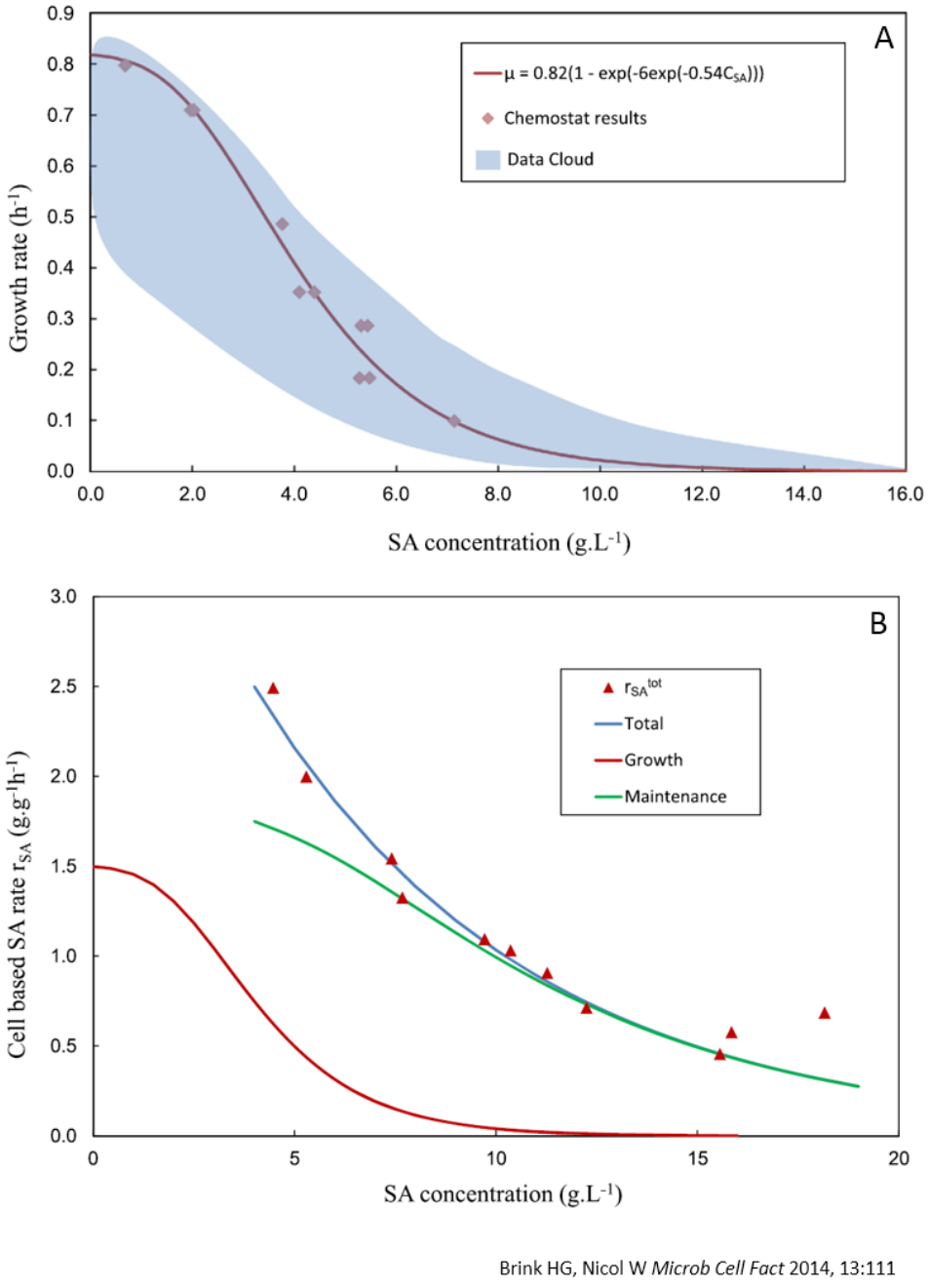

Brink HG, Nicol W *Microb Cell Fact* 2014, 13:111

Figure 2.7. The (A) growth rate and (B) specific succinic acid productivity of *A. succinogenes* decrease with increasing succinic acid concentration [16]**.** In (A), a succinic acid inhibition model is proposed which follows the "data cloud" comprising results from a number of batch SA production studies on *A. succinogenes*. In (B), the transition from growth-driven to maintenance-driven SA production is illustrated.

Table 2.7. Representative continuous bio-succinic acid production studies with *A. succinogenes* on glucose.

Strain	Mode	Titre[a] (g L^{-1})	Yield (g g^{-1})	Productivity (g $L^{-1}h^{-1}$)	Reference
130Z	Continuous; biofilm	10.4	0.72	2.08	[37]
130Z	Continuous; biofilm	13.4	0.50	6.63	[36]
130Z	Continuous; biofilm	11.3	0.69	6.35	[38]
130Z	Continuous; biofilm	48.5	0.91	9.40[b]	[15]
130Z	Continuous; biofilm	32.5	0.90	10.80	[13]
130Z	Continuous; biofilm	7.7	0.69	17.10	[16]
130Z	Continuous; chemostat	7.1	0.61	1.80	[16]
CCTCC M2012036	Continuous; biofilm	55.3	0.80	2.77	[39]

[a]The values for each performance indicator are not necessarily from the same experiment within each study, but rather the highest value attained for each.

[b]Not given in paper, but provided by author.

2.4 STEADY-STATE FERMENTATION ANALYSIS

In addition to the process advantages of operating a fermenter continuously (2.3 Continuous succinic acid production), continuous operation lends itself particularly well to accurately study the behaviour and physiology of microorganisms. Continuous bioreactors can achieve steady-state where all conditions within the reactor remain constant over time. The constant environmental conditions then bolster the assumption that the organism attains metabolic steady-state at a particular environmental condition [118]. This is because the rates of metabolite production and substrate consumption must also remain constant over time since there is no accumulation of metabolites or substrate within the reactor. In addition, the constant environmental conditions allow cells to maintain metabolic steady-state for extended periods providing an extended window for analysis. Therefore, steady-state conditions allow for more accurate measurement of carbon flux in metabolic networks through analysis of extracellular metabolite concentrations, something that is not easily done in batch fermentations where more complicated transient methods must be employed [119].

Continuous operation also allows for proper quantification of the dilution effects caused by the addition of neutralising agents for pH control and antifoam for foam suppression. Furthermore, no

volume changes occur through sampling or pH control because the reactor volume can be controlled in a continuous system. Combined, these factors allow for accurate mass and redox balances, which are instrumental in understanding metabolic flux distributions in an organism and for assessing the completeness of fermentation data. For this reason, metabolic fluxes are best determined and interpreted under steady-state conditions [45].

2.4.1 THE MASS BALANCE

The most illuminating tool for analysing fermentation data is the mass balance. A mass balance essentially follows the notion of "what goes in, must come out". In bioreaction engineering, this is most easily performed as an elemental balance where all the elements entering the system as components of the substrate(s) (e.g. carbon, hydrogen, oxygen, nitrogen) must appear in the products (including biomass) or unconverted substrate(s). No specific knowledge of the metabolism of the microbial strain is needed in performing an overall mass balance, which makes this approach particularly useful and broadly applicable. Rather, it is only necessary to have measurements of the extracellular metabolites and substrates and to be judicious on what products the organism is expected to produce and excrete. Closure of the mass balance is instructive as incompleteness indicates that metabolites have not been accounted for, or that the metabolite or substrate measurements are inaccurate. Mass balance closure can be defined as the ratio of the stoichiometric amount of substrate required to produce the measured metabolite concentrations (based on an elemental balance), and the actual amount of substrate consumed. Following an incomplete mass balance, a more thorough analysis or the fermentation system is required. A generalised approach to elemental balancing and mass balances in fermentation systems is given by Villadsen et al. [32].

2.4.2 THE REDOX BALANCE

Second to the mass balance, and delving a step deeper into the workings of the microbial host, the redox balance provides further insight into fermentation data and the behaviour of the biocatalyst. A redox balance is essentially an electron balance where all electrons lost from one entity are necessarily gained by another entity. In biological reactions, there are unique carriers of electrons that are generally cofactors of enzymatic reactions. The main redox carriers are nicotinamide adenine dinucleotide (NADH), nicotinamide adenine dinucleotide phosphate (NADPH) and flavin adenine dinucleotide ($FADH_2$), but for simplicity, it is acceptable to represent them collectively as NADH. As such, NADH can be viewed as the single currency of reductive power [32]. In addition, many organisms can interconvert NADH and NADPH by the oxido-reductase enzyme, NADPH:NADH

transhydrogenase [32]. When NADH donates reductive power (as hydrogen atoms) to a metabolite, the metabolite is reduced while NADH is oxidised to NAD^+. Conversely, when a metabolite "sheds" electrons, NAD^+ will accept these electrons (as two hydrogen atoms) and be reduced to NADH (Figure 2.8). Accordingly, if a metabolite loses reductive power, one expects to see an increase in NADH (i.e. an increase in the reductive power currency) and vice versa. Note, in biological redox reactions, a proton is always associated with an electron and therefore electron transfer is accompanied by proton transfer and occurs as a hydrogen atom.

Within a balanced biochemical network, all NADH produced in one part of the network must be consumed in another part of the network. This criterion can be used to determine limitations of a biochemical network (e.g. maximum product yields on a particular substrate) and to assess the completeness of a particular fermentation system. Similar to an incomplete mass balance, an incomplete redox balance suggests that metabolites have not been fully accounted for, or that the expected metabolic network of the organism is inaccurate compared to the true, active metabolic network. For example, Bradfield and Nicol [15] explored redox balances in succinic acid fermentations by *A. succinogenes* and found that the detected metabolites and substrate levels could not account for total redox requirements. This suggests that either an alternative metabolic pathway is active, metabolites are unaccounted for, or that there is an external influence on the redox balance, possibly within the fermentation medium.

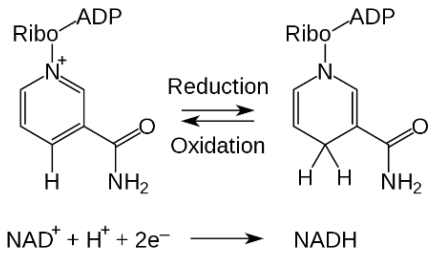

Figure 2.8. Redox reactions of nicotinamide adenine dinucleotide, the redox currency. Reduction of NAD^+ leads to NADH and oxidation of NADH yields NAD^+. (Image: Tim Vickers, public domain).

A useful way to analyse a metabolic network and to perform redox balances is to use overall reaction pathways. An overall pathway is essentially a summation of all intermediate metabolic reactions that lead from substrate to end-product within a biochemical network. Overall pathways are dealt with extensively by Villadsen et al. [32] and examples as applied to various succinate-producers, including *A. succinogenes*, are given by van Heerden and Nicol [25]. Pathways can be net liberators of reductive power (NADH), where the substrate progressively becomes oxidised, or net consumers of reductive power where the final metabolites are more reduced (collectively) than the substrate. In a fully defined and balanced system, the sum of NADH (and other reducing equivalents) involved in all the pathways should be zero.

In the case of *A. succinogenes*, the formation of succinic acid can be seen as an overall reductive process since the metabolites are more reduced than the substrate, given a carbon-balanced pathway. Equation 2-1 represents the overall pathway from glucose to succinic acid, essentially the C_4 branch. For the C_3 branch, the overall pathways from glucose to acetic acid, formic acid and pyruvic acid (PYR) are net oxidative processes yielding NADH. The overall pathways of the C_3 route are given by Equations 2-2 to 2-4 and include both routes of pyruvate oxidation (i.e. PFL and PDH/FDH). Equation 2-5 represents the complete recycling of carbon through the oxidative pentose phosphate pathway (OPPP) where glucose is fully converted to CO_2 and reductive power. Equations 2-6 to 2-10 give the carbon mole (C-mole) equivalents of Equations 2-1 to 2-5 as C-mole is a useful unit to maintain consistency when analysing metabolic flux. In addition, when carbohydrate sources have the same C:H:O proportion, such as glucose ($C_6H_{12}O_6$) and xylose ($C_5H_{10}O_5$), the C-mole balances reduce to the same form.

$$\textbf{SA}: C_6H_{12}O_6(\text{Glc}) + 2\text{NADH} + 2CO_2 \rightarrow 2C_4H_6O_4(\text{SA}) + 2H_2O \quad \textbf{2-1}$$

$$\textbf{PFL}: C_6H_{12}O_6(\text{Glc}) + 2H_2O \rightarrow 2C_2H_4O_2(\text{AA}) + 2CH_2O_2(\text{FA}) + 2\text{NADH} \quad \textbf{2-2}$$

$$\textbf{PDH}: C_6H_{12}O_6(\text{Glc}) + 2H_2O \rightarrow 2C_2H_4O_2(\text{AA}) + 4\text{NADH} + 2CO_2 \quad \textbf{2-3}$$

$$\textbf{PYR}: C_6H_{12}O_6(\text{Glc}) \rightarrow 2C_3H_4O_3(\text{Pyr}) + 2\text{NADH} \quad \textbf{2-4}$$

$$\textbf{OPPP}: C_6H_{12}O_6(\text{Glc}) + 6H_2O \rightarrow 6CO_2 + 12\text{NADPH} \quad \textbf{2-5}$$

$$\textbf{SA}: CH_2O(\text{Glc}) + \frac{1}{3}\text{NADH} + \frac{1}{3}CO_2 \rightarrow \frac{4}{3}CH_{\frac{3}{2}}O(\text{SA}) + \frac{1}{3}H_2O \quad \textbf{2-6}$$

$$\textbf{PFL}: CH_2O(\text{Glc}) + \frac{1}{3}H_2O \rightarrow \frac{2}{3}CH_2O(\text{AA}) + \frac{1}{3}CH_2O_2(\text{FA}) + \frac{1}{3}\text{NADH} \quad \textbf{2-7}$$

$$\textbf{PDH}: CH_2O(\text{Glc}) + \frac{1}{3}H_2O \rightarrow \frac{2}{3}CH_2O(\text{AA}) + \frac{2}{3}\text{NADH} + \frac{1}{3}CO_2 \quad \textbf{2-8}$$

$$\textbf{PYR}: CH_2O(\text{Glc}) \rightarrow CH_{\frac{4}{3}}O(\text{Pyr}) + \frac{1}{3}\text{NADH} \quad \textbf{2-9}$$

$$\textbf{OPPP}: CH_2O(\text{Glc}) + H_2O \rightarrow CO_2 + 2\text{NADPH} \quad \textbf{2-10}$$

If the metabolite concentrations are known, the stoichiometry of these equations can be used to determine the respective amounts of NADH and the consistency of the system can be assessed. However, as discussed above, this is most accurate under steady-state conditions in a continuous reactor.

3 | FERMENTATIVE PRODUCTION OF SUCCINIC ACID ON MODEL SUBSTRATES

The choice of feedstock is an essential component of fermentations as it has a large influence on process development and the economic viability of the overall process [9]. Furthermore, the type of feedstock largely determines the suitability of the microbial host, since the strain must efficiently grow on the carbohydrates present in the feedstock and achieve high product yields. To achieve sustainable production of chemicals, it is necessary to use a renewable feedstock. Renewable feedstocks include lignocellulose (e.g. woody and herbaceous biomass) and sugar- or starch-rich crops (e.g. sugar cane, wheat, corn) [120]. Carbohydrates can be extracted or released from these feedstocks by numerous pretreatment approaches [40] and subsequently used in a fermentation process. In sugar- and starch-rich crops, the primary monosaccharide is glucose, whereas in lignocellulosic biomass, the primary monosaccharides, on average, are xylose and glucose [121]. Therefore, it is expected that sustainable, bulk fermentation processes will utilise feedstreams containing a large proportion of glucose and/or xylose. To this end, it is important to determine process limitations and biocatalyst behaviour on glucose and xylose in the context of bio-succinic acid production. Such an understanding will help define upper limits on fermentation performance and assist in optimising fermenter design. Furthermore, insight into the behaviour of the microbial host on these model substrates is crucial for process optimisation and to identify potential targets for metabolic engineering of the organism for enhanced succinic acid production.

This chapter is an extension of previous work on continuous succinic acid production by *A. succinogenes* where glucose was used as the substrate [15]. Here, the hemicellulose-derived, C_5 monosaccharide – xylose – is used as the substrate in similar continuous biofilm fermentations and the results are compared to the previous study on glucose. In particular, mass and redox balances are used to analyse the fermentation data under steady-state conditions across three different dilution rates. Furthermore, attempts are made to reconcile the observed metabolic activity with the expected central metabolism of the organism. The majority of the content in this chapter formed part of work published under Bradfield & Nicol in *Bioprocess and Biosystems Engineering* [122].

3.1 EXPERIMENTAL

3.1.1 THE CONTINUOUS, EXTERNALLY RECYCLED BIOFILM REACTOR

A custom, externally recycled bioreactor/fermenter (Figure 3.1) was used for the continuous xylose fermentations. The reactor consisted of a glass cylinder enclosed by an aluminium base and head. Mixing was achieved by circulation of the fermentation broth through an external recycle line connected at the base of the reactor and suspended into the centre of the reactor body via the reactor head. Flow through the recycle line was maintained at rates between 500 and 700 mL min^{-1} (100 to 140 rpm) by a Watson-Marlow 323S (Watson-Marlow, UK) peristaltic pump fitted with a 313D pump head. The operational or design volume of the reactor was held constant at approximately 360 mL by controlling the liquid level using an overflow tube connected to an outlet pump. The outlet pump also served as a seal between the reactor and the environment, contributing to system sterility. To prevent airborne contaminants from entering the system, 0.2-µm Midisart 2000 PTFE membrane filters (Sartorius, Germany) were fitted to all vents and gas inlets.

Support structures were included in the fermenter to increase cell density by providing increased surface area for biofilm attachment, growth and stability. The supports included tightly bound wooden sticks (run 1), silicone-tubing segments (run 2) and loosely spaced wooden sticks (run 3). Different types of supports were used in each of the three xylose fermentations (3.1.5) in an attempt to overcome blockages of the system due to excessive biofilm growth. All supports were cleaned with distilled water and dried prior to insertion. A distributor plate was inserted above the region containing the support structures to contain the supports and provide a liquid head for volume and foam control.

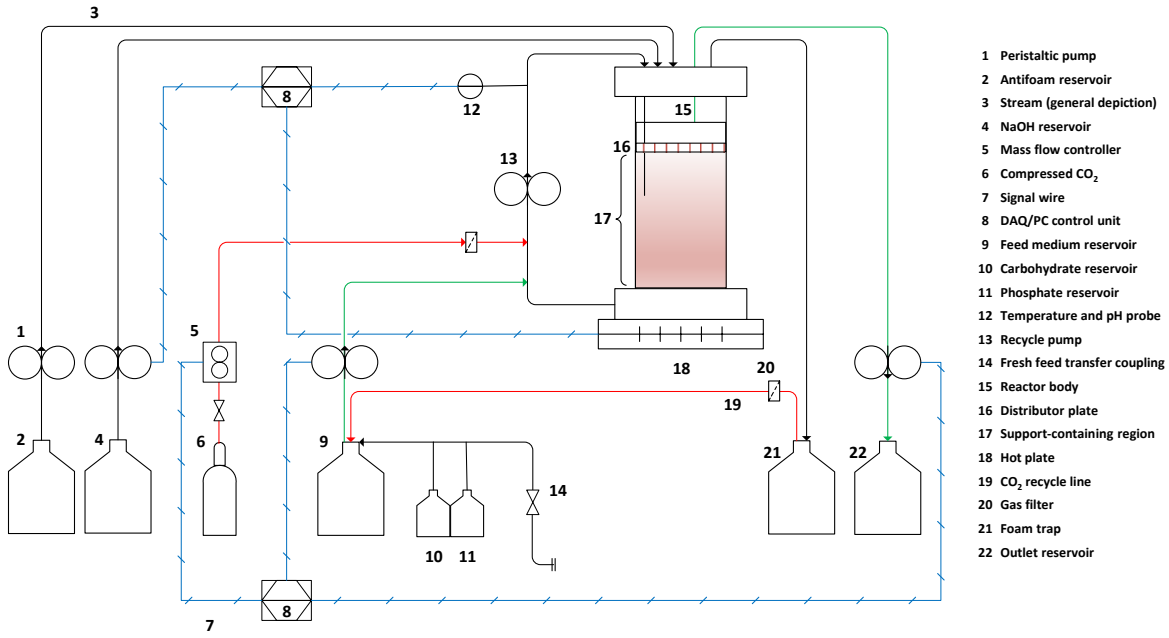

Figure 3.1. Schematic of the continuous, externally recycled biofilm reactor. Not to scale. For simplicity, not all gas vents are shown.

Temperature and pH were measured by a Ceragel CPS71D glass electrode (Endress+Hauser, Germany) housed in an aluminium holder connected within the recycle line. The electrode was coupled to a Liquiline CM442 unit (Endress+Hauser, Germany) which processed analogue and digital signals. Feed medium and CO_2 gas (Afrox, South Africa) were fed directly into the recycle line to enhance mixing and dissolution of gas. In addition, undissolved CO_2 gas venting the system via the foam trap was recycled to the feed reservoir to establish a CO_2 head, thereby driving CO_2 saturation of the feed and displacing any residual air in the reservoir headspace (molar mass CO_2 > molar mass air) which assisted in maintaining anaerobic conditions. Concentrated NaOH (10 M), used for pH control, was dosed directly into the fermentation broth through a continuous Marprene tube via the reactor head to avoid contact with the aluminium components, as concentrated NaOH readily corrodes aluminium (i.e. $2Al + 2NaOH + 2H_2O \rightarrow 2NaAlO_2 + 3H_2$). A 10% v/v solution of Antifoam SE-15 (Sigma-Aldrich, Germany) was added in a dropwise fashion via the reactor head to supress foam when needed. Antifoam selection is described in 3.1.8 below. It was observed that antifoam is most effective when fed directly onto a foam formation.

The reactor system (reactor, fittings, feed, antifoam and bottles), excluding the highly corrosive NaOH solution, was autoclaved at 121 °C for 60 min. The three components of the feed (3.1.3 below) were contained in separate bottles to prevent unwanted interactions during autoclaving, such as Maillard reactions and the precipitation of metal ions by phosphates. After inoculation (~10 mL seed culture; 3.1.4 below), the fermenter was operated in batch mode to increase cell density and then

switched to continuous mode at a low dilution rate (0.05 h^{-1}) to avoid cell washout while decreasing the concentration of acids. Once a stable biomass population was established (as determined by reactor productivity), the dilution rate was increased to between 0.1 h^{-1} and 0.3 h^{-1} to accelerate the formation of biofilm. Online replenishment of feed was achieved as described in [123] where a U-coupling comprising a double-valve system was sterilised in oil at 140 °C and served as a link between a replenishment reservoir and the main feed reservoir.

3.1.2 CONTROL AND MONITORING

Control and monitoring of the fermentation system were centralised around a cDAQ-9184 (National Instruments, USA) data acquisition device linked to a desktop computer running a custom LabVIEW™ program. A current output module (NI 9265; National Instruments, USA), and a voltage and current input module (NI 9207; National Instruments, USA) communicated with instrumentation through analogue control signals (4 – 20 mA; 0 – 5 V). All signals were processed and logged in the LabVIEW™ program. The control system managed pH, temperature, feed and exit pump speeds, and CO_2 flow rates. In addition, the system provided a real-time calculation of the average base flow rate which essentially reflects acid productivity and can be used to estimate succinic acid productivity [38,123]. Furthermore, since base and antifoam addition dilute the feed entering the reactor, the average base and antifoam flow rates are used to determine the extent of dilution which is used to adjust the concentrations of components in the feed medium. The dilution adjustment is crucial to the accuracy of the mass balances.

pH and temperature were controlled at 6.80 ± 0.01 and 37.0 ± 0.1 °C respectively. pH was controlled by means of an on-off strategy where an internal relay in the Liquiline unit controlled the dosing of a 10-N NaOH solution based on feedback from the pH electrode. The speed of the dosing pump was controlled by LabVIEW™ in an attempt to maintain an average dosing time-fraction of “50% on” to avoid crystallisation of NaOH within the Marprene line. Temperature was controlled by a PID feedback controller developed in LabVIEW™ which determined the duration for which the hotplate situated beneath the reactor base remained “on”. Online controller tuning was performed when needed, especially after changes in the dilution rate. The flow rate of CO_2 gas was controlled at 0.10 vvm by a Brooks 5850S (Brooks, Hungary) mass flow controller with a maximum flow output of 100 mL min^{-1}. The computer used for control was accessible via the internet which allowed for remote adjustment of set points and general monitoring using the TeamViewer remote access application. This is especially useful because continuous processing necessitates long periods of unattended operation.

3.1.3 FERMENTATION MEDIUM

The fermentation or feed medium was consistent with that used in the comparative glucose study [15] and comprised three separate solutions (A, B and C; Table 3.1) based on a simplified version of the formulation of Urbance et al. [33]. The sodium/potassium phosphate buffer of Urbance et al. [33] was replaced by a purely potassium-based buffer to reduce the sodium concentration in the fermentation broth since NaOH was used for pH control. Corn steep liquor (CSL) was clarified by heating a 200-g L^{-1} solution of stock CSL at 105 °C for 15 min, then cooling at 4 °C until the solids had settled out. The resulting supernatant was used as the "clarified" CSL and stored at 4 °C.

Table 3.1. Medium composition used for the continuous xylose fermentations. All chemicals were obtained from Merck KgaA (Germany), unless stated otherwise.

Component	Concentration (g L^{-1})
A. Nitrogen, salts and nutrients	
NaCl	1.0
$MgCl_2 \cdot 6H_2O$	0.2
$CaCl_2 \cdot 6H_2O$	0.2
Sodium acetate	1.36
Clarified corn steep liquor (Sigma-Aldrich)	10.0
Yeast extract	6.0
Antifoam SE-15 (Sigma-Aldrich)	0.5 mL/L
$Na_2S \cdot 9H_2O$*	0.36
B. Phosphates	
KH_2PO_4	3.2
K_2HPO_4	1.6
C. Substrate	
Xylose	50-85

*Used initially to assist with anoxic conditions in the feed, but removed once recycling of CO_2 into the feed reservoir was applied.

3.1.4 THE MICROORGANISM

Actinobacillus succinogenes 130Z (DSM 22257; ATCC 55618) [30] was acquired from the German Collection of Microorganisms and Cell Cultures (DSMZ). Cultures were maintained in 66 % w/w glycerol solutions at -40 °C for medium-terms and in tryptone soy broth (TSB) suspensions at 4 °C for short-terms. Inoculum was incubated at 37 °C and 150 rpm for 16 – 24 h in 30 mL sealed vials containing 15 mL sterilised TSB at 30 g L^{-1}. Prior to inoculation, the inoculum was analysed by HPLC to ensure purity and consistent metabolite distributions. The presence of succinic-, acetic- and

formic acids indicated a viable inoculum, while the presence of lactic acid and/or the absence of succinic acid indicated a spoilt inoculum.

3.1.5 STEADY-STATES

A total of three independent fermentations were performed, each covering dilution rates of 0.05 h^{-1}, 0.10 h^{-1} and 0.30 h^{-1} with a total fermentation time across all three fermentations of approximately 1,500 hours. Steady-states were achieved at each dilution rate in each fermentation. Averages for each output variable (i.e. yield, productivity, titre, etc.) are based on the steady-state results at each dilution rate for each fermentation. In the case where multiple steady-states were obtained at a single dilution rate within a fermentation, the average of these steady-states was used in determining the average for the variable. Using a single set of steady-state data from each fermentation ensured that the overall average was not biased towards any one fermentation and that an equal contribution was made from each fermentation. Standard deviation, calculated using the overall averages from each independent fermentation (three values in total), was used to reflect the variation in each variable. The redox analyses performed on the third fermentation include averages of all the steady-state data within that fermentation.

As per definition of a continuous reactor, only when the system exhibited steady-state behaviour were the samples included in the data sets. Steady-state (or pseudo steady-state) was assumed when (i) the time-averaged NaOH flowrate remained within 5% of a 4-h average and (ii) metabolite and residual xylose concentrations showed fluctuations within 3% over a period of at least two volume turnovers.

3.1.6 MASS BALANCE CALCULATIONS

Mass balances (2.4.1) were performed by calculating the stoichiometric amount of substrate required to produce the measured metabolite concentrations based on elemental balances, and comparing this amount to the actual amount of substrate consumed. The elemental balances were performed on C, H and O between the carbohydrate substrate and the products, since for each element appearing in the substrate, an equal amount must appear in the products. The products comprise all the measured metabolites of the fermentation (i.e. succinic-, acetic-, formic- and pyruvic acid), and H_2O. Since CO_2 can serve as both a substrate and a metabolite, it remains an unknown in the system and its net production or consumption will be reflected in the mass balance solution. The elemental balances in this case provide three equations (C, H and O), and given a system of M products (including CO_2 and H_2O), M-3 specifications (measurements) are required in

order to solve for the unknown metabolite production rates and the corresponding element-balanced substrate consumption rate. The system can be solved using linear algebra techniques. Once the substrate consumption rate is determined, it is divided by the actual (measured) substrate consumption rate and expressed as a percentage that represents the mass balance closure. Note, the accuracy of the mass balance is dependent upon including all the metabolites in the calculation, if metabolites are neglected, the closures will necessarily be lower. In addition, it is important to have accurate estimates of the average base and antifoam flow rates to factor in dilution of the substrate and other components in the feed (3.1.2 above). A generalised approach to elemental balancing is presented in [32].

3.1.7 ANALYTICAL METHODS

Sampling of the reactor was performed on a bed of ice to suppress metabolic activity outside of the reactor and ensure that the composition of the sample represented that of the fermentation broth. The concentrations of organic acids, ethanol and xylose present in the feed medium and fermentation broth were determined by means of high-performance liquid chromatography (HPLC). The HPLC system comprised an Agilent 1260 Infinity HPLC (Agilent Technologies, USA), equipped with a 300 mm x 7.8 mm Aminex HPX-87H ion-exchange column (Bio-Rad Laboratories, USA), and an RI detector. For the first two fermentations, a 5 mM solution of H_2SO_4 at a flowrate of 0.6 mL min^{-1} served as the mobile phase with column and RID temperatures of 60.0 °C and 55.0 °C, respectively. To avoid co-elution of xylose and pyruvate, a more acidic, 20 mM solution of H_2SO_4 (all else equal) was used for the mobile phase in the third fermentation. In the given HPLC system, organic acid retention times decrease with increasing mobile phase acidity, whereas carbohydrate retention times are minimally influenced. It was found that suitable xylose and pyruvic acid separation occurred with a 20 mM H_2SO_4 mobile phase without observable co-elution of other compounds.

3.1.8 ANTIFOAM SELECTION

There are various types of antifoam used for foam suppression in fermentations, yet the properties of each are not well documented and compatibility with a specific microorganism must be determined experimentally. To this end, three antifoam varieties from Sigma-Aldrich were tested on cultures of *A. succinogenes*. Each type of antifoam (A, Y30 and SE-15) was added to a separate 15-mL solution of 30 g L^{-1} TSB with a control containing no antifoam. The solutions were autoclaved, cooled, then inoculated with a stock culture of *A. succinogenes* and incubated at 37 °C overnight. From Figure 3.2 it can be seen that final SA titres are slightly lower in the presence of antifoam, but

there are only minor differences between the different antifoam types. Cultures grown in the presence of SE-15 showed more repeatable succinic acid titres than those of Y30 and when compared to A, resulted in succinic acid titres closer to the control. Furthermore, SE-15 can be repeatedly autoclaved and can be added to the fermentation medium or dosed directly to the

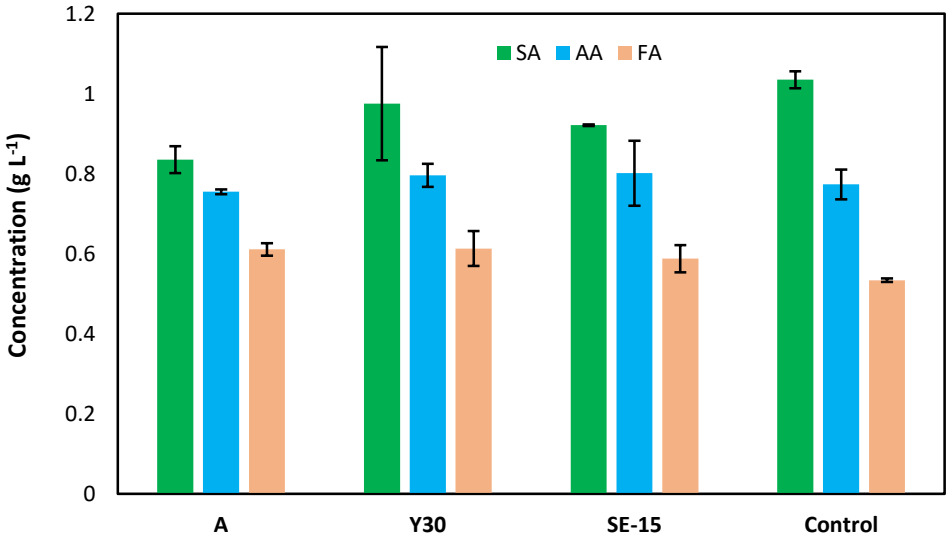

bioreactor as needed. Therefore, SE-15 was selected for fermentation work.

Figure 3.2. Comparison of different antifoam varieties. Experiments were performed in duplicate. SA = succinic acid; AA = acetic acid; FA = formic acid.

3.2 CONTINUOUS XYLOSE FERMENTATIONS

Succinic acid was successfully produced continuously from xylose by *A. succinogenes* in the custom biofilm reactor in three separate fermentations each including dilution rates (D) of 0.05 h^{-1}, 0.10 h^{-1} and 0.30 h^{-1}. The fermentations spanned a total of approximately 1,500 hours cumulatively and showed generally good stability. The only major operational challenge was caused by accumulation of biofilm which led to clogging of the support packing resulting in regions of preferential flow, hence different supports were tried in each fermentation in an attempt to overcome this issue. Erosion or sloughing of the biofilm, known features of biofilm behaviour [124], resulted in disturbances of the steady-states. However, biofilm was able to regrow and once the fermenter had stabilised, steady-states were re-established.

The SA productivity and rate of xylose consumption were similar in all three fermentations (Figure 3.3). Therefore, the performance of the three fermentations can be directly compared despite different types of biofilm supports being employed in each fermentation. Similarly, the rate of glucose consumption in the previous, comparative study [15] compared remarkably well with the

average rate of xylose consumption in this study (Figure 3.4A). Therefore, it is reasonable to make direct comparisons between the two studies despite the use of different packing/support types. As such, it was found that while the rates of xylose and glucose consumption were similar, the SA productivity was noticeably lower for the xylose fermentations (Figure 3.4B) and varied between 1.5 g L^{-1} h^{-1} and 3.4 g L^{-1} h^{-1}. A maximum SA productivity of 3.6 g L^{-1} h^{-1} (single steady-state) was obtained at D = 0.3 h^{-1} which is 18.1% lower than the maximum achieved on glucose (4.4 g L^{-1} h^{-1}) across the same range of dilution rates. The only other prominent pure xylose fermentation study with *A. succinogenes* reports a productivity of 0.54 g L^{-1} h^{-1} [97]. The nearest approximations to pure xylose fermentations are those on lignocellulosic biomass containing high xylose concentrations where the best SA productivities reported are: 0.99 g L^{-1} h^{-1} on acid-pretreated sugarcane bagasse [125], 1.01 g L^{-1} h^{-1} on sugar cane bagasse [110], and 1.21 g L^{-1} h^{-1} on straw hydrolysate [62]. Liang et al. [126] achieved productivities of 2.31 g L^{-1} h^{-1} and 1.69 g L^{-1} h^{-1} on sugar cane bagasse and corn stover hydrolysate, respectively, using engineered strains of *E. coli*. Although fermentation inhibitors may have negatively impacted productivities in these studies, the sugar streams also contained glucose which likely increased SA productivities above that of a pure xylose stream due to the higher yields attainable on glucose, as seen in the comparison made in this study. Importantly, all these studies were conducted in batch or repeat-batch mode and the high productivities achieved in this study highlight the processing benefits of operating continuously. Moreover, the use of biofilm to increase cell densities and enhance productivities is clearly demonstrated in the current study, which is consistent with previous studies on biofilm reactors [127].

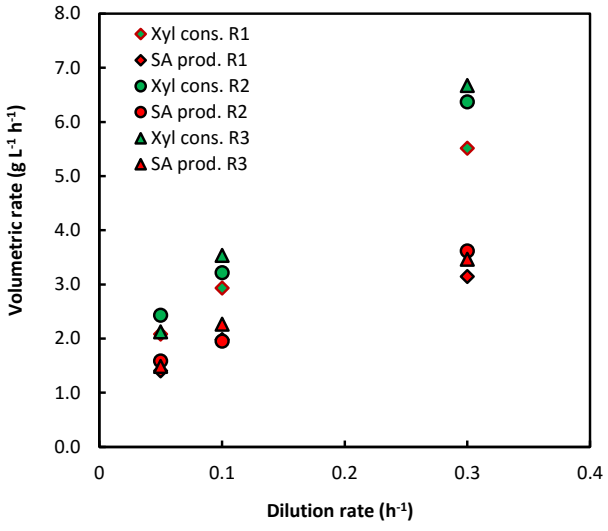

Figure 3.3. Volumetric rate of succinic acid production (*SA prod.*) and xylose consumption (*Xyl cons.*) for all three fermentation runs (*R*). Support types: *R1* tightly bound wooden sticks, *R2* silicone segments, *R3* loosely spaced wooden sticks.

The lower SA productivities on xylose correspond to lower SA concentrations (C_{SA}) (Figure 3.4C), where C_{SA} was between 10.9 g L^{-1} and 29.4 g L^{-1} on average. The acetic acid concentration (C_{AA}) ranged from 3.6 g L^{-1} to 6.0 g L^{-1} (Figure 3.4D) increasing at lower dilution rates but to a lesser extent than in the glucose study, whereas the formic acid concentration (C_{FA}) remained between 2.5 g L^{-1} and 2.8 g L^{-1}. Overall, the metabolite concentrations in the xylose fermentations followed similar trends to those of the glucose fermentations and no ethanol formation was observed. Furthermore, no lactic acid was observed which is in agreement with previous studies on *A. succinogenes* [41,74] and which further contradicts the claims of *A. succinogenes* being an efficient lactate producer [80], as discussed in the Literature section (2.2.1).

The average yield of succinic acid on xylose was between 0.55 g g^{-1} and 0.68 g g^{-1} and increased with decreasing dilution rate (Figure 3.4E). The previous study on xylose reported a yield of 0.76 g g^{-1} in batch mode [97], and similar to the productivity comparison, studies with *A. succinogenes* using xylose-rich lignocellulosic feed streams report higher overall yields (e.g. 0.79 g g^{-1} on sugarcane bagasse hydrolysate [125] and 0.83 g g^{-1} on straw hydrolysate [62]). However, as mentioned before, the lignocellulosic feed streams all contained glucose which likely increased the overall yield above that of pure xylose. More importantly, the SA yield on xylose was substantially lower than that on glucose across all dilution rates which dovetails with the correspondingly lower C_{SA} values in Figure 3.4C. Given that the rate of xylose consumption was similar to that of glucose, a lower SA yield at similar overall by-product concentrations implies that there is mass unaccounted for in the system. In other words, in the xylose runs, C_{SA} together with the by-product concentrations is lower than the equivalent amount in the glucose fermentations and can therefore not account for the total amount of xylose consumed.

The average SA/AA mass ratio (Y_{AASA}), or selectivity to SA (since AA is the major by-product), was higher at lower dilution rates implying that carbon flux to SA increased as the dilution rate decreased (i.e. as acid titres increased), which relates to the higher SA yields at lower dilution rates. Also, Y_{AASA} (3.0 g g^{-1} – 5.0 g g^{-1}) was similar for both xylose and glucose fermentations (Figure 3.4F) which indicates that a similar flux shift towards SA occurred with both substrates. Similar to the glucose study, the FA/AA mass ratio (Y_{AAFA}) on xylose showed a decreasing trend with decreasing dilution rate, but to a lesser extent, which corresponds to the trend in C_{FA}. A decrease in Y_{AAFA} implies that pyruvate dehydrogenase and/or formate dehydrogenase activity is greater at lower dilution rates as detailed in previous continuous fermentations on glucose by *A. succinogenes* [13,15]. However, the dehydrogenase activity appears to be lower in the case of xylose since Y_{AAFA} does not decrease to the same extent as in the glucose study.

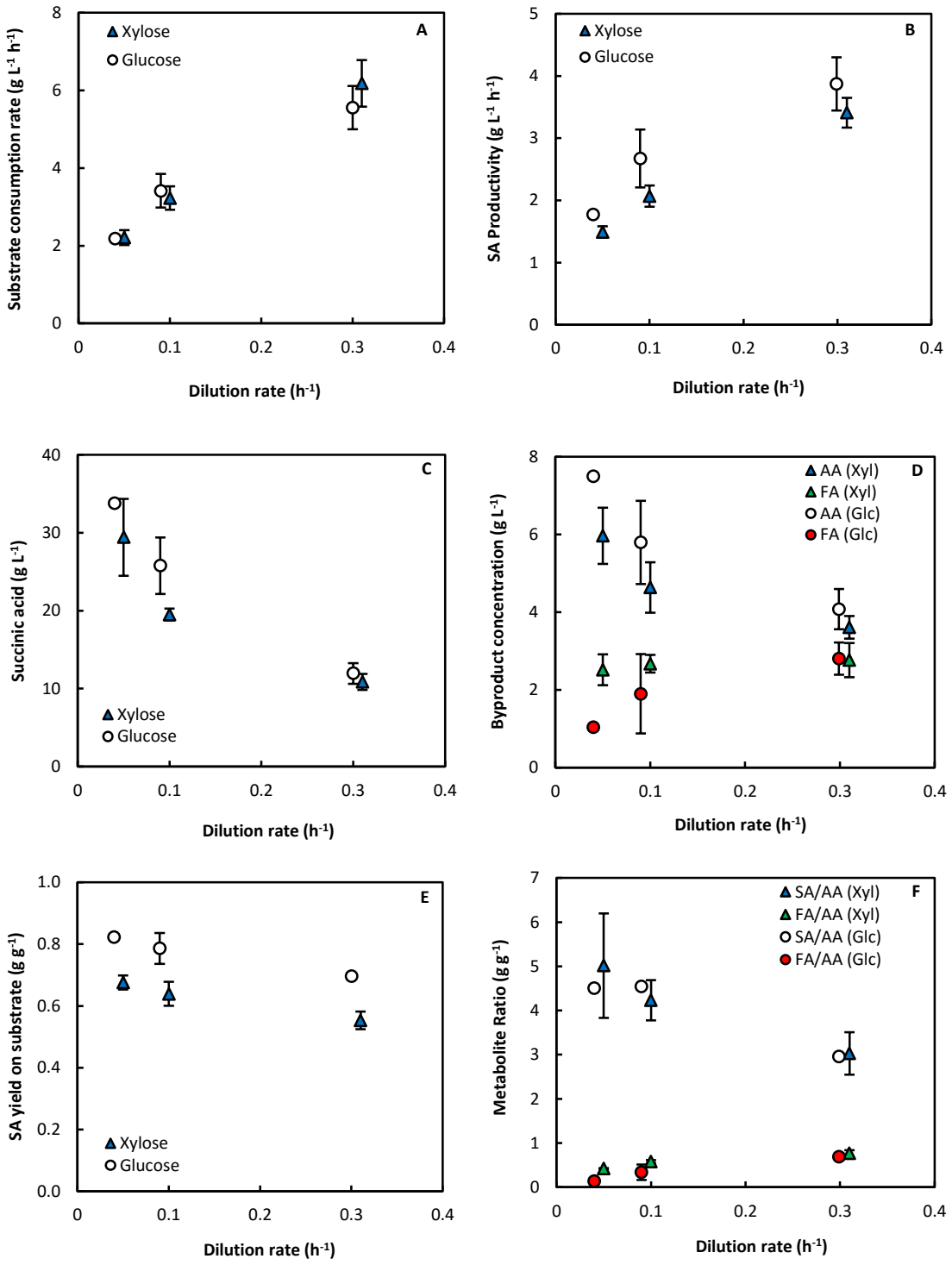

Figure 3.4. Comparison of continuous xylose and glucose fermentations. For xylose, each *data point* represents the average of the steady-states at each dilution rate for all three fermentations. Glucose data are from [15]. *Error bars* represent the standard deviation (σ) for each data set. Where *error bars* are not visible, the markers are covering the bars and σ is small. Xylose (*Xyl*) and glucose (*Glc*) runs were performed at the same dilution rates, but the glucose data sets are shifted to the left on the x-axis in each graph to compare the error bars more clearly with those of xylose. *SA*: succinic acid, *AA*: acetic acid, *FA*: formic acid. Only steady-state data points are included.

Regarding the stability and time-course of the fermentations, it can be seen that once stable biofilm was achieved, steady-state conditions remained fairly stable in terms of productivity (Figure 3.5A) and yield (Figure 3.5B), especially at the lower dilution rates. At D = 0.3 h^{-1} there appears to be more scatter in the variables (last two points at 0.3 h^{-1}), most likely due to biofilm development under lower acid titres, where sections of biofilm detached along with regions of gradual regrowth. It is interesting to note that steady-states at D = 0.05 h^{-1} were essentially repeatable at three distinct time intervals during the fermentation.

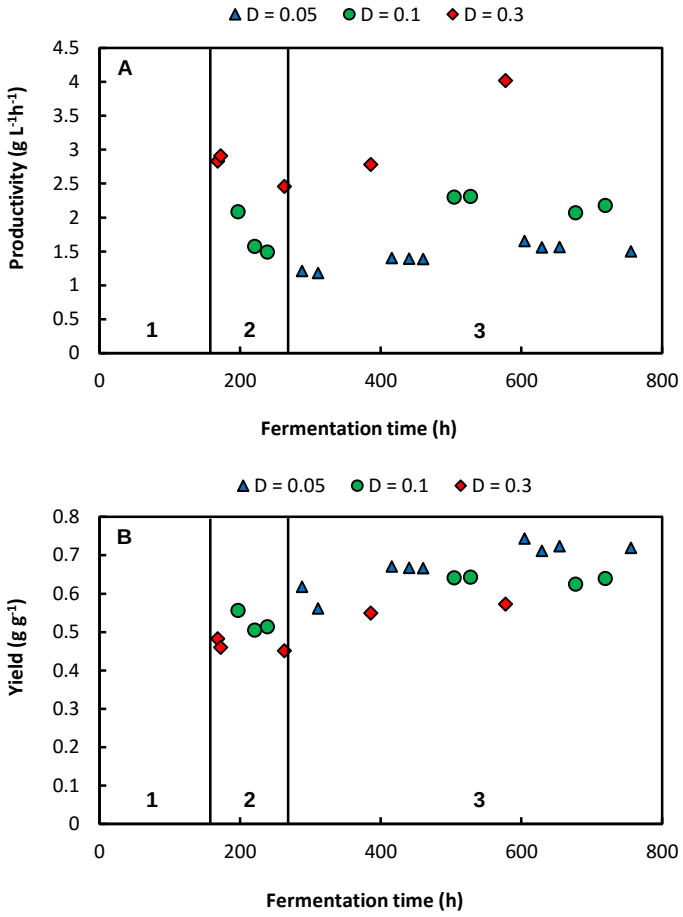

Figure 3.5. Time profile of the third xylose fermentation for (A) succinic acid productivity and (B) succinic acid yield on xylose. In each figure, *region 1* represents the start-up and biofilm growth phase, *region 2* shows a disturbance causing loss of productivity and a decrease in yield, and *region 3* is where stable operation and steady-states were achieved. Not all data points are under steady-state conditions and only representative data are included to highlight the overall trend of the fermentation. In addition, dilution rates were varied and repeated during the fermentation.

3.3 MASS AND REDOX BALANCES

While the results of section 3.2 above are valuable from a processing standpoint and suggest that *A. succinogenes* can effectively convert a xylose-rich feedstock to SA, it is instructive to further understand the differences between the xylose and glucose fermentations. To investigate the yield

differences between the two fermentations, and the possibility of unaccounted mass as suggested above, the mass balances of each system were compared. Mass balances were performed by calculating the stoichiometric amount of substrate required to produce the measured metabolite concentrations based on elemental balances, and comparing this amount to the actual amount of substrate consumed (see 3.1.6). The mass balance closures were found to be lower for the xylose fermentations (Table 3.2). The previously mentioned studies on xylose-containing fermentations by *A. succinogenes* do not interpret the results using mass balances and are performed exclusively in batch reactors where mass balances cannot be accurately performed, therefore no mass balance comparisons are available.

Table 3.2. Fermentation data for the glucose and xylose studies, including mass balance closures.

Substrate	D (h^{-1})	Mass balance closure (%)	Substrate consumed ($g\ L^{-1}$)	C_{SA} ($g\ L^{-1}$)	C_{AA} ($g\ L^{-1}$)	C_{FA} ($g\ L^{-1}$)
Xylose*	0.05	73.0	46.5	30.8	5.5	2.3
	0.1	74.4	29.8	19.1	4.3	2.6
	0.3	74.6	18.7	10.7	3.5	2.7
Glucose	0.05	90.9	41.7	33.8	7.5	1.0
	0.1	89.0	33.0	25.8	5.8	1.9
	0.3	91.2	17.1	11.9	4.1	2.8

*The xylose data are for the first two fermentations only.

Incomplete mass balance closures can be attributed to undetected metabolites or biomass growth when no dry cell weight (DCW) measurements are included in the mass balance. In biofilm fermentations, cell mass accumulates in the fermenter [127], and erosion and sloughing of biofilm [124] cause segments to exit the fermenter unpredictably. As such, DCW measurements either do not account for biomass incorporated into the biofilm or contain biofilm fragments of accumulated biomass that overestimate mass measurements, therefore DCW in a biofilm reactor is not a true reflection of biomass growth or suspended cell concentrations. Consequently, it is difficult to determine the amount of substrate used for biomass growth at steady-state during a biofilm fermentation. However, the growth rate of *A. succinogenes* has been shown to decrease significantly with increasing C_{SA} due to product inhibition and becomes negligible beyond a C_{SA} of 15 g L^{-1} in continuous fermentations [16], and cell growth terminates at a C_{SA} of around 13 g L^{-1} in batch fermentations [35]. In addition, it has been shown that over extended periods of steady-state operation (96 h) in a biofilm fermentation with *A. succinogenes*, DCWs were low on average (0.19 g L^{-1}) compared to the average amount of glucose consumed (42 g L^{-1}) [15] and so at most 0.45% of

the glucose consumed was used for biomass. In light of these two observations, and considering that C_{SA} was between 10.9 g L^{-1} and 29.4 g L^{-1} throughout this study (including the third fermentation), it was assumed that substrate consumption through biomass growth was negligible. Any contribution of biomass growth to the overall mass balance would be more apparent at high dilution rates (e.g. 0.3 h^{-1}) where C_{SA} is lower (10.9 g L^{-1}), however mass balance closures were similar across all dilution rates (Table 3.2). As such, it was assumed that biomass growth at steady-state had a negligible contribution to the mass balance across all dilution rates and it was suspected that an undetected metabolite was produced.

An undetected metabolite implies that either an intermediate metabolite in the established central metabolism is being excreted or alternative metabolic pathways are active. *A. succinogenes* lacks a complete TCA cycle due to the absence of the genes encoding isocitrate dehydrogenase and citrate synthase which form part of the oxidative branch of the TCA cycle [41]. Furthermore, it has been shown that *A. succinogenes* lacks glyoxylate and Entner-Doudoroff pathways [41]. Therefore, the only route of SA synthesis is via the reductive branch of the TCA cycle. Besides succinic acid, the main reported end products during *A. succinogenes* fermentations are acetic acid, formic acid and ethanol [74]. In addition, intermediates in the TCA cycle (i.e. fumarate, malate, oxaloacetate and citrate) have not been observed in previous studies of *A. succinogenes* or in our laboratory, despite a report of citrate lyase activity in *A. succinogenes* cell extracts [74]. α-Ketoglutarate synthesis has also been ruled out [81]. However, Lin et al. [29] reported appreciable pyruvic acid concentrations (~4.8 g L^{-1}) together with succinic-, acetic- and formic acid in batch fermentations of glucose with *A. succinogenes*. Furthermore, Guettler et al. [30] reported small amounts of pyruvic acid when *A. succinogenes* was grown on an enriched medium. Despite good mass balance closures without pyruvic acid production in the comparative glucose fermentations, pyruvic acid was considered a likely candidate for the missing metabolite.

Analysing a known solution of xylose and pyruvic acid by HPLC showed complete co-elution of the two species as seen by a single, enlarged peak on the chromatogram. By applying the same HPLC method as in the first two fermentations, but with a more acidic mobile phase (20 mM versus 5 mM H_2SO_4), it was possible to separate the peaks distinctly. Note, glucose and pyruvic acid do not co-elute when using a 5 mM solution of H_2SO_4 as the mobile phase, therefore if pyruvic acid was present in the comparative glucose study, it would have been detected by HPLC.

Given the new analysis method, a third xylose fermentation was performed. The third fermentation revealed that pyruvic acid was indeed produced at appreciable concentrations at all three dilution rates with an associated improvement in the mass balances compared to the first two fermentations

(Figure 3.6). Note, Figure 3.4 above is based on all three fermentations since none of the fermentation variables, except yield and xylose consumption rate, were influenced by the detection of pyruvate. Yield and xylose consumption rate were marginally affected because residual xylose forms the basis of each calculation and the quantification of residual xylose was impacted by co-elution of pyruvic acid. Fortunately, since high xylose feed concentrations resulted in residual xylose concentrations substantially greater than the detected pyruvic acid concentrations, the presence of pyruvate was shown to negligibly influence the xylose peak area, as seen by similar yields and xylose consumption rates when including and excluding the third fermentation data in the calculation of averages. Differences in the chromatogram response factors of xylose and pyruvate led to the improved mass balance closures.

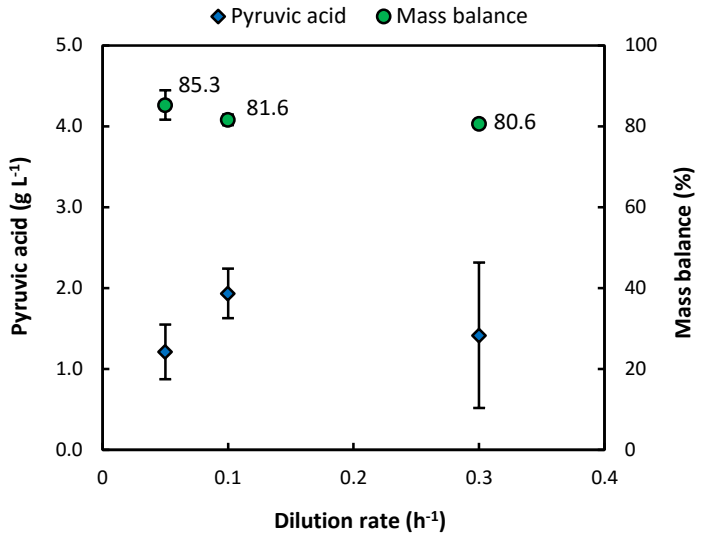

Figure 3.6. Results of the third fermentation where pyruvic acid was detected by a modified HPLC method. Each *point* represents the average of the steady-states achieved at each dilution rate.

Despite the improvement in mass balance closures with the inclusion of pyruvic acid, complete closures were not achieved and closures for xylose data were still poorer than those of the glucose. However, the improvement in mass balance closures, together with a more accurate picture of the metabolite distribution during xylose fermentations, underscores the necessity and utility of performing mass balances on fermentation data. In addition, with an improved view of the active metabolic network of *A. succinogenes* when fermenting xylose, it becomes possible to perform redox balances with better accuracy which are instructive in understanding metabolic flux distributions. These benefits further highlight the advantages of steady-state analysis which is only possible during continuous operation.

Redox balances were performed by considering the NADH contributions from the overall, balanced metabolic pathways that convert xylose to metabolites. The overall pathways can be viewed as either reductive or oxidative, where a net production of NADH in a pathway is viewed as oxidative while a net consumption of NADH is reductive (2.4.2). In a redox balanced system, the net NADH of the oxidative and reductive pathways should be zero. Similar to Equations 2-1 to 2-5, Equations 3-1 to 3-4 give overall pathways for the molar conversion of xylose (Xyl) to excreted metabolites with the associated amounts of NADH. The overall pathways can be further visualised with reference to the expected central metabolic network of *A. succinogenes* when using xylose as the substrate (Figure 3.7), which is a snippet of the more complete central metabolic network (Figure 2.4). Since evidence of pyruvate excretion has been demonstrated in the current study, the network includes a terminal pyruvate branch. An equation for cell growth has been excluded as detailed in the above discussion.

$$\textbf{PDH/FDH}: C_5H_{10}O_5(\text{Xyl}) + \frac{5}{3}H_2O \rightarrow \frac{5}{3}C_2H_4O_2(\text{AA}) + \frac{10}{3}\text{NADH} + \frac{5}{3}CO_2 \quad \textbf{3-1}$$

$$\textbf{PFL}: C_5H_{10}O_5(\text{Xyl}) + \frac{5}{3}H_2O \rightarrow \frac{5}{3}C_2H_4O_2(\text{AA}) + \frac{5}{3}CH_2O_2(\text{FA}) + \frac{5}{3}\text{NADH} \quad \textbf{3-2}$$

$$\textbf{Pyr}: C_5H_{10}O_5(\text{Xyl}) \rightarrow \frac{5}{3}C_3H_4O_3(\text{Pyr}) + \frac{5}{3}\text{NADH} \quad \textbf{3-3}$$

$$\textbf{SA}: C_5H_{10}O_5(\text{Xyl}) + \frac{5}{3}\text{NADH} + \frac{5}{3}CO_2 \rightarrow \frac{5}{3}C_4H_6O_4(\text{SA}) + \frac{5}{3}H_2O \quad \textbf{3-4}$$

Equation 3-1 represents the formation of acetic acid (AA) via the pyruvate dehydrogenase (PDH) route, and Equation 3-2 represents the formation of acetic acid and formic acid (FA) via the pyruvate formate-lyase (PFL) route. If formic acid is further converted to CO_2 and NADH by formate dehydrogenase (FDH), the overall pathway is equivalent to Equation 3-1. Pyruvic acid (Pyr) production followed by excretion is given by Equation 3-3, and succinic acid (SA) formation is represented by Equation 3-4 and involves a net consumption of NADH. Thus, Equations 3-1 to 3-3 can be seen as the oxidative pathways, while Equation 3-4 can be seen as the reductive pathway. Note, in balancing xylose uptake via the non-oxidative pentose phosphate pathway (Figure 3.7), three xylose molecules are converted to two fructose-6-phosphate (F6P) molecules and one glyceraldehyde-3-phosphate molecule, yielding five phosphoenolpyruvate molecules which in turn produce five NADH molecules. Therefore, for each xylose molecule consumed, 5/3 NADH molecules are generated. Performing an NADH balance using the measured metabolites as described here can be seen as a product-based redox balance since the closure is relative to the measured metabolites (products) only.

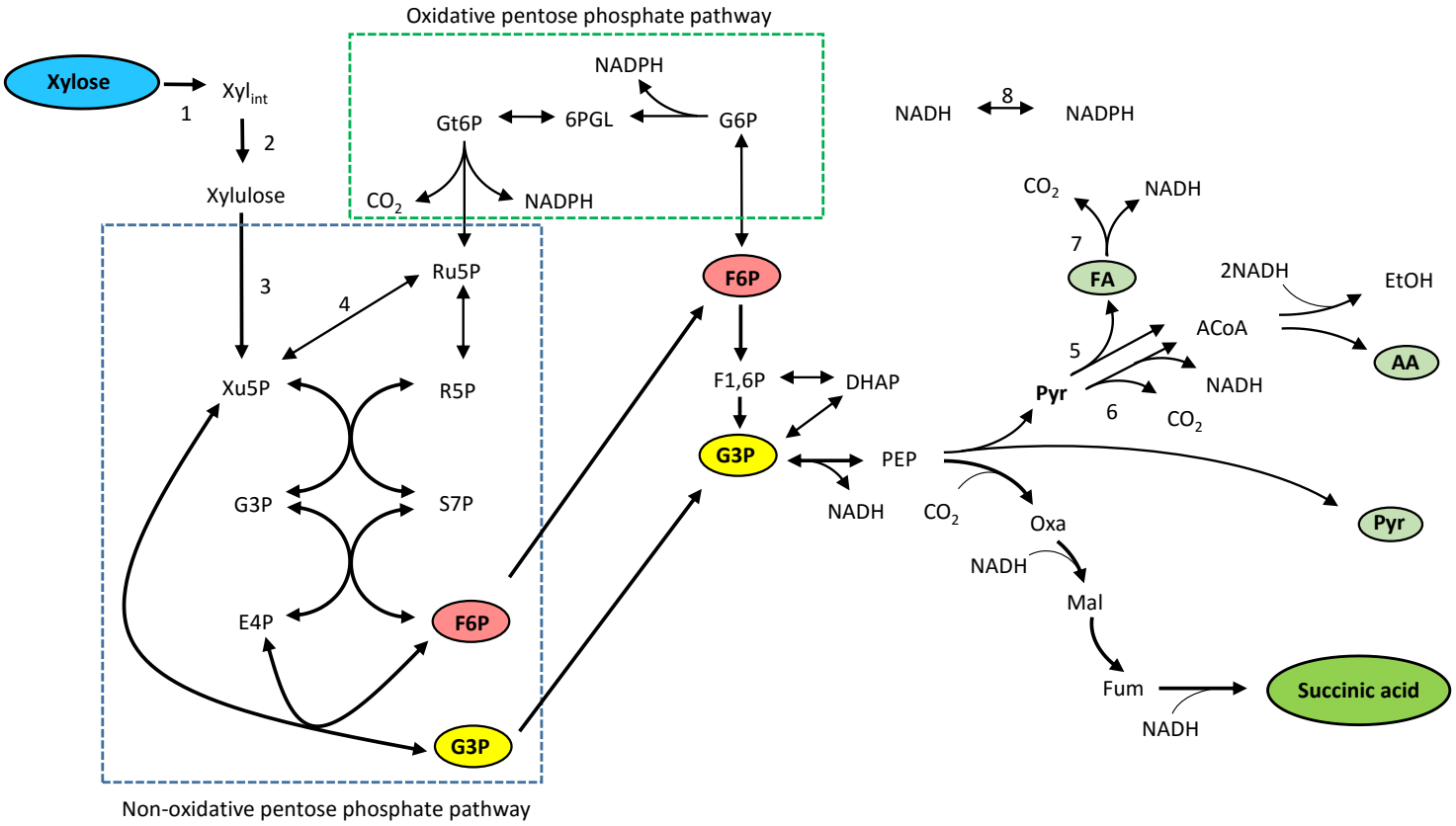

Figure 3.7. Expected central metabolic network of *A. succinogenes* showing the uptake of xylose and subsequent conversion to succinic acid and by-products. The figure is based on insight from the published genome of *A. succinogenes* [41,77,128]. Relevant enzymes with EC numbers: 1 High affinity ATP-dependent xylose transporter (3.6.3.17); 2 xylose isomerase (5.3.1.5); 3 xylulose kinase (2.7.1.17); 4 ribulose-phosphate 3-epimerase (5.1.3.1); 5 pyruvate formate-lyase (2.3.1.54); 6 pyruvate dehydrogenase (1.2.4.1; 1.8.1.4; 2.3.1.12); 7 formate dehydrogenase (1.2.1.2); 8 transhydrogenase (1.6.1.2). *Xyl$_{int}$* intracellular xylose, *Xu5P* xylulose-5-phosphate, *Ru5P* ribulose-5-phosphate, *R5P* ribose-5-phosphate, *G3P* glyceraldehyde-3-phosphate, *S7P* sedoheptulose-7-phosphate, *E4P* erythrose-4-phosphate, *F6P* fructose-6-phosphate, *PEP* phosphoenolpyruvate, *Pyr* pyruvate, *AA* acetic acid, *FA* formic acid, *EtOH* ethanol.

Using the measured metabolite concentrations from each steady-state in the third fermentation (i.e. including pyruvate), the NADH in each pathway was calculated using Equations 3-1 to 3-4, and the produced and consumed NADH amounts were compared. From Figure 3.8A it can be seen that more NADH was consumed than produced and the deviation is more pronounced at increasing amounts of NADH consumption. Furthermore, the deviation increased with decreasing dilution rate (i.e. increasing acid titres) which dovetails with increased Y_{AASA} at lower dilution rates since more carbon is directed towards the reductive, C_4 pathway. The implication of excessive NADH consumption is that the oxidative pathways of the metabolic network (Figure 3.7; excluding the oxidative pentose phosphate pathway for now) are unable to generate the NADH required for the observed amount of SA production. This notion can be visualised in Figure 3.8B where the total amount of xylose consumed in order to satisfy the product-based redox balance (ΔX_r) is compared to the xylose consumed in each pathway based on Equations 3-1 to 3-4 and the corresponding metabolite measurements. Across all dilution rates, the sum of the xylose consumed in each pathway does not account for the total ΔX_r and another pathway ("other pathway") is required in each case to make up the xylose deficit. Moreover, it is precisely this "other pathway" (necessarily oxidative) that supplies the NADH required to close the product-based redox balance.

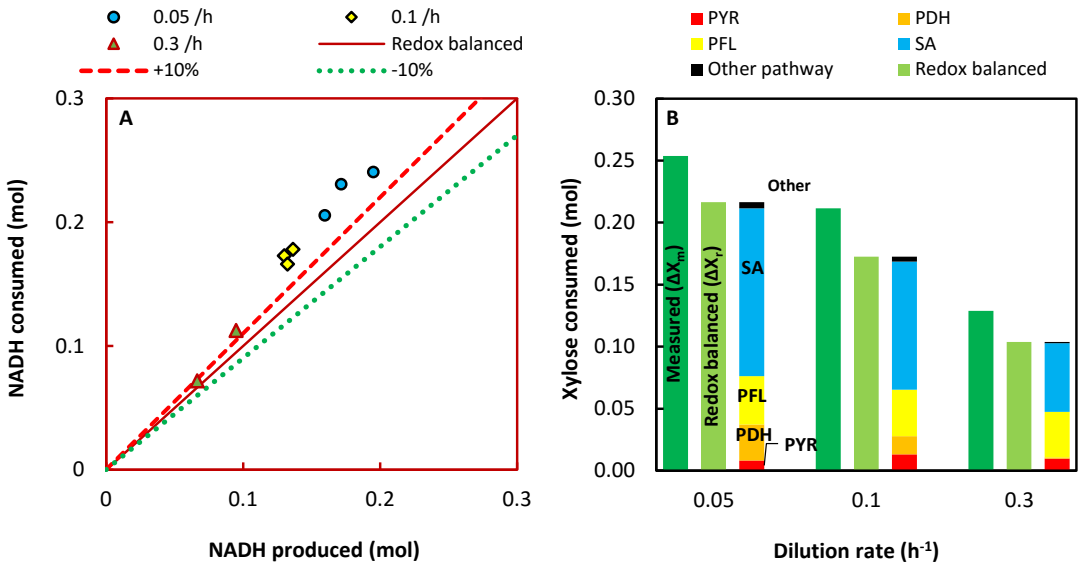

Figure 3.8. Redox balances of the third xylose fermentation. (A) Parity plot of the NADH produced in the oxidative pathways versus the NADH consumed in the reductive pathway for each steady-state across all three dilution rates (0.05, 0.1 and 0.3 h^{-1}), using the excreted metabolite concentrations. In a redox balanced system, the points would lie on the *solid diagonal*. **(B)** A comparison of the actual (measured) xylose consumed (ΔX_m) to the xylose required to satisfy the product-based redox balance (ΔX_r), and the individual contribution of each detected metabolic pathway to xylose. For each dilution rate, the averages of the metabolites and xylose consumed of all the steady-states are used in calculating individual pathway contributions and xylose consumed.

A possible metabolic pathway that can supply reduction power and that is within the metabolism of *A. succinogenes* is the oxidative pentose phosphate pathway (OPPP). The OPPP provides a route

from glycolysis to the non-oxidative pentose phosphate pathway (NPPP) with an associated release of reduction power as NADPH (Figure 3.7). If a fraction of the F6P produced in the NPPP is cycled through the OPPP instead of proceeding through glycolysis, an overall pathway can be defined where xylose is converted to CO_2 and NADPH exclusively (Equation 3-5). Also, since transhydrogenase activity has been detected in *A. succinogenes* [77], the NADPH produced in the OPPP can be oxidised to $NADP^+$ with the associated reduction of NAD^+ to NADH, which can then serve as the unaccounted NADH needed for the observed SA production.

$$\textbf{OPPP}: C_5H_{10}O_5(\text{Xyl}) + 5H_2O \rightarrow 5CO_2 + 10\text{NADPH} \qquad \textbf{3-5}$$

If one assumes that the xylose consumed in the "other pathway" segment occurs via the OPPP, it is possible to re-check the overall redox distribution similar to the calculation in Figure 3.8A, but with the inclusion of the designated OPPP xylose using Equation 3-5. This results in perfect closure of the redox balance and supports the notion that reduction power is generated through the OPPP. Therefore, the OPPP is a likely candidate pathway not only due to its presence in the central metabolism of *A. succinogenes*, but also because it can oxidise xylose to the exact extent needed to satisfy the product-based redox balance. Furthermore, it has been previously shown that carbon flux through the pentose phosphate pathway (PPP) in a mutant strain of *E. coli*, grown on glucose, increased by 325% with increasing succinic acid production resulting from increased CO_2 flow rates [129]. Increased flux through the PPP can be attributed to an increased demand for reduced cofactors at greater CO_2 concentrations. Also, given that the biochemical route of xylose uptake is via the PPP, increased expression of the PPP is expected in xylose fermentations as has been reported with *Saccharomyces cerevisiae* [130] and *Aspergillus niger,* where glucose-6-phosphate dehydrogenase activity was shown to be 92.4% greater in cells grown on xylose compared to those grown on glucose [131].

A further consequence of the stoichiometry of Equation 3-5 is the distinct difference in proportion between the NADH discrepancy (Figure 3.8A) and the “other pathway” segment (Figure 3.8B). Since a single mole of xylose can provide ten moles of NADH (as NADPH), only a minor consumption of carbon via the OPPP would be sufficient to account for the deficit in reduction power. For example, at the highest C_{SA} in this study when D = 0.05 h^{-1} (third fermentation), the OPPP would consume only 2.4% of the total carbon (ΔX_r) to close the redox balance. Therefore, the product-based redox balance can be closed by consuming only a small fraction of xylose in the OPPP. However, this does not close the overall mass balance and the gap between ΔX_r and the actual amount of xylose consumed (ΔX_m) remains (Figure 3.8B).

Given that the HPLC configuration with both mobile phases was capable of detecting all the organic acids in the central metabolism of *A. succinogenes* and no unidentified peaks were observed with no further traces of co-elution, it is unlikely that the unaccounted mass is an organic acid. To this end, it is possible that gaseous CO_2 is the missing metabolite. CO_2 can only be generated by simultaneously forming reduction power via the OPPP - the likely route whereby this is achieved. This implies that excess reduction power will be produced if CO_2 is used to close the mass balance. It is clear from the product distribution that the known pathways cannot consume this additional reduction power and accordingly it must be consumed by an external oxidising agent. Since the fermentations occurred under anaerobic conditions, the oxidising agent would likely be a component within the fermentation medium. One possible candidate is yeast extract since it is known to behave as an external electron acceptor in glycerol fermentations with *A. succinogenes* [132] and could therefore react with reduced cofactors from the cell. If this is the case, then the fraction of carbon (as xylose) consumed in the OPPP would increase from 2.4% to 16.5% in the example above, where the increased consumption translates directly to CO_2 production. Since this increase is considerably high and would necessitate a substantial amount of oxidant in the broth, it is more likely that a smaller fraction of additional carbon is lost as CO_2 via the OPPP, thereby improving but not fully closing the mass balance. The incomplete mass balance is informative and does not detract from the process relevance of the results, rather it invites further investigation on xylose metabolism of *A. succinogenes*.

3.4 CONCLUSIONS

This chapter demonstrates that *A. succinogenes* can successfully and efficiently convert xylose to succinic acid in a continuous, biofilm reactor. Furthermore, succinic acid production on xylose compares well with that on glucose, but lower succinic acid yields, titres and productivities were observed. By-product concentrations on xylose were overall similar to those on glucose, but with lower acetic acid and higher formic acid levels. Akin to glucose fermentations, xylose fermentations displayed incomplete mass balances, but to a larger extent. Pyruvic acid excretion, as detected by a modified HPLC method, improved but did not fully close the mass balances. Furthermore, redox balances of the observed metabolites showed an overconsumption of reduction power, and carbon flux through the oxidative pentose phosphate pathway (OPPP) was shown to be a plausible source of the additional reduction power which affords elevated C_4 pathway flux. However, inclusion of OPPP flux was unable to close the overall mass balance. In this regard, it is possible that a fraction of carbon is lost as CO_2 via an overactive OPPP where oxidation of the additional reduction power

(beyond that needed to close the redox balance) occurs external to the metabolism, possibly by an oxidant in the fermentation medium.

Overall, the results are useful to integrated biorefinery development as they suggest that xylose-rich, lignocellulosic feedstocks, such as corn stover hydrolysate, may be suitable for SA production by *A. succinogenes*. In addition, the results provide a comparative baseline for future work involving more complex, biomass feedstocks. Going forward, process optimisation is essential and a cheaper fermentation medium should be explored (e.g. replacement of yeast extract by corn steep liquor or using spent yeast from ethanol production) as well as the tolerance of the organism to potential inhibitors present in actual biorefinery streams.

4 | THE PENTOSE PHOSPHATE PATHWAY AS A SOURCE OF ADDITIONAL REDUCTION POWER

It has been shown that succinic acid production occurs in preference to the main by-products acetic- and formic acid at elevated succinic acid concentrations under continuous biofilm conditions, resulting in an increase in the succinic acid yield on glucose [15] and xylose (Chapter 3). The improvement in yield has been linked to a shift in metabolic flux distribution where the organism enters a non-growth or stationary phase [16]. Furthermore, mass and redox balance closures based on excreted metabolites, were found to be incomplete under these conditions and no additional metabolites or sources of reduction power were detected. *A. succinogenes* has an incomplete TCA cycle and lacks a glyoxylate shunt [41], therefore by-product formation via fermentative pathways, particularly acetate and formate, is necessary to balance redox in succinate production. However, if there is an associated decrease in by-product formation with increasing SA production, reduction power must be generated elsewhere in the metabolism to sustain flux to SA. To this end, it was hypothesised that the incomplete redox balance closures are due to increased carbon flux through the oxidative pentose phosphate pathway (OPPP). Increased OPPP flux generates reduction power as NADPH which can be converted to NADH by transhydrogenase in *A. succinogenes* [77] and used in the reductive branch of the TCA cycle. The OPPP has the potential to produce the same outcome as a complete TCA cycle or glyoxylate shunt, as it is capable of generating sufficient reduction power for homosuccinate fermentation.

Metabolic flux analysis (MFA) or flux balancing [133], can be used to demonstrate that the OPPP is a plausible explanation for the observed metabolic behaviour. However, MFA alone cannot be used to confirm OPPP flux because CO_2 is the only end-product of the OPPP and CO_2 production is not unique to the OPPP. Therefore, a more direct method is needed to detect OPPP flux. Nevertheless, with available metabolite measurements, MFA can be used to estimate OPPP fluxes and provide a theoretical basis for comparison. As discussed in 2.4, continuous operation is the most suitable mode for MFA [45] as it offers both process and metabolic steady-state conditions. These conditions allow for more accurate and simplified flux analysis compared to batch operation. In addition, continuous operation of biofilm reactors leads to enhanced productivities [127] making it the likely choice for industrial scale succinic acid production by *A. succinogenes*. Therefore, gaining insight into the metabolism of the chosen microbial host under conditions similar to those of bulk scale

production is particularly advantageous as it aids process optimization and hints at potential targets for strain improvement.

In the current chapter, the hypothesis of OPPP flux serving as a source of additional reduction power in continuous glucose and xylose fermentations is explored at four different dilution rates. OPPP flux was qualitatively determined by means of glucose-6-phosphate dehydrogenase assays of biofilm extracts coupled to a kinetic model. In addition, MFA was used to determine the expected or theoretical flux relationships when the OPPP is assumed to supply the reduction power needed to satisfy the redox balance. The flux relationships determined from the kinetic model were then compared to the expected flux relationships to confirm the accuracy of the observed OPPP flux. The majority of the content in this chapter has been included in an article submitted under Bradfield & Nicol to *Applied Microbiology and Biotechnology*.

4.1 EXPERIMENTAL

4.1.1 CONTINUOUS FERMENTATIONS

Fermentations were performed with *A. succinogenes* as prepared in 3.1.4, at dilution rates between 0.02 and 0.3 h^{-1} in a custom, externally-recycled bioreactor system, similar to that used in Chapter 3 (3.1.1). The volume was maintained at 360 mL by means of an overflow tube connected to an exit pump. pH and temperature were controlled at 6.80 ± 0.01 and 37.0 ± 0.1 °C respectively, as detailed in 3.1.2. A 10% v/v solution of Antifoam SE-15 (Sigma-Aldrich, Germany) was dosed onto the liquid headspace as needed. The average flow rates of NaOH and antifoam were determined in real-time over a 4-hr period and used to adjust feed concentrations due to dilution of the feed. Furthermore, the time-profile of the average NaOH flow rate was used in estimating steady-state conditions. CO_2 gas (Afrox, South Africa) was fed directly into the recycle line at 0.1 vvm to ensure CO_2 saturation of the fermentation broth – essential for succinic acid production. To ensure anaerobic conditions, CO_2 venting from the reactor was recycled via the foam trap to the feed medium reservoir to create a CO_2 headspace, ensuring CO_2 saturation of the feed and preventing air from entering the system. The reactor and liquid reservoirs (excluding NaOH) were autoclaved together at 121 °C for 60 min, with the three parts of the feed medium kept separate.

Steady-state conditions were determined from constant metabolite concentrations and a flat NaOH dosing profile, as described in 3.1.5. For each substrate, steady-state conditions at an intermediate succinic acid concentration (~30 g L^{-1}) were performed in duplicate to show repeatability of fermentation performance. The duplicates occurred at the beginning and end of the fermentation. The duplicate for glucose was excluded in the assay analyses because it was taken two weeks after the final steady-state and there appeared to be a substantial amount of dead biomass in the fermenter. As a result, the scrubbed DCW was 212% greater than the initial value, but at an equivalent reactor productivity. The repeat point for the xylose fermentation was taken within four days after the final steady-state and no signs of extensive dead biomass were observed.

To increase cell density in the reactor, four wooden sticks wrapped in mutton cloth and fixed to a top distributor plate were inserted into the reactor (Figure 4.1). The stick structure served as a support surface for biofilm attachment, growth and stability. The number of sticks was limited to four to prevent biofilm overgrowth, blockage of the reactor and obstruction of mass transfer. As a result, less biofilm was present in the fermenter compared to previous fermentations using a similar fermentation setup, including that used in Chapter 3 and in [13,15].

Figure 4.1. The support structure used for biofilm attachment. (A) Biofilm attached to the support structure consisting of four, cloth-bound wooden sticks after termination of the fermentation. **(B)** The same support structure as in (A) after removal of the biofilm revealing the extent of biofilm attachment.

Fermentation medium

The fermentation medium (Table 4.1) was similar to that used in Chapter 3. Sodium acetate was removed from the initial formulation as sodium is present in the form of NaCl and through the addition of NaOH for pH control, and acetate is produced by *A. succinogenes* as acetic acid. Similarly, the concentration of NaCl was reduced to 0.5 g L^{-1}. The concentrations of the phosphates in the potassium phosphate buffer were reduced by half as the concentration used is Chapter 3 was found to be excessive. Corn steep liquor (CSL) was clarified as described in Chapter 3 (3.1.3). The three parts of the fermentation medium (A, B and C) were autoclaved separately and only combined once at ambient temperature to prevent unwanted interactions, such as Maillard reactions and precipitation of metal ions by phosphates.

Table 4.1. Medium composition used for the continuous fermentations. All chemicals were obtained from Merck KgaA, unless stated otherwise.

Component	Concentration (g L^{-1})
A. Nitrogen, salts and nutrients	
NaCl	0.5
$MgCl_2 \cdot 6H_2O$	0.2
$CaCl_2 \cdot 6H_2O$	0.2
Clarified corn steep liquor (Sigma-Aldrich)	10.0
Yeast extract	6.0
Antifoam SE-15 (Sigma-Aldrich)	0.5 mL/L
B. Phosphates	
KH_2PO_4	1.6
K_2HPO_4	0.8
C. Substrate	
Glucose/xylose	60

4.1.2 ANALYTICAL METHODS

Fermentation broth was sampled via the outlet line onto a bed of ice to supress metabolic activity of the cells once outside the fermenter. The concentration of organic acids, ethanol and both carbohydrate substrates present in the feed medium and fermentation broth were measured by means of high-performance liquid chromatography (HPLC). The system comprised an Agilent 1260 Infinity HPLC (Agilent Technologies, USA), equipped with a 300 × 7.8 mm Aminex HPX-87H ion-exchange column (Bio-Rad Laboratories, USA), and an RI detector. Two methods were used for HPLC analysis to overcome co-elution of xylose and pyruvate, as described in 3.1.7. In the first method, a 5-mM solution of H_2SO_4 at a flowrate of 0.6 mL min^{-1} served as the mobile phase with column and RID temperatures of 60.0 and 55.0 °C, respectively. In the second method, a 20-mM solution of H_2SO_4 was used with all other parameters the same as the first method.

Dry cell weight (DCW) was determined by centrifuging a known volume of fermentation broth, washing the resulting cell pellets with distilled water, then centrifuging again and discarding the supernatant. The remaining pellets were dried at 80 °C until constant mass, from which the concentration of cell mass was determined. To minimise the effect of biofilm fluctuations on suspended DCWs, samples were taken for the duration of at least one volume turnover. DCWs were performed on the fermentation broth after biofilm scrubbing to determine the cell content present in the biofilm sample and the enzyme assays. Attempts to separate cells and extracellular polymeric substance from the biofilm showed poor repeatability compared to a previous study [16]. Therefore,

the DCW of scrubbed biofilm was used as a measure of the total biomass content of each sample and was assumed to be an accurate representation of the total biomass content in the reactor.

4.1.3 PREPARATION OF CELL EXTRACTS

In situ removal of biofilm (i.e. scrubbing) was achieved by varying the direction and increasing the speed of the recycle pump to create turbulence, thereby shearing off portions of the attached biofilm. In addition, a magnetic stirrer bar was located below the support structure and activated to increase turbulence during biofilm scrubbing. Biofilm-rich fermentation broth was then extracted from the fermenter via a suction line that ran from the head of the reactor to the lower portion of the support structure, positioned to maximize contact with the wooden sticks and extract biofilm in preference to fermentation broth.

Samples of scrubbed biofilm (40 mL) were centrifuged at 4,000 × *g* for 25 min at room temperature. The resulting cell pellets were combined and resuspended in Tris-HCl (pH 7.4) to a volume of 10 mL. From the 10-mL suspension, three 2-mL samples were centrifuged at 10,000 × *g* for 10 minutes at 4 °C. The resulting cell pellets were then combined and resuspended in Tris-HCL (pH 7.4) to a final volume of 6 mL. The suspension was then disrupted on ice by sonication (Branson 250 probe sonicator, USA) using ten pulsed cycles of 15 s with a 1-minute resting period. The sonicator was set to power level 4 and 40% duty cycle. Cell extracts were then centrifuged at 16,000 × *g* for 30 min at 4 °C. The supernatant containing soluble cell extracts () was then used for enzyme assays.

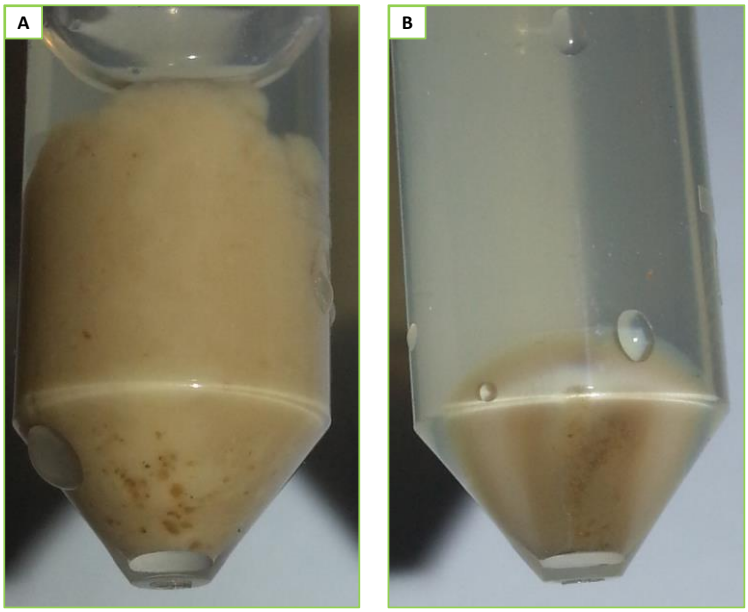

Figure 4.2. Biomass pellets before and after disruption by sonication. (A) Cleaned and centrifuged scrubbed biomass before sonication. **(B)** Centrifuged solution of biomass after sonication. The clearly defined layers present in the cell pellet indicates successful disruption of the cell wall.

4.1.4 ENZYME ASSAYS

The presence and activity of glucose-6-phosphate dehydrogenase (G6PDH) was determined spectrophotometrically by observing the increase in absorbance at 340 nm which corresponds to NADPH production [134]. The assay solution consisted of reaction cocktail, cell extracts and substrate. The reaction cocktail (pH 7.4) consisted of 100 mM glycylglycine buffer (Sigma-Aldrich, Germany), 3.2 mM $NADP^+$ (Melford, UK), and 18 mM $MgCl_2$ (Sigma-Aldrich, Germany). Since phosphoglucose isomerase (PGI) activity interferes with G6PDH activity by reacting with glucose-6-phosphate (G6P), a kinetic model that included both enzymatic reactions was developed. Five different combinations of G6P (Sigma-Aldrich, Germany) and fructose-6-phosphate (F6P) (Sigma-Aldrich, Germany) starting concentrations were used in the assay system (Table 4.2) to fit kinetic parameters to the model.

Enzyme assays were performed in 24-well plates at 37 °C using a SpectraMax Paradigm microplate reader (Molecular Devices, USA). In each assay, reagent cocktail was added to the well first followed by 100 µL of cell extracts, substrate was then added to a final volume of 1.5 mL corresponding to a path length of 1 cm. The volume of reagent cocktail was dependent on the volume of substrate added. Assays were performed in succession at each concentration condition. No change in absorbance was observed when adding cell extracts to reaction cocktail without substrate, which implies that any observed activity was a result of enzyme specificity for the added substrate. Absorbance readings were taken every 15 s over a 10-minute interval at each condition and an extinction coefficient of 6.22 $mM^{-1}cm^{-1}$ was used to relate absorbance readings to NADPH concentration.

Table 4.2. The enzyme assay system used for developing a kinetic model that includes phosphoglucose isomerase and glucose-6-phosphate dehydrogenase activity. Volumes indicate the amount added to the plate well.

Condition	53 mM G6P added (µL)	49 mM F6P added (µL)	[G6P] in assay solution (mM)	[F6P] in assay solution (mM)
Low G6P	10	0	0.35	0
High G6P	300	0	10.63	0
Low F6P	0	10	0	0.33
High F6P	0	300	0	9.87
Equilibrium*	300	100	10.63	3.29

*Equilibrium concentrations for phosphoglucose isomerase are from [135].

4.1.5 MODELS AND COMPUTATIONS

Mass and redox balances were performed as in Chapter 3 (3.1.6 & 3.3). Cell mass as DCWs was also included in the mass balance in this chapter, therefore nitrogen was included in the elemental balance and the standard composition for biomass on a C-mole basis, $CH_{1.8}O_{0.5}N_{0.2}$ [32], was used.

4.1.5.1 FLUX MODEL

Metabolic flux models were developed for glucose (Figure 4.3A) and xylose (Figure 4.3B) based on the established metabolic pathways and the genome of *A. succinogenes* [41,77,128]. A matrix-based description of the metabolic network, as reviewed in [133], was used for metabolic flux analysis of each network. The method entails defining a unique flux (v) for each pathway in the network, on a carbon-mole (C-mole) basis, then using nodal, NADH and stoichiometric balances together with known metabolite production rates to define the system. For the system to be fully defined, the number of equations and specifications must equal the number of fluxes. Since the system is linear, it can be solved by linear algebra techniques using Equation 4-1 [136]. The complete matrix system for each flux model is provided below each model in Figure 4.3.

$$\boldsymbol{S} \times \boldsymbol{v} = \boldsymbol{b} \qquad 4\text{-}1$$

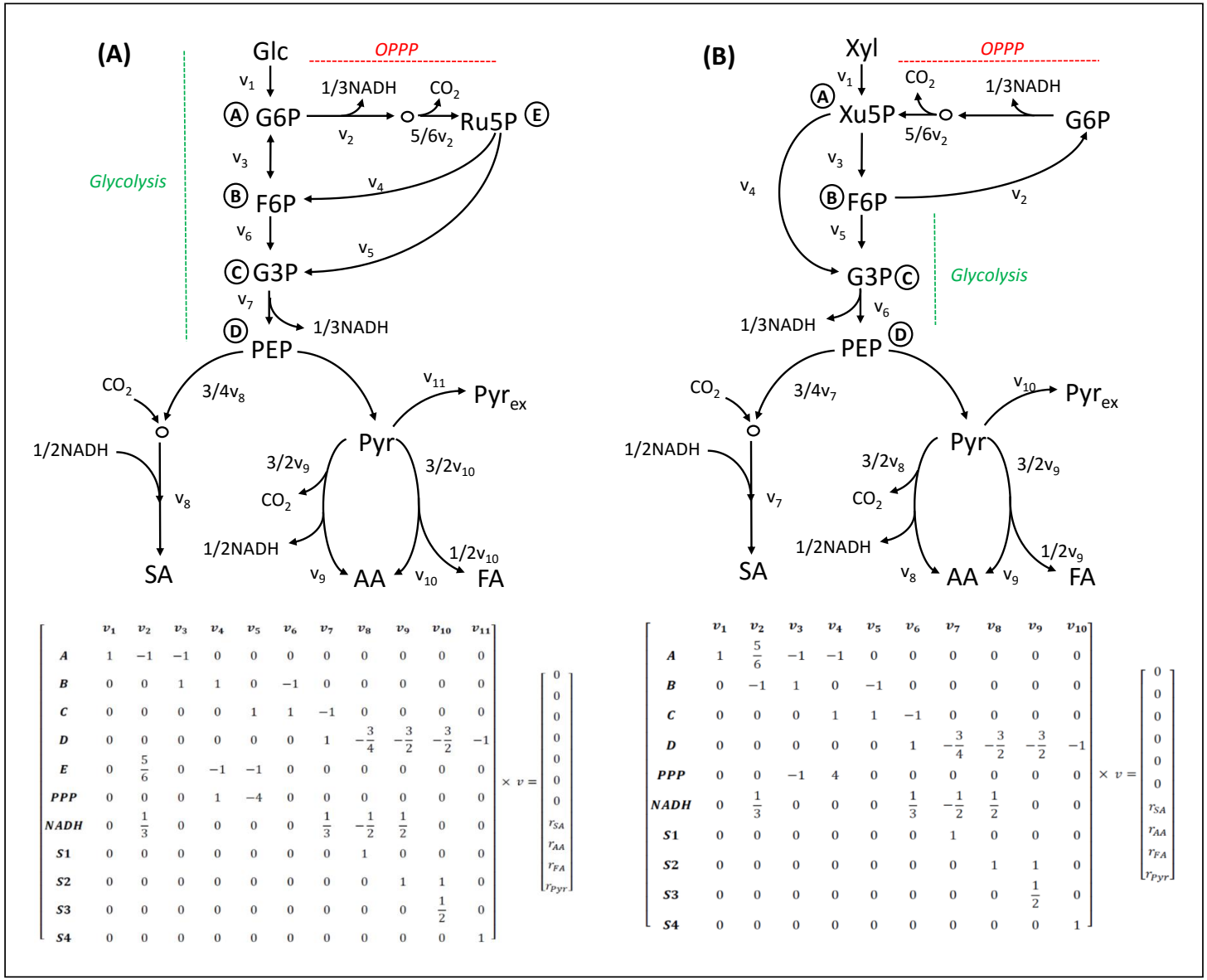

$$\begin{bmatrix} & v_1 & v_2 & v_3 & v_4 & v_5 & v_6 & v_7 & v_8 & v_9 & v_{10} & v_{11} \\ A & 1 & -1 & -1 & 0 & 0 & 0 & 0 & 0 & 0 & 0 & 0 \\ B & 0 & 0 & 1 & 1 & 0 & -1 & 0 & 0 & 0 & 0 & 0 \\ C & 0 & 0 & 0 & 0 & 1 & 1 & -1 & 0 & 0 & 0 & 0 \\ D & 0 & 0 & 0 & 0 & 0 & 0 & 1 & -\frac{3}{4} & -\frac{3}{2} & -\frac{3}{2} & -1 \\ E & 0 & \frac{5}{6} & 0 & -1 & -1 & 0 & 0 & 0 & 0 & 0 & 0 \\ PPP & 0 & 0 & 0 & 1 & -4 & 0 & 0 & 0 & 0 & 0 & 0 \\ NADH & 0 & \frac{1}{3} & 0 & 0 & 0 & 0 & \frac{1}{3} & -\frac{1}{2} & \frac{1}{2} & 0 & 0 \\ S1 & 0 & 0 & 0 & 0 & 0 & 0 & 0 & 1 & 0 & 0 & 0 \\ S2 & 0 & 0 & 0 & 0 & 0 & 0 & 0 & 0 & 1 & 1 & 0 \\ S3 & 0 & 0 & 0 & 0 & 0 & 0 & 0 & 0 & 0 & \frac{1}{2} & 0 \\ S4 & 0 & 0 & 0 & 0 & 0 & 0 & 0 & 0 & 0 & 0 & 1 \end{bmatrix} \times v = \begin{bmatrix} 0 \\ 0 \\ 0 \\ 0 \\ 0 \\ 0 \\ 0 \\ r_{SA} \\ r_{AA} \\ r_{FA} \\ r_{Pyr} \end{bmatrix}$$

$$\begin{bmatrix} & v_1 & v_2 & v_3 & v_4 & v_5 & v_6 & v_7 & v_8 & v_9 & v_{10} \\ A & 1 & \frac{5}{6} & -1 & -1 & 0 & 0 & 0 & 0 & 0 & 0 \\ B & 0 & -1 & 1 & 0 & -1 & 0 & 0 & 0 & 0 & 0 \\ C & 0 & 0 & 0 & 1 & 1 & -1 & 0 & 0 & 0 & 0 \\ D & 0 & 0 & 0 & 0 & 0 & 1 & -\frac{3}{4} & -\frac{3}{2} & -\frac{3}{2} & -1 \\ PPP & 0 & 0 & -1 & 4 & 0 & 0 & 0 & 0 & 0 & 0 \\ NADH & 0 & \frac{1}{3} & 0 & 0 & 0 & \frac{1}{3} & -\frac{1}{2} & \frac{1}{2} & 0 & 0 \\ S1 & 0 & 0 & 0 & 0 & 0 & 0 & 1 & 0 & 0 & 0 \\ S2 & 0 & 0 & 0 & 0 & 0 & 0 & 0 & 1 & 1 & 0 \\ S3 & 0 & 0 & 0 & 0 & 0 & 0 & 0 & 0 & \frac{1}{2} & 0 \\ S4 & 0 & 0 & 0 & 0 & 0 & 0 & 0 & 0 & 0 & 1 \end{bmatrix} \times v = \begin{bmatrix} 0 \\ 0 \\ 0 \\ 0 \\ 0 \\ 0 \\ r_{SA} \\ r_{AA} \\ r_{FA} \\ r_{Pyr} \end{bmatrix}$$

Figure 4.3. Simplified metabolic networks of *A. succinogenes* used for calculating oxidative pentose phosphate pathway flux from experimental metabolite measurements for (A) glucose and (B) xylose. Pathways are based on [41,77,81,128]. Each flux is denoted by *v* and represents the rate of carbon moles through a particular branch of the network. Nodes are given by ringed capital letters. The related matrix system (Equation 4-1) for each network is given below each diagram. In the matrices, *capital letters* correspond to the ringed letters in the diagram and denote nodal balances, *NADH* denotes the redox balance, *PPP* denotes a stoichiometric specification for the pentose phosphate pathway and *S* denotes a metabolite specification. Specifications were given as per the measured metabolite rates (*r*). Not all intermediates are included and biomass formation is excluded. AA acetic acid, FA formic acid, G3P glyceraldehyde-3-phosphate, G6P glucose-6-phosphate, Glc glucose, PEP phosphoenolpyruvate, Pyr pyruvate, Pyr_{ex} extracellular pyruvate, Ru5P ribulose-5-phosphate, SA succinic acid, Xu5P xylulose-5-phosphate, Xyl xylose.

4.1.5.2 ENZYME KINETIC MODEL

The parameters of the Michaelis-Menten model, K_m and V'_{max}, for the G6PDH reaction were determined by fitting the model to the NADPH concentration profiles generated from the enzyme assays. V'_{max} represents the specific reaction rate normalized to cell concentration in the assay for each steady-state. Fits were performed on the entire data set (all five steady-states) for each substrate using non-linear, least-squares optimization in Matlab (*Appendix A: Matlab programme for kinetic fits*). Only data from the first 5 min of each assay was included in each fit to ensure that the $NADP^+$ concentration was sufficiently high and did not influence the rate of the reaction. This allows for a simplified kinetic model where the rate dependency on $NADP^+$ is zero order and therefore can be excluded from the kinetic expression. Glucose data sets were used initially to solve for K_m, which was then fixed in determining the V'_{max} values for the xylose data sets to maintain consistency. The mean absolute percentage error between the model and the experimental data for an entire data set was used to indicate the quality of the fit.

4.2 CONTINUOUS GLUCOSE AND XYLOSE FERMENTATIONS

Similar to previous continuous, biofilm studies on *A. succinogenes* [13,15,16], in the current study, the succinic acid yield on substrate (Figure 4.4A) and the ratio of succinic acid to acetic acid (Y_{AASA}; Figure 4.4B) increased with increasing succinic acid titre (C_{SA}). Furthermore, the formic acid-to-acetic acid ratio (Y_{AAFA}) decreased with increasing C_{SA} (Figure 4.4B), indicating increased pyruvate- or formate dehydrogenase activity [15]. In addition, Y_{AASA} values exceeded the limits defined by the active metabolism where full pyruvate formate-lyase activity allows for a maximum Y_{AASA} value of 1.97 g g^{-1}, while full pyruvate/formate dehydrogenase activity allows for a maximum Y_{AASA} value of 3.93 g g^{-1} [15].

It has been suggested that these trends are linked to a titre-dependent shift in metabolism from a growth to a non-growth or stationary mode [15,16], with associated incomplete closures of mass and redox balances. In the current study, average mass balance closures (Figure 4.5A) were 91% and 84% for glucose and xylose respectively and decreased with increasing C_{SA}, which is in agreement with previous observations. In addition, redox balance closures (Figure 4.5B) showed greater deviations at higher C_{SA} values. Moreover, the shift from growth to non-growth metabolism at increasing titres is exemplified by Figure 4.6 where dry cell weights (DCW) of the fermentation broth decreased with increasing C_{SA}. Samples for determination of suspended DCWs were collected over an extended period to account for biomass fluctuations due to biofilm dynamics. In each fermentation, the duplicate point near a C_{SA} of 30 g L^{-1} showed good repeatability and conformed to

the trend of the other steady-states points. Pyruvic acid concentrations were between 0.80 and 3.21 g L^{-1} for the xylose fermentation and between 0.34 and 0.99 g L^{-1} in the glucose fermentation. SA yields and mass balance closures in the xylose fermentation were distinctly lower than those for glucose, in accordance with previous observations [122].

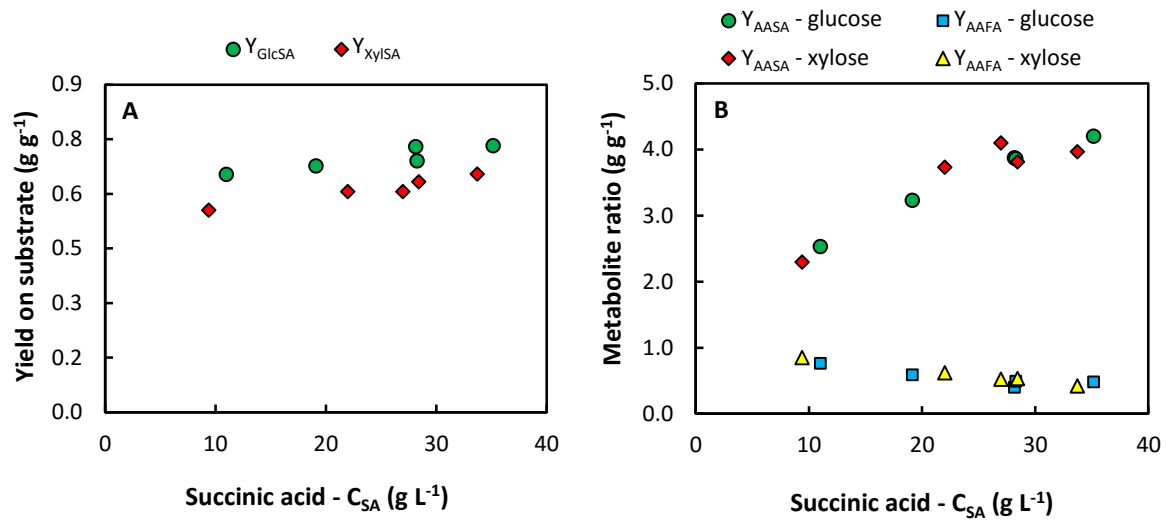

Figure 4.4. Succinic acid yield and metabolite ratios of the continuous fermentations. Similar trends were observed compared to previous studies in **(A)** the yield of succinic acid on glucose (Y_{GlcSA}) and xylose (Y_{XylSA}), and **(B)** the metabolite ratios (Y_{AASA} = succinic acid/acetic acid; Y_{AAFA} = formic acid/acetic acid).

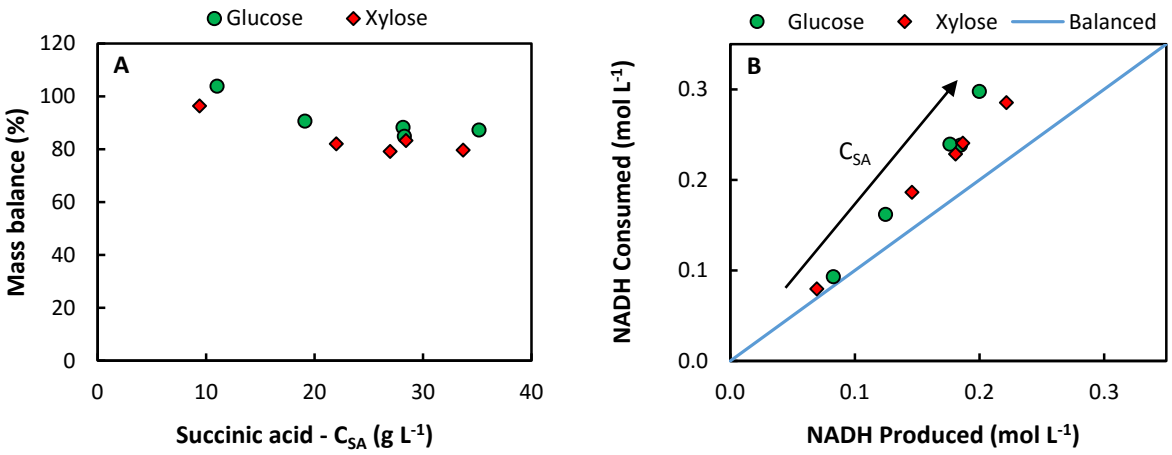

Figure 4.5. Mass and redox balances of the continuous fermentations. (A) Mass balance closures and **(B)** a redox (as NADH) parity plot showed similar trends to previous studies. Production and consumption of NADH are based on overall pathways and metabolite measurements on a molar basis. In **(B)**, the black arrow indicates the direction of increasing succinic acid concentration.

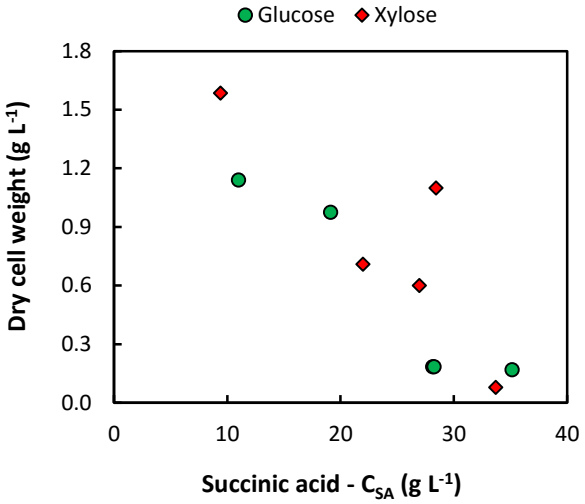

Figure 4.6. Dry cell weights of the continuous fermentations. Dry cell weights were determined from samples with a collection period of at least one volume turnover to account for fluctuations caused by the dynamic nature of biofilm.

The parity plot, that reflects incomplete closure of the redox balance (Figure 4.5B), reveals that more NADH is being consumed in succinic acid production than is being generated by the central metabolic network of *A. succinogenes* based on the concentrations of excreted metabolites (Figure 4.3; excluding the pentose phosphate pathway). Furthermore, the deviation increases with increasing C_{SA}. Biomass is an unlikely source of the additional reduction power since the deviation in the redox balance closure increases as the suspended DCW decreases with increasing C_{SA} (Figure 4.6). Furthermore, biomass (as suspended DCW) only accounts for 0.35% of total glucose consumption when redox balance deviations are at their highest. In addition, *A. succinogenes* has an incomplete TCA cycle, and lacks Entner-Doudoroff and glyoxylate pathways [41], and no additional metabolites or sources of reduction power were detected. These observations are in agreement with previous studies, and together with the limited metabolic network of *A. succinogenes*, led to the hypothesis that the oxidative pentose phosphate pathway (OPPP) is a plausible source of the unaccounted reduction power [15,122,137].

Glycolysis, together with a complete TCA cycle or a glyoxylate shunt, can generate sufficient reduction power to achieve homosuccinate fermentation [25]. The OPPP is also capable of generating the required reduction power for homosuccinate fermentation by carbon cycling between glycolysis and the OPPP [32]. Therefore, there are three routes coupled to glycolysis by which homosuccinate fermentation can be attained with a theoretical maximum yield of succinic acid on glucose of 1.12 g g^{-1} [15]. With regard to the OPPP, homosuccinate fermentation can be achieved if 85.7% of total glucose (on a molar basis) is channelled through the OPPP (Figure 4.7) and back to glycolysis after a minor loss of carbon from the pathway as CO_2. However, there is a net consumption of CO_2 (decrease in the CO_2 yield on glucose) in succinic acid production which

increases with increasing succinic acid yield, or increasing OPPP-to-substrate uptake flux (Figure 4.6), defined here as α for the flux models in Figure 4.3 (Equation 4-2).

$$\alpha = \frac{v_2}{v_1} \qquad 4\text{-}2$$

Therefore, carbon is not lost from the system as CO_2 even though CO_2 is produced concomitant with NADPH production. To further explore the hypothesis, in the current study we performed enzyme assays on cell extracts of biofilm samples taken *in situ* at each dilution rate, to determine the presence of OPPP activity.

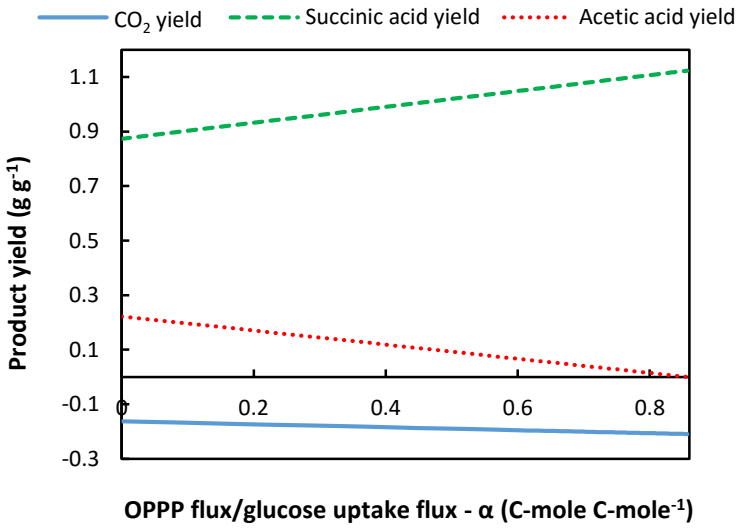

Figure 4.7. The yield of CO_2, succinic acid and acetic acid on glucose as a function of increasing values of α (Equation 4-2). The ratio of fluxes (α) corresponds to Figure 4.3A where a similar matrix system was used. The model assumes exclusive pyruvate dehydrogenase activity (i.e. no pyruvate formate-lyase activity) and no pyruvate excretion, for simplification, and to define the system for maximum CO_2 production. The theoretical maximum yield (homosuccinate fermentation) occurs when 85.7% of total carbon (molar basis) splits to the OPPP from glycolysis. This can be calculated by specifying zero acetic acid formation and solving for α. A decrease in CO_2 yield implies that CO_2 consumption increased with an increase in OPPP flux.

4.3 GLUCOSE-6-PHOSPHATE DEHYDROGENASE AND ENZYME KINETICS

In glucose metabolism, glucose-6-phosphate (G6P) serves as the branch point from glycolysis to the OPPP (Figure 4.3A), while for xylose, G6P forms part of the recycle loop that channels carbon from glycolysis back to the pentose phosphate pathway via the OPPP (Figure 4.3B). In both cases, glucose-6-phosphate dehydrogenase (G6PDH) is involved in catalysing the first reaction of the OPPP (G6P → 6-phosphoglucono-δ-lactone (6PGL), Figure 4.8), consequently the activity of this enzyme provides an indication of the flux through the OPPP. In addition, the reaction converts $NADP^+$ to NADPH allowing the activity of the enzyme to be determined spectrophotometrically [134].

G6P is the required substrate for G6PDH assays, however, since cell extracts contain a number of soluble proteins, phosphoglucose isomerase (PGI) is likely to be present and react with G6P. Therefore, the assay system included F6P and G6P at various concentrations (Table 4.2) in order to develop a kinetic model *in vitro* that would account for the PGI reaction and allow for a more accurate determination of the rate of the G6PDH reaction (Figure 4.8). An additional concern is that 6PGL can be further converted to 6-phosphogluconate (6PG) by lactonase (LAC), which in turn is converted to ribulose-5-phosphate (Ru5P) by 6-phosphogluconate dehydrogenase (6PGDH) with associated formation of NADPH. However, since the G6PDH reaction is conventionally considered the rate limiting step in the OPPP [138], it was assumed that the LAC and 6PGDH reactions were not limiting and relatively instantaneous. Consequently, the rate of NADPH formation was considered to be twice that of the G6PDH reaction to simplify fitting of the kinetic model. In addition, the concentration of $NADP^+$ was maintained in excess to ensure a zero order rate dependency on $NADP^+$, thereby further simplifying the kinetic model.

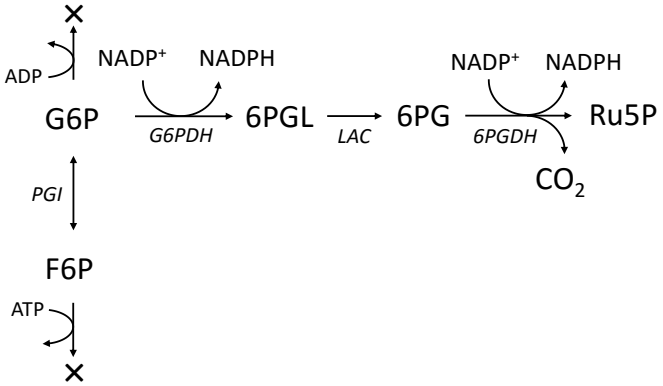

Figure 4.8. Reaction scheme used for developing the kinetic model from the enzyme assays. Reactions could not proceed beyond G6P and F6P in glycolysis as the required cofactors (ADP and ATP) were excluded from the assays. The rates of the LAC and 6PGDH reactions were assumed to be instantaneous relative to the G6PDH reaction since this is considered the rate limiting step of the OPPP. 6PG 6-phosphogluconolactone, 6PGL 6-phosphoglucono-δ-lactone, F6P fructose-6-phosphate, G6P glucose-6-phosphate, Ru5P ribulose-5-phosphate, *6PGDH* 6-phosphogluconate dehydrogenase, *G6PDH* glucose-6-phosphate dehydrogenase, *LAC* lactonase, *PGI* phosphoglucose isomerase.

Michaelis-Menten kinetics were used to model both the G6PDH and the reversible PGI reactions. The hypothesis of OPPP activity implies that the rate of the G6PDH reaction should vary across dilution rates (i.e. different acid titres) and therefore the enzyme concentration and activity will be different in each assay. Furthermore, the DCW for each sample is different and in combination with the differences in enzyme concentration, implies that the maximum specific reaction rate (V'_{max}) is unique for each steady-state condition. Therefore, separate fits are required for V'_{max} at each steady-state. Kinetic parameters for the PGI reaction were obtained from [135], however maximum rates

for the forward and reverse directions were related by the Haldane relationship and remained variable in the model.

G6PDH activity was observed across all steady-state conditions in both glucose (V'_{max} between 8.17 × 10^{-5} and 2.82 × 10^{-4} $mmol_{G6P}$ $g_{cells}^{-1}s^{-1}$) and xylose (V'_{max} between 8.86 × 10^{-5} and 1.47 × 10^{-4} $mmol_{G6P}$ $g_{cells}^{-1}s^{-1}$) fermentations indicating the presence of OPPP flux. Moreover, the presence of G6PDH activity in the xylose fermentations strongly supports the hypothesis, since G6P only features in the OPPP in xylose metabolism, whereas in glucose metabolism, G6P forms part of glycolysis. Therefore, the presence of G6PDH activity under non-growth conditions (as reflected by DCW (Figure 4.6)) indicates that a definite OPPP flux occurred in the xylose-grown cells. Fits of the assay data to the kinetic model gave a mean absolute percentage error of 4.9% and 4.5% across all glucose and xylose data sets respectively (Figure 4.9A). The fitted K_m value of 0.26 mM for G6P was similar to that reported for G6PDH from other bacteria (0.11 mM for *Leuconostoc mesenteroides* [139]; 0.17 mM for *Zymomonas mobilis* [140]).

Furthermore, it was found that the rate of the PGI reaction was substantially greater than that of the G6PDH reaction since the fitted rate constants of the G6PDH reaction were essentially the same for G6P-only and F6P-only starting concentrations, at each of the two concentration levels (Figure 4.9B). This is further confirmed by maximum rates of up to 2500 times greater for the forward PGI reaction compared to the G6PDH reaction, and indicates that the conversion of F6P to G6P is relatively instantaneous. Therefore, the PGI reaction did not have a considerable effect on the rate of the G6PDH reaction, but rapid equilibrium meant that a portion of G6P was constantly being lost to F6P, thus lowering the effective G6P concentration available for the G6PDH reaction.

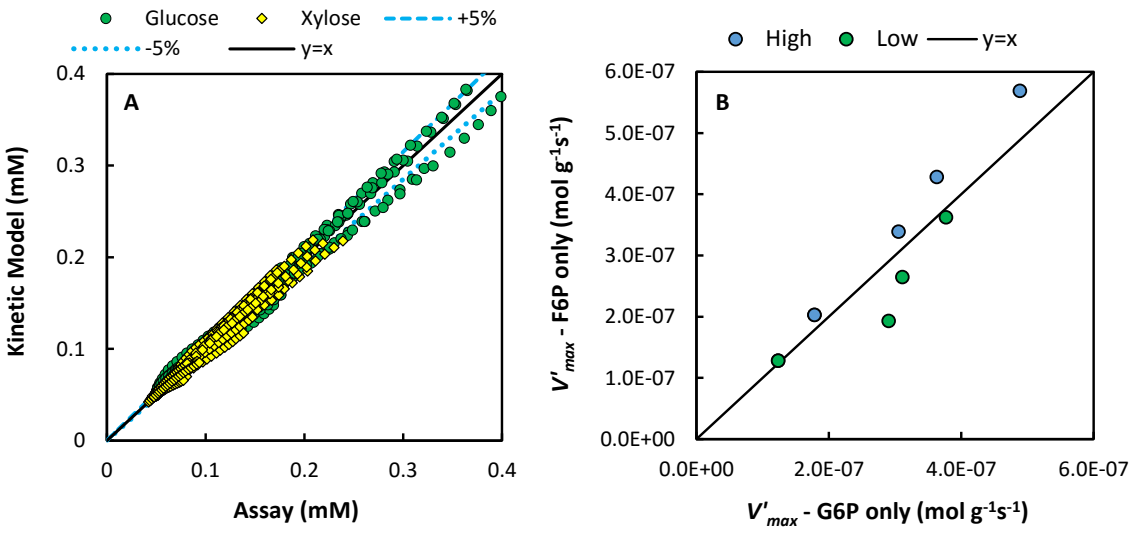

Figure 4.9. Insight into the enzyme assays and the kinetic model for glucose-6-phosphate dehydrogenase. (A) The complete set of modelled and experimental (assay) NADPH concentrations, including a 5% deviation region. The model was fitted to assay readings taken every 15 s over a comparison period of 300 s. **(B)** Comparison of the rate of the G6PDH reaction when using only G6P or only F6P as substrates in the assay for high and low concentration levels of each. For each concentration level, the points of the duplicate dilution rate overlap precisely, therefore only four points are visible for each concentration level, but five points are actually present. The independence of the G6PDH reaction rate on starting substrate implies that the PGI reaction is relatively instantaneous and does not influence the rate of the G6PDH reaction.

4.4 FLUX ANALYSIS AT THE GLUCOSE-6-PHOSPHATE NODE

The maximum specific rates (V'_{max}) for the G6PDH reaction determined from the assays and the kinetic model give an experimental indication of OPPP flux. In addition to the experimental rates, fluxes were determined from metabolic network models for each substrate (Figure 4.3) and the measured metabolite concentrations. The models include the OPPP in order to provide a theoretical reference against which the experimental data can be compared as part of testing the hypothesis. Since overall substrate uptake flux regulates the magnitude of individual pathway fluxes, it is necessary to normalize individual fluxes to substrate uptake flux. To this end, α (Equation 4-2) represents the ratio of OPPP flux to substrate flux (or substrate uptake rate) and gives the theoretical split of carbon into the OPPP at the G6P node on a molar rate basis.

In order to compare the experimentally determined rates to α, it is necessary to use the same basis. The ideal experimental equivalent is to use the biomass based rate of G6P production divided by the biomass based rate of substrate uptake (r'_s; [$mol_{subs}\ g_{biomass}^{-1}\ s^{-1}$]), however, these rates are not explicitly known. Nevertheless, the biomass based G6P rate can be approximated by the experimentally determined specific reaction rate (i.e. V'_{max}), although the true rate is likely to be lower since intracellular metabolite concentrations in the central metabolism (including PPP) of *E. coli* have been shown to be near the K_m value [141]. Also, since the total biomass content in the fermenter (C^f_x) cannot be determined for each steady-state, r'_s is unknown. However, the volumetric

rate of substrate consumption is known (r_s; [mol_{subs} $L_{reactor}^{-1}$ s^{-1}]) which enables the definition of *γ* (Equation 4-3) as an experimental approximation of α:

$$\gamma = \frac{V'_{max}}{r'_s} = \frac{V'_{max}}{r_s} C_x^f \qquad \left[\frac{mol_{G6P}}{mol_{subs}}\right] \qquad \textbf{4-3}$$

Given the uncertainty in both the intracellular metabolite concentrations and C^f_x, a direct quantitative comparison between α and γ is not possible. However, if one assumes that C^f_x is constant and that intracellular intermediate concentrations in the central metabolism are similar across all steady-states, a trend comparison of the experimental and theoretical rate relationships is possible. In Figure 4.10, the two ratios are compared with the underlying assumption that scalar differences between the two y-axes are based on unknowns that remained constant across all steady-states.

The trends in OPPP flux relative to total substrate uptake flux determined from the enzyme kinetic model (*γ*) compare well with the trends from the flux models (*α*) (Figure 4.10). For glucose (Figure 4.10A), the shape and relative magnitudes of α and γ are similar across all C_{SA} values. For xylose (Figure 4.10B), the shapes of the trends are similar but relative magnitudes are different, yet both show an increasing trend with increasing C_{SA}. Importantly, since the experimentally observed flux behaviour on both substrates matches the increasing trend of the flux models, based on the inclusion of the OPPP in the models, it implies that the experimental trends do indeed reflect OPPP flux with the same characteristics as the models. Also, since the trends of the experimental fluxes match those of the models for two independent fermentations using different substrates, the hypothesis of increasing OPPP activity with increasing C_{SA} is strongly supported. Therefore, evidence is provided of OPPP flux leading to the production of additional reduction power in biofilms of *A. succinogenes*.

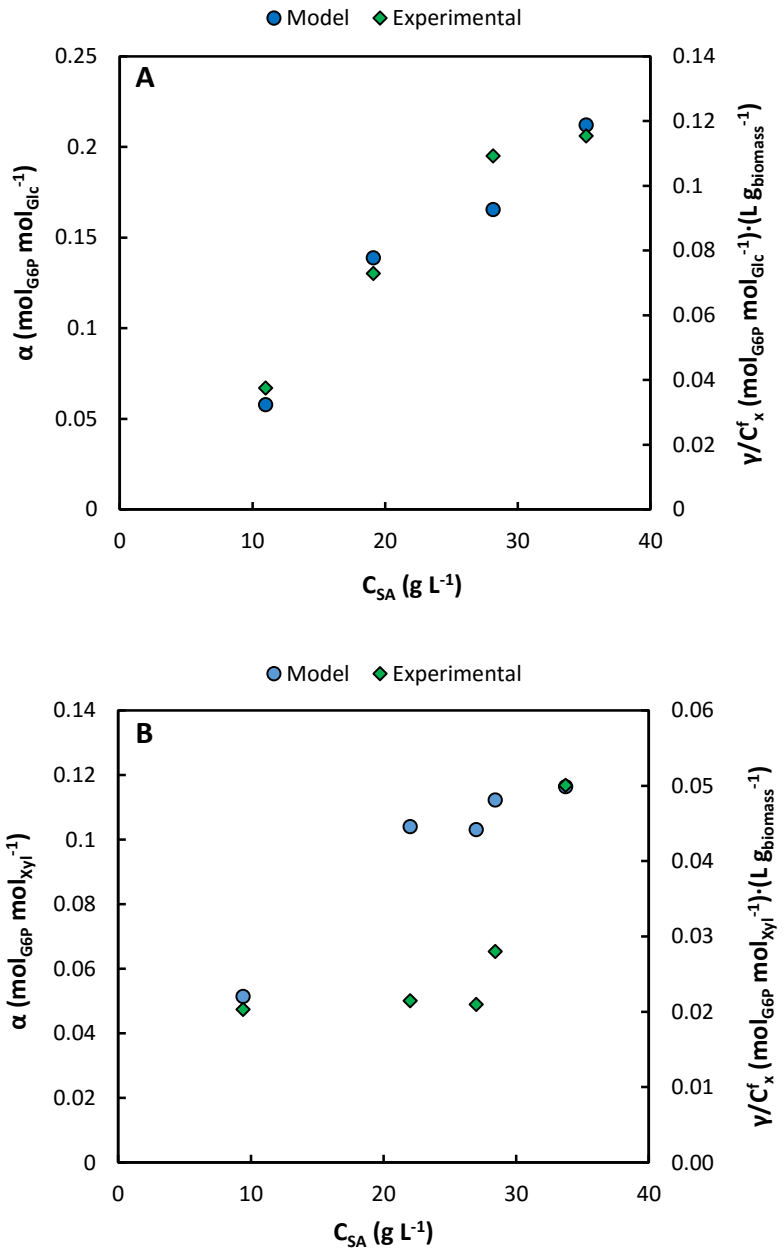

Figure 4.10. Experimental (enzyme kinetic model) and modelled (flux model) ratios of OPPP flux-to-total substrate uptake flux versus succinic acid concentration for (A) glucose and (B) xylose. The experimental flux relationships are represented by γ (Equation 4-3), while those of the flux model are given by α (Equation 4-2) corresponding to the metabolic networks of Figure 1.

The benefits of upregulating OPPP for increased succinic acid production have been demonstrated with genetically modified strains of *A. succinogenes* [44] where G6PDH genes were overexpressed, yet this behaviour has not previously been demonstrated in wild-type *A. succinogenes*. Additionally, to date, no studies have been performed on metabolic flux distributions in non-growing *A. succinogenes* cells. ^{13}C-metabolic flux analysis of growing cells of *A. succinogenes* from batch fermentations gave γ (or α) values of up to 6.9% [128] and 5% [77] on a defined medium. The flux models in the current study give α values between 5.8% and 21.2% for glucose, and 6.2% to 14.0%

for xylose, where values increase with increasing C_{SA}. Therefore, at the low C_{SA} conditions, where growth is minimal yet apparent (Figure 4.6), the flux ratios compare well with the previous studies, however as the cells enter a stationary phase due to growth inhibition at high C_{SA}, flux through the OPPP increases as indicated experimentally. A similar result was observed in [142] where OPPP flux increased by 83% in non-growing cells compared to growing cells of wild-type *Bacillus subtilis*. Under non-growing conditions, γ values in *Bacillus subtilis* cells of up to 64% were observed, suggesting that the values predicted by the models in the current study are reasonable.

Although OPPP activity can lead to closure of the redox balance, the mass balance remains unchanged since the only by-product of the OPPP is CO_2 and there is a net consumption of CO_2 within the system across all ratios of OPPP-to-substrate uptake flux (Figure 4.7). In our previous work, we speculated that if OPPP flux was greater than the amount required to close the redox balance, additional reduced cofactors would be produced which cannot be consumed in the central metabolism. To ensure an overall redox balance of the system, the reduced cofactors must necessarily be oxidized external to the cell, possibly by an electron accepter (oxidising agent) in the feed such as, for example, yeast extract [132]. In such a scenario, CO_2 consumption would be lower and there may be a net production of CO_2 under sufficiently high OPPP fluxes, thereby accounting for the incomplete mass balance. Including an NADH sink in the flux models (Figure 4.3) to account for this effect, showed that the trends in OPPP flux versus substrate uptake flux is essentially the same as those in Figure 8, but the magnitudes are substantially higher. Therefore, our speculation regarding the incomplete mass balance closures may be correct but does not dovetail quantitatively with the results from the current study and more investigation is required.

4.5 CONCLUSIONS

This chapter provides evidence of increased oxidative pentose phosphate pathway (OPPP) flux, relative to overall substrate uptake flux, at increasing acid titres in *A. succinogenes* biofilms under continuous operation. The relative increase in OPPP flux, under non-growth conditions, generates additional reduction power as NADPH which can be converted to NADH by transhydrogenase. Consequently, increased flux through the reductive branch of the TCA cycle is possible which ultimately leads to improved succinic acid yields on substrate. The behaviour was observed for glucose and xylose substrates and compares well with metabolic flux models that include the OPPP. Overall, the results are useful as they suggest potential targets for metabolic engineering of the organism, such as upregulation of the OPPP, and provide insight into the organism under conditions relevant to scaling up of a succinic acid production process based on *A. succinogenes*.

5 | SUCCINIC ACID PRODUCTION ON A XYLOSE-ENRICHED BIOREFINERY STREAM

Chapters 3 and 4 explored production of succinic acid by *A. succinogenes* on two model substrates – xylose and glucose. The results showed that the microbial strain is able to successfully produce SA at competitive productivities, yields and titres on both substrates. While these results are promising, it is important to test the ability of the organism on a more process-relevant feedstream. From the perspective of a lignocellulosic biorefinery, such a stream will be rich in the two model monosaccharides, but will also contain other hemicellulose-derived sugars. In order for a fermentation process to be economically viable, it is essential that the microbial host achieve high yields on all the carbohydrates present in the feedstream. Furthermore, the release of microbial inhibitors during pretreatment such as furfural, hydroxymethylfurfural (HMF), acetic acid, and lignin-derived low molecular weight phenolic compounds is an additional major consideration when developing a biorefinery-relevant fermentation process [143]. The organism must be able to tolerate the inhibitors while still achieving high product yields or the feedstream must be detoxified prior to the fermentation step which will increase process costs.

To date, most studies on *A. succinogenes* that utilise renewable feedstocks lack process-relevant pretreatment methods (i.e. typically batch, autoclave-type reactions with sulphuric acid) and so do not accurately portray realistic biorefinery conditions. A more relevant pretreatment process has been developed which is capable of producing xylose-enriched streams from biomass at the pilot scale by a combination of deacetylation (alkaline wash) and continuous dilute acid pretreatment [83,144,145]. The xylose-enriched stream can then be separated from the residual cellulose-enriched solids [146] and used as a distinct process stream for chemicals or fuels production. Since succinic acid is considered a top value-added, biomass-derived chemical [147], it can serve as a target molecule from microbial conversion of xylose-rich hydrolysates.

To this end, Chapter 5 explores the feasibility of using process-relevant, xylose-enriched, corn stover hydrolysate as a feedstream for succinic acid production by *A. succinogenes,* and forms the more applied component of the thesis. The work in this chapter was conducted in collaboration with the National Renewable Energy Laboratory (NREL; Colorado, USA) and was split into two main parts. In the first part, initial batch work was conducted to determine the behaviour of the organism on

hemicellulose-derived carbohydrates, mock hydrolysates and two actual hydrolysates, namely dilute acid pretreated hydrolysate (DAP-H) and deacetylated, dilute acid pretreated hydrolysate (DDAP-H). The preliminary batch work was published under Salvachua et al. in *Biotechnology for biofuels* [148]. For brevity, this chapter includes only a brief summary of the relevant batch results with reference to the publication.

The second part, which constitutes the main focus and contents of this chapter, sought to (i) increase productivities over the preliminary batch fermentations by employing a continuous, biofilm system and (ii) determine whether the observed yield advantages offered by biofilms of *A. succinogenes* can be achieved on non-detoxified, process-relevant feed streams. Firstly, continuous fermentations of xylose were performed in a custom, stirred, biofilm reactor to establish a performance baseline. Thereafter, detailed continuous fermentations of DDAP-H were performed using the same system across four different dilution rates. Similar to Chapter 3, mass and redox balances were used to determine the completeness of the continuous fermentation data and to interpret the results with respect to the central carbon metabolism of *A. succinogenes*. The continuous work was published under Bradfield et al. in *Biotechnology for biofuels* [137] and forms the bulk of this chapter.

5.1 EXPERIMENTAL

5.1.1 THE CONTINUOUS, STIRRED-TANK BIOFILM REACTOR

Unlike the external-recycle reactor used in Chapter 3 and Chapter 4 (*3.1.1*), here a stirrer-tank reactor was used for the continuous fermentations (Figure 5.1) of *A. succinogenes* (*3.1.4*). The reactor consisted of a 1.6-L BioFlo 3000 unit (New Brunswick Scientific, USA) customised to operate continuously. The working or design volume (overall reactor volume based on the vessel size) was controlled at 1.3 L by means of an overflow tube connected to an exit pump. A liquid-free headspace assisted with foam control. The supply of CO_2 (General Air, USA) gas to the fermenter was controlled manually at a fixed rate of 0.10 vvm by means of a 65-mm aluminium rotameter (Cole-Parmer, USA), and fed through a submerged sparger located beneath the agitation shaft. All gas entering and exiting the fermenter, and venting from reservoirs, passed through Millex-FG 0.2 µm PTFE filters (Millipore, USA) to ensure sterility. Gas venting through the head of the fermenter was passed through a drainable foam trap to prevent blockage of the vent filter. Quantification of foam volume (foam overflow into the foam trap) contributed to overall dilution rate calculations in instances of extensive foaming. Temperature was controlled at 37 ^{o}C by means of a thermocouple, housed within a stainless-steel cover submerged in the fermenter, coupled to a PID controller within the BioFlo system. pH was controlled at 6.80 using a gel-filled 405-DPAS probe (Mettler Toledo, Switzerland) coupled to a PID controller which regulated the dosing of an unsterilised 10 N NaOH solution (Fisher Scientific, USA). A 10% v/v solution of Antifoam SE-15 (Sigma-Aldrich, USA) was dosed as needed into the headspace during operation to suppress foaming.

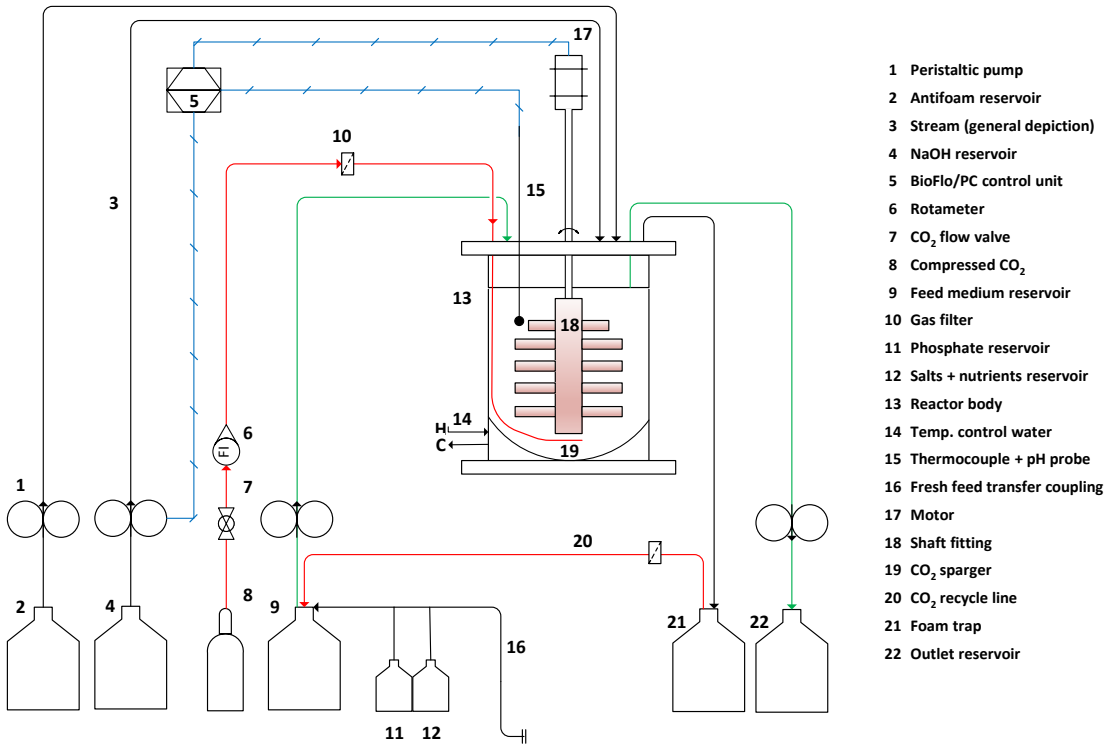

Figure 5.1. Schematic of the continuous, stirred-tank biofilm reactor. Not to scale. For simplicity, not all gas vents are shown and the control integration with the BioFlo unit is simplified. The pH probe and thermocouple are separate units but are represented as a single unit in the figure.

To increase cell density in the reactor through biofilm growth and attachment, a novel agitator fitting was developed (Figure 5.2). The fitting comprised a central porous polypropylene (PP) tube perforated with a multitude of holes into which porous PP or silicone arms were affixed. The central tube was attached to the agitator shaft by means of stainless steel brackets allowing for easy detachment. The basis for the design was to provide additional surface area for biofilm attachment and support whilst achieving sufficient mixing and homogeneity of the fermentation broth through stirring. For example, the surface area-to-volume ratio of the reactor increased from 0.34 cm^2 cm^{-3} (excluding the agitator fitting) to 1.36 cm^2 cm^{-3} and 1.31 cm^2 cm^{-3} when using the silicone and PP fittings (excluding porosity) respectively. In addition, stirring would provide liquid circulation through the protruding arms via the central tube thereby enhancing liquid flow through the internal regions of the fitting. The design was tested in an initial xylose fermentation run, using silicone protruding arms, and due to positive results, it was also employed in the hydrolysate fermentations where porous PP arms were used to further increase surface area since good attachment to the central PP tube was demonstrated in the xylose run.

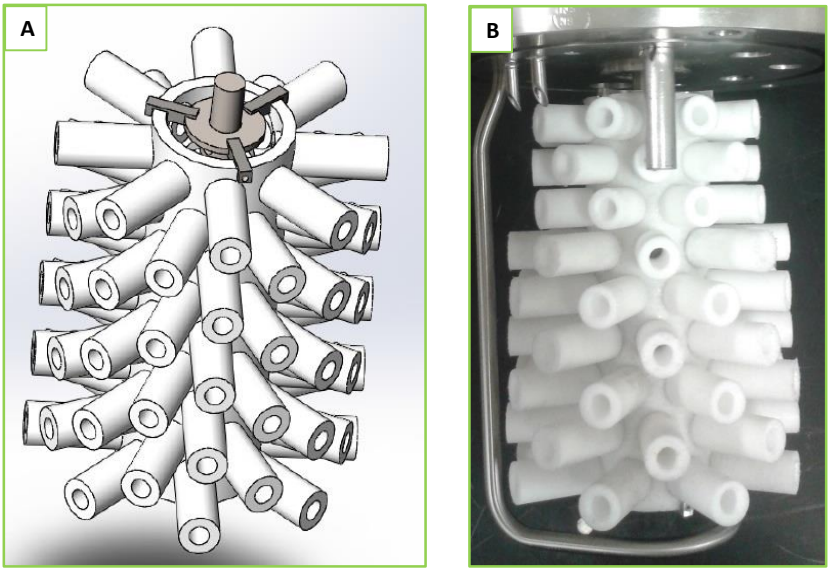

Figure 5.2. Novel agitator fittings used to increase cell density in the biorefinery stream fermentations. (A) A 3D rendering of the fitting with polypropylene (PP) protruding arms. **(B)** The actual PP fitting attached to the agitator shaft. The upper protruding arms were shortened to accommodate the pH probe and thermocouple.

The complete fermenter setup (reactor, tubing, and reservoirs) was autoclaved at 121 °C for 60 min to 75 min (depending on the volume of feed used), with the three medium parts kept in separate bottles to prevent unwanted reactions as in Chapter 3. Once the system had cooled, the medium parts were mixed into a single bottle. In the case of hydrolysate fermentations, the reactor contained approximately 1 L of a TSB-hydrolysate mixture (3:1) during autoclaving to serve as a start-up growth medium and to ensure that the pH probe remained wet. Similar to the inoculum preparation, hydrolysate was included to facilitate adaptation of the culture to the hydrolysate and to avoid shocking the organism when the fermenter was switched to the DDAP-H stream.

Fermentations were initialised by operating in batch mode for 16 to 24 hours after inoculation and once the sugar concentrations were sufficiently low, the system was switched to continuous mode by feeding the fermentation medium at a low dilution (~0.01 h^{-1}) rate to avoid cell washout. Since the TSB-hydrolysate mixture within the fermenter only features during the start-up phase of the process, it is unlikely that potentially unwanted reactions caused by autoclaving the mixture will have an influence on the steady-state results under continuous conditions. Also, steady-state conditions occurred long after the start-up batch, therefore the TSB-hydrolysate mixture would have been extensively diluted or completely washed out at this point. The first fermentation was performed using xylose (~60 g L^{-1}) as the only carbohydrate substrate to establish a baseline for the DDAP-H fermentations and to test the ability of the agitator fittings to increase cell density. The DDAP-H fermentations were repeated in duplicate and steady-states were obtained at dilution rates of 0.02 h^{-1}, 0.03 h^{-1} to 0.04 h^{-1} with a combined fermentation time of approximately 1,550 hours. A single-steady state was achieved at 0.05 h^{-1} in the second DDAP-H fermentation.

5.1.2 CORN STOVER HYDROLYSATE

Corn stover harvested in Emmetsburg, IA, USA underwent deacetylation, followed by acid impregnation and pilot-scale pretreatment, as described in [149]. Deacetylation was performed by mixing dry corn stover with a 0.4% w/w sodium hydroxide solution and holding for 2 h at 80 °C. Following this, a dilute solution of sulphuric acid (0.8 % w/w) was added to drained solids from the deacetylation process for acid impregnation, after which the acid-impregnated solids were mixed at room temperature for 2 h followed by dewatering using a screw press. The deacetylated, acid-impregnated corn stover then underwent pilot-scale acid hydrolysis pretreatment in a horizontal pretreatment reactor (Metso Inc., USA) at 150–170 °C with residence times of 10 – 20 min. The resulting deacetylated corn stover hydrolysate (DDAP-H) was stored in drums at 5 °C. Prior to preparation of the fermentation medium, the xylose-rich liquid fraction of the DDAP-H was separated from the glucose-rich solids fraction by means of a mechanical press. The liquid fraction was utilised in this study with the average composition in the fermenter feed stream given in Table 5.1.

Table 5.1. Composition of the diluted DDAP-H in the fermentation medium as fed to the fermenter. Undiluted DDAP-H constituted approximately 65% v/v of the fermentation medium.

Compound	Feed (g L^{-1})
Glucose	8.3
Xylose	52.6
Galactose	3.7
Arabinose	5.3
Acetic acid	0.9
Furfural	0.62
HMF	0.11

5.1.3 FERMENTATION MEDIUM

The fermentation medium (Table 5.2) used in the biorefinery stream fermentations was similar to that used in Chapter 3 and Chapter 4 (3.1.3 & 4.1.1) with a few modifications to reduce the cost of the medium due to the applied nature of the study. Sodium acetate was removed from the initial formulation because sodium is present in the form of NaCl and through the addition of NaOH for pH control, and acetate is produced by *A. succinogenes* as acetic acid. Similarly, the concentration of NaCl was reduced to 0.5 g L^{-1}. The concentrations of the phosphates in the potassium-phosphate buffer were reduced by half because the concentrations were found to be excessive as seen by residual phosphate peaks (as phosphoric acid) on the HPLC chromatograms in previous

fermentations. Corn steep liquor (CSL) was clarified in the same way as in Chapter 3 (3.1.3) but stored at 5 °C, and the three parts of the fermentation medium (A, B and C) were autoclaved separately as before.

Table 5.2. Medium composition used for the continuous fermentations in the stirred-tank reactor. All chemicals were obtained from Sigma-Aldrich (USA), unless stated otherwise.

Component	Concentration (g L^{-1})
A. Nitrogen, salts and nutrients	
NaCl (Fisher Scientific, USA)	0.5
$MgCl_2 \cdot 6H_2O$	0.2
$CaCl_2 \cdot 6H_2O$	0.2
Clarified corn steep liquor	10.0
Yeast extract (BD, USA)	6.0
Antifoam SE-15	0.5 mL/L
B. Phosphates	
KH_2PO_4	1.6
K_2HPO_4	0.8
C. Substrate*	
Xylose	60
DDAP-H	Table 5.1

*The carbohydrate source was either xylose or DDAP-H.

5.1.4 ANALYTICAL METHODS

Carbohydrates and organic acids

High-performance liquid chromatography (HPLC) was used to analyse the composition of the fermentation medium and the fermenter outlet. Organic acids and fermentation inhibitors (HMF and furfural) were detected by means of an Agilent 1100 system (Agilent Technologies, USA) fitted with a refractive index detector (RID) and an Aminex HPX-87H ion-exchange column (Bio-Rad Laboratories, USA). The mobile phase was 0.01 N (5 mM) H_2SO_4 at a flow rate of 0.6 mL min^{-1}. Column and RID temperatures were maintained at 85 °C and 55 °C, respectively. A sample injection volume of 6 µL was used. Carbohydrates (glucose, xylose, arabinose and galactose) were detected using the same system type and parameters as before except with a Phenomenex SP0810 column (Phenomenex, USA) and deionised water as the mobile phase. A YSI 7100 MBS (YSI Life Sciences, USA) was used for glucose and xylose detection at low concentrations due to reduced sensitivity of the respective HPLC system at low sugar concentrations. Note, the method used for pyruvic acid detection in Chapter 3 was developed after this study and was therefore not employed here.

Phenolic compounds

Analysis of phenolic compounds from the feed and outlet dilutions was performed on an Agilent 1100 system equipped with a G1315B diode array detector (DAD) and an Ion Trap SL (Agilent Technologies, USA) mass spectrometer (MS) with in-line electrospray ionization (ESI). Each sample was injected undiluted at a volume of 50 µL into the LC/MS system. Compounds were separated using an YMC C30 Carotenoid 0.3 µm, 4.6 x 150 mm column (YMC America, USA) at an oven temperature of 30 °C. The chromatographic eluents consisted of A) water modified with 0.03% formic acid, and B) 9:1 acetonitrile and water also modified with 0.03% formic acid. At a flow rate of 0.7 mL min^{-1}, the eluent gradient was as follows: 0-3 min, 0% B; 16 min, 7% B; 21 min, 8.5% B; 34 min, 10% B; 46 min, 25% B; 51-54 min, 30% B; 61 min, 50% B; and lastly 64-75 min, 100% B before equilibrium. Deionized water (Barnstead Easy Pure^{II}, USA), acetonitrile (HPLC grade, Fisher Scientific, USA), and formic acid with a purity of 98% (Sigma-Aldrich, USA) were used as HPLC solvents and modifiers.

Flow from the HPLC-DAD was directly routed in series to the ESI-MS ion trap. The DAD was used to monitor chromatography at 210 nm for a direct comparison to MS data. Source and ion trap conditions were calibrated with Agilent ESI-T tuning mix (P/N:G2431A), while tuning parameters were optimized under negative-ion mode by direct infusion of standards for major contributing compounds. MS and MS/MS parameters are as follows: smart parameter setting with target mass set to 165 Da, compound stability 70 %, trap drive 50 %, capillary at 3500 V, fragmentation amplitude of 0.75 V with a 30 to 200 % ramped voltage implemented for 50 ms, and an isolation width of 2 m/z (He collision gas). The ESI nebulizer gas was set to 60 psi, with dry gas flow of 11 L min^{-1} held at 350 °C. MS scans and precursor isolation-fragmentation scans were performed across the range of 40-350 Da.

5.1.5 DATA COLLECTION AND ANALYSIS

Online monitoring of the process parameters was performed by means of BioCommand software (New Brunswick Scientific, USA). The weighted time-average of the NaOH flow rate was calculated in real-time by a custom programme and used as an indication of steady-state. Once the time-averaged NaOH flow rate remained within 5% of the average over at least a 24-hour period, and sugar and metabolite concentrations remained within 3% over the same interval, the system was considered to be at pseudo steady-state. Furthermore, samples were taken daily to assess the transient behaviour of the system. The time-averaged NaOH flow rate, together with the antifoam flow rate, were used in calculating a dilution factor to adjust the inlet concentration of the substrates and other

compounds of relevance due to dilution by the additional flow. The accuracy and completeness of the data were assessed by performing overall mass balances as detailed in 3.1.6.

5.2 PRELIMINARY BATCH FERMENTATIONS

As described in [148], preliminary batch fermentations were performed on *A. succinogenes* to determine its behaviour and SA production performance on: (i) the four main hemicellulose-derived carbohydrates present in corn stover hydrolysate (i.e. glucose, xylose, arabinose and galactose), (ii) mock hydrolysates containing the same four carbohydrates and putative microbial inhibitors (acetic acid, furfural and HMF) and, (iii) two xylose-enriched hydrolysates derived from pilot-scale pretreatments, namely deacetylated, dilute acid pretreated hydrolysate (DDAP-H) and regular dilute acid pretreated hydrolysate (DAP-H).

It was found that the order of preference or efficiency in carbohydrate conversion was glucose, xylose, arabinose and then galactose (Figure 5.3). Glucose, xylose and arabinose were consumed simultaneously with galactose consumption occurring once glucose neared full conversion. Similar yields were obtained on pure glucose (0.72 g g^{-1}) and xylose (0.70 g g^{-1}) streams while the yield of DDAP-H (0.74 g g^{-1}) clearly outperformed that of DAP-H (0.52 g g^{-1}). Furthermore, the maximum productivity on DDAP-H (1.27 g $L^{-1}h^{-1}$) far exceeded that of DAP-H (0.27 g $L^{-1}h^{-1}$) but was lower than mock DDAP-H (1.57 g $L^{-1}h^{-1}$) and pure xylose (1.79 g $L^{-1}h^{-1}$) and glucose (1.63 g $L^{-1}h^{-1}$) streams. In addition, furfural was converted to furfuryl alcohol and consequently decreased to zero (Figure 5.4), together with HMF, during the course of the batch fermentations. Overall, the results demonstrate that *A. succinogenes* is capable of fermenting non-detoxified corn stover hydrolysate at competitive yields and productivities and that deacetylation is an effective pretreatment step to reduce inhibitory effects of hydrolysate.

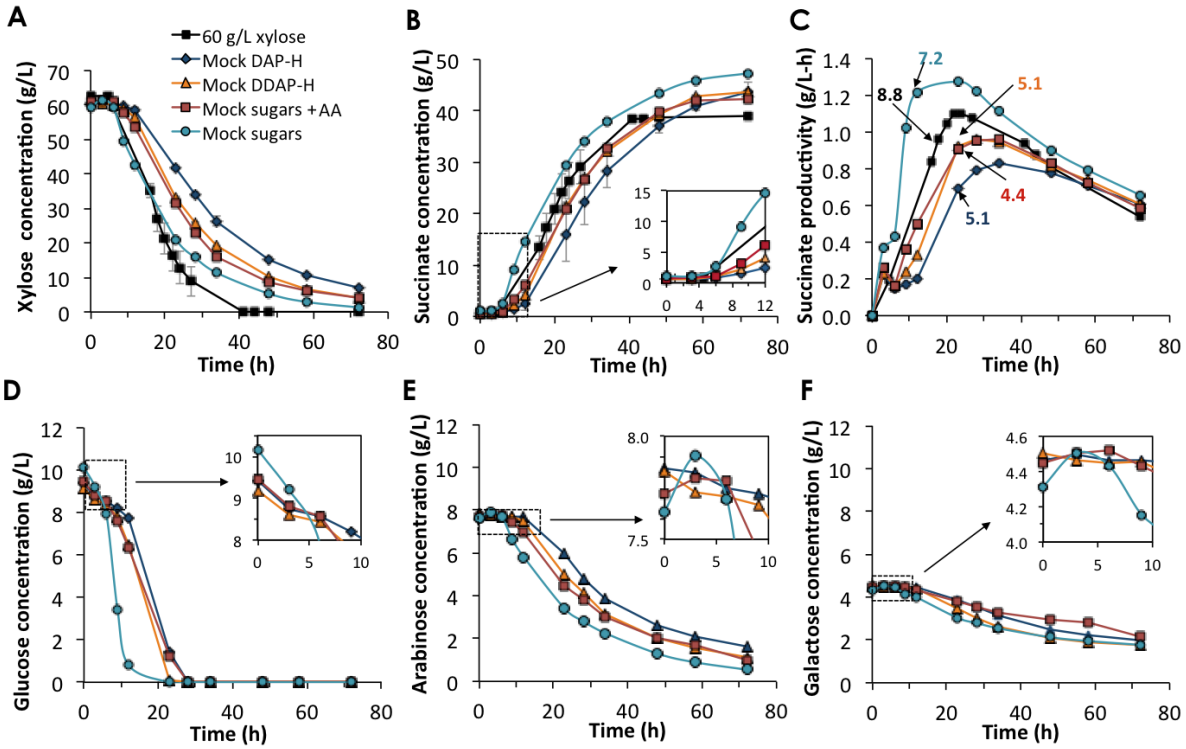

Figure 5.3. Succinic acid production and sugar consumption by *A. succinogenes* in mock media in the preliminary batch fermentations [148]**.** Profiles of xylose **(A)** glucose **(D)** arabinose **(E)** and galactose **(F)** consumption, succinate production **(B)** and succinate productivity **(C)** by *A. succinogenes* of different mock hydrolysates. Productivity is calculated as succinate concentration divided by the fermentation time at each point. Sugars and inhibitors in the different media are (1) mock DAP-H = sugars (80 g L^{-1}) + furfural (1.7 g L^{-1}) + HMF (0.17 g L^{-1}) + AA (5.8 g L^{-1}), (2) mock DDAP-H = sugars (80 g L^{-1}) + furfural (1.7 g L^{-1}) + HMF (0.17 g L^{-1}) + AA (2.3 g L^{-1}), (3) mock sugars + AA = sugars (80 g L^{-1}) + AA (5.8 g L^{-1}), and (4) mock sugars = only sugars (80 g L^{-1}). Insets in the graphs **B**, **D**, **E**, and **F** present the profiles corresponding to the first few hours of fermentation. The numbers in **C** indicate the time point where the maximum cell density (OD_{600}) was reached and the specific OD_{600} value for each culture.

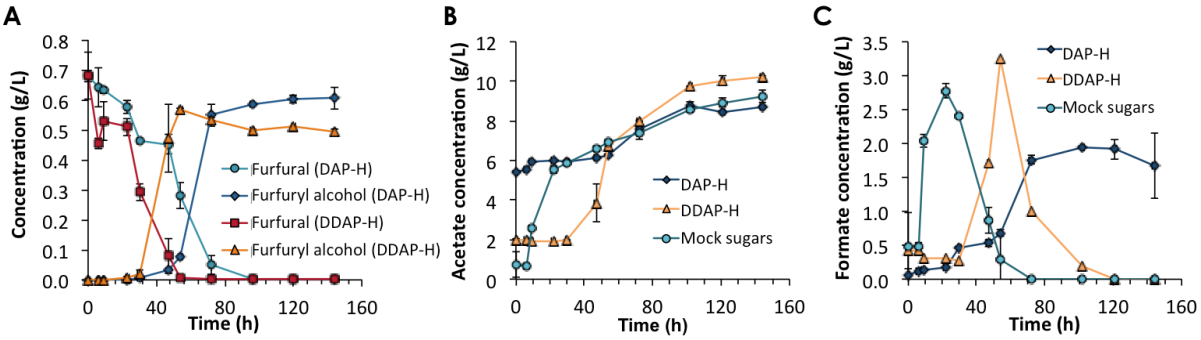

Figure 5.4. Inhibitors and co-products metabolism during preliminary batch fermentations [148]**.** Profiles of **(A)** furfural conversion to furfuryl alcohol in DAP-H and DDAP-H and **(B)** acetate production and **(C)** formate production and metabolism in mock sugars, DAP-H, and DDAP-H.

5.3 BASELINE CONTINUOUS XYLOSE FERMENTATION

An initial continuous fermentation was performed using a clean (inhibitor free), xylose feed stream to establish a baseline against which the hydrolysate fermentation runs could be compared, as xylose is the major sugar in dilute-acid pretreated hydrolysates [144,150–152]. A xylose feed

concentration of 60 g L^{-1} was chosen since this was the estimated concentration of xylose in the mock and hydrolysate runs (80 g L^{-1} total sugars) of our preliminary batch study [148]. A second objective of the initial fermentation was to ensure that the novel agitator fitting was capable of facilitating biofilm attachment and support, preferably for extended periods of operation.

Steady-states were achieved at dilution rates (D) of 0.05 h^{-1} and 0.10 h^{-1} (Table 5.3) with succinic acid as the major product, and acetic acid (AA) and formic acid (FA) as by-products. The productivity benefits of operating continuously with a biofilm reactor are highlighted when comparing the SA productivity attained in this study (1.5 – 2.6 g L^{-1} h^{-1}) to that of the preliminary xylose batch study (60 g L^{-1} feed) of 0.94 g L^{-1} h^{-1} [148] and to a similar study by Liu et al. [97] of 0.54 g L^{-1} h^{-1}. Furthermore, the productivity compares well with the continuous xylose fermentations conducted in Chapter 3 [122] where productivities of 1.5 g L^{-1} h^{-1} to 3.4 g L^{-1} h^{-1} were attained at Ds between 0.05 h^{-1} and 0.3 h^{-1}. Note, productivity is calculated using the overall operational reactor volume (1.3 L) and the volumes of the agitator and fitting form part of this volume.

Table 5.3. Summary of the performance of the stirred, continuous biofilm reactor on a clean xylose feedstream.

Dilution rate (h^{-1})	Productivity (g $L^{-1}h^{-1}$)	SA[a] (g L^{-1})	Yield on xylose (g g^{-1})	SA/AA[b] (g g^{-1})	FA[c]/AA (g g^{-1})	Sugar conversion (%)	Effective xylose feed (g L^{-1})
0.05	1.54	32.5	0.72	4.2	0.36	80	57.0
0.10	2.64	26.4	0.77	4.2	0.37	60	56.7

[a] succinic acid; [b] acetic acid; [c] formic acid

The maximum SA titre in this study (32.5 g L^{-1}) is lower than that of the preliminary batch study (38.4 g L^{-1}), whereas the maximum yield is greater (0.77 g g^{-1} vs 0.70 g g^{-1}) and both values compare remarkably well with that of Liu et al. [97] (32.6 g L^{-1} and 0.77 g g^{-1}), thereby further motivating continuous operation. In addition, it was found that the agitator fitting effectively facilitated biofilm attachment and support during continuous operation. Biofilm attached to all surfaces of the silicone protruding arms and the inner tube of the fitting, and also to the glass walls and internals of the fermenter (Figure 5.5). Prior to inoculation, the pH response to base addition was found to be rapid, which suggests that effective mixing was achieved by the agitator. Therefore, the agitator fitting provided adequate support for biofilm and did not compromise mixing of the broth. In addition, minimal loss of cells was observed in the reactor effluent, further indicating the effectiveness of the fitting.

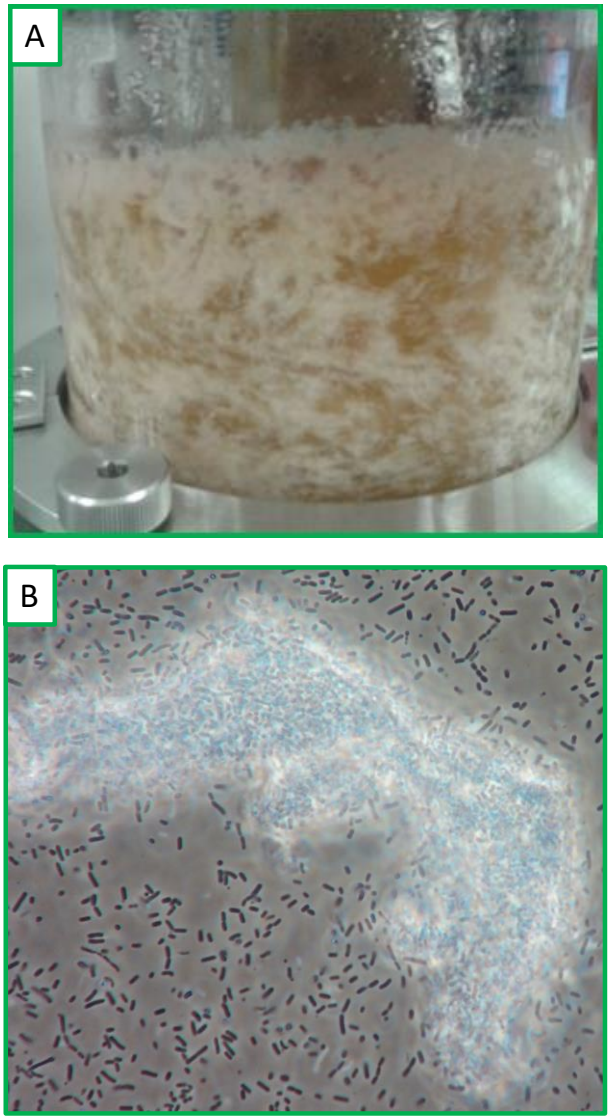

Figure 5.5. Biofilm and cell morphology of *A. succinogenes* grown on xylose. (A) Biofilm attachment occurred on the walls of the fermenter and the agitator which is not visible due to the density of the biofilm and the opacity of the broth. **(B)** A micrograph of *A. succinogenes* cells grown on xylose. The dense portion is a clump of detached biofilm.

5.4 CONTINUOUS HYDROLYSATE (DDAP-H) FERMENTATIONS: EFFECT OF DILUTION RATE

Following the promising results of the pure xylose fermentations, continuous fermentations of xylose-enriched, deacetylated, dilute-acid pretreated corn stover hydrolysate (DDAP-H) were performed. The DDAP-H was prepared by a two-stage pretreatment of corn stover comprising a mild alkaline wash with NaOH followed by dilute acid pretreatment (DAP) with H_2SO_4 (see *5.1.2 above*). Deacetylation is effective at removing a significant amount of acetic acid from the hydrolysate [145], which is beneficial since acetic acid is known to be inhibitory to the growth of *A. succinogenes* [29,153]. Deacetylation also partially removes lignin from the cell wall, which potentially could reduce inhibition due to low molecular weight phenolics. The DDAP-H consisted mainly of C_5 and C_6 carbohydrates at a total concentration of 104.8 g L^{-1} along with fermentation inhibitors such as

furfural and HMF (originating from sugar degradation during DAP [143]), and acetic acid. Although the expected xylose concentration in the hydrolysate streams of the preliminary batch study was 60 g L^{-1} (with a corresponding total sugars concentration 80 g L^{-1}), fluctuations in the total and relative sugar concentrations between hydrolysate batches resulted in an actual xylose feed concentration of between 52 and 58 g L^{-1}. Therefore, in the present study, the pressed hydrolysate was diluted (Table 5.1) to achieve an operational xylose concentration within this range for direct comparison with the DDAP-H results of the preliminary study [148].

The DDAP-H fermentations were performed in duplicate at dilution rates of 0.02 h^{-1}, 0.03 h^{-1} and 0.04 h^{-1}. Steady-states were achieved at all three dilution rates with a single steady-state achieved at a dilution rate of 0.05 h^{-1} to gain insight into the response of the system at higher dilution rates. The dynamic behaviour of the system, discussed further in *5.8 below*, was instructive in selecting optimal dilution rates, in developing a start-up procedure for stable continuous operation and in assessing steady-state stability. It was found that the succinic acid concentration (C_{SA}) remained fairly constant at between 38.6 g L^{-1} and 39.6 g L^{-1} on average across all three duplicated dilution rates (Figure 5.6A), and decreased to 33.7 g L^{-1} at D = 0.05 h^{-1}. However, C_{SA} was shown to increase with decreasing dilution rate in previous continuous studies with *A. succinogenes* [13,16,39], although these studies did not include all the low Ds used in the current study. Despite the constant C_{SA} values, the concentrations of the major by-products, acetic acid (C_{AA}) and formic acid (C_{FA}), showed similar trends to previous continuous fermentations where C_{AA} decreased with decreasing D, and C_{FA} remained near, or equal, to zero (Figure 5.6B), with the only exception being the concentration at D = 0.05 h^{-1} where C_{AA} decreased along with C_{SA}.

Similar to the trend in C_{SA}, the yield of SA on carbohydrates (Y_{sSA}) remained fairly constant (0.76 to 0.78 g g^{-1}) across the lower three dilution rates and decreased to 0.69 g g^{-1} at D = 0.05 h^{-1} (Figure 5.6C). Furthermore, the yields remained below the overall theoretical maximum of 1.12 g g^{-1} [25] (on a glucose basis, but this holds for all carbohydrates in this study due to the same degree of reduction seen in the identical C:H:O ratios), and within the limits defined by the accepted metabolic pathways of 0.66 g g^{-1} to 0.87 g g^{-1} [15]. Despite this, the SA/AA ratios (Y_{AASA}) exceeded those dictated by the same pathways (1.97 g g^{-1} and 3.93 g g^{-1}) and ranged between 5.2 g g^{-1} and 7.9 g g^{-1} whereas the FA/AA ratio (Y_{AAFA}) remained constant at zero due to the absence of FA (Figure 5.6D). Since C_{SA} remained constant at a constant Y_{sSA} with a corresponding decrease in Y_{AASA} at increasing Ds, it implies that carbon was increasingly channelled to AA but not away from SA. However, in the case of a constant yield when all metabolites are accounted for, it is expected that as C_{AA} increased, C_{SA} should have decreased.

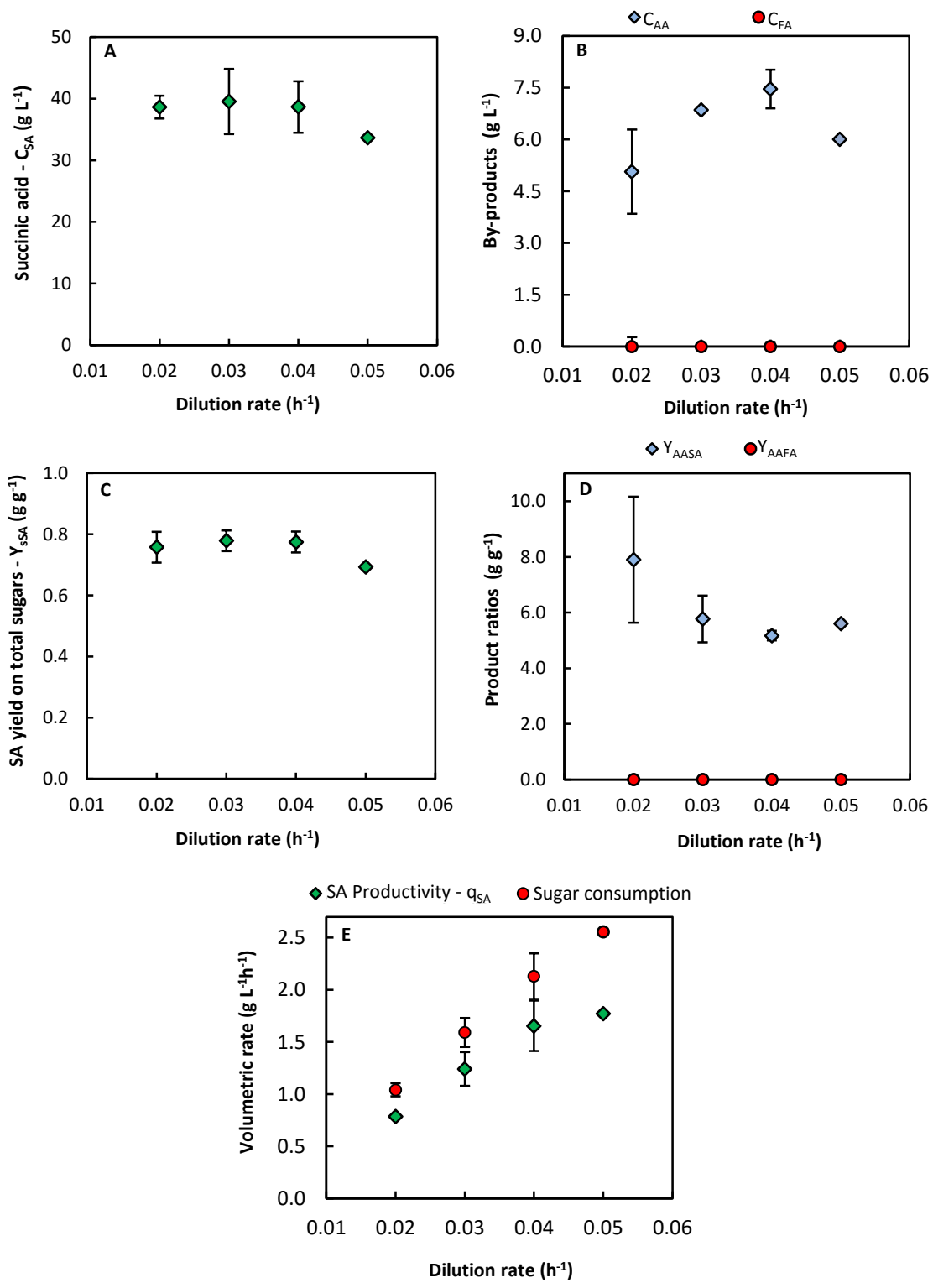

Figure 5.6. Fermentation performance on DDAP-H as a function of dilution rate. Concentrations of **(A)** succinic acid, and **(B)** the major by-products acetic acid and formic acid; **(C)** the yield of succinic acid on total sugars consumed; **(D)** metabolite ratios indicating selectivity to succinic acid (Y_{AASA}) and the route of pyruvate consumption (Y_{AAFA}); **(E)** volumetric rate of carbohydrate consumption and succinic acid productivity. *Error bars* represent standard deviation and are hidden by the markers in cases where the deviation is negligible. No repeats were performed at D = 0.05 h^{-1}.

The SA productivity (q_{SA}) was found to be competitive and ranged between 0.78 g L^{-1} h^{-1} and 1.65 g L^{-1} h^{-1} for the lower three dilution rates (Figure 5.6E). In addition, q_{SA} increased linearly up to a D of 0.04 h^{-1} due to C_{SA} remaining fairly constant, but flattened out somewhat at D = 0.05 h^{-1} due to a correspondingly lower C_{SA}. The total sugars consumption rate increased linearly across all dilution rates including 0.05 h^{-1}. The highest q_{SA} of 1.77 g L^{-1} h^{-1} was achieved at D = 0.05 h^{-1} with a corresponding total sugars consumption rate of 2.56 g L^{-1} h^{-1}. The decrease in Y_{sSA} at D = 0.05 h^{-1} is also reflected by the increased difference between the rate of sugars consumption and the rate of SA production when compared to the lower Ds. The non-linear increase in q_{SA} in moving from a D of 0.04 h^{-1} to 0.05 h^{-1} with a corresponding linear increase in the rate of sugar consumption, together with a poorer yield at 0.05 h^{-1}, is suggestive of a shift in the metabolic flux distribution.

Despite the linear increase in sugar consumption rate with dilution rate, the conversion of total sugars decreased gradually with increasing dilution rate from 81.3% at D = 0.02 h^{-1} to 73.7% at D = 0.05 h^{-1} (Figure 5.7A). The order of preference in sugar utilisation by *A. succinogenes*, as reflected by the conversion of each sugar (Figure 5.7B), was glucose (94.3 – 97.5%), xylose (73.0 – 83.2%), arabinose (61.5 – 70.0%) and galactose (37.9 – 47.9%). However, all sugars were consumed simultaneously suggesting the absence of carbon catabolite repression, in agreement with the results of the preliminary batch study on DDAP-H [148] where the sugars were consumed simultaneously but at different rates with the same utilisation preferences as seen in the present study. Interestingly, the conversion of xylose at 0.05 h^{-1} in the DDAP-H fermentation (73.0%) was somewhat lower than that of the baseline xylose fermentation at the same D (79.6%) with a similar xylose feed concentration - likely due to the preference for glucose.

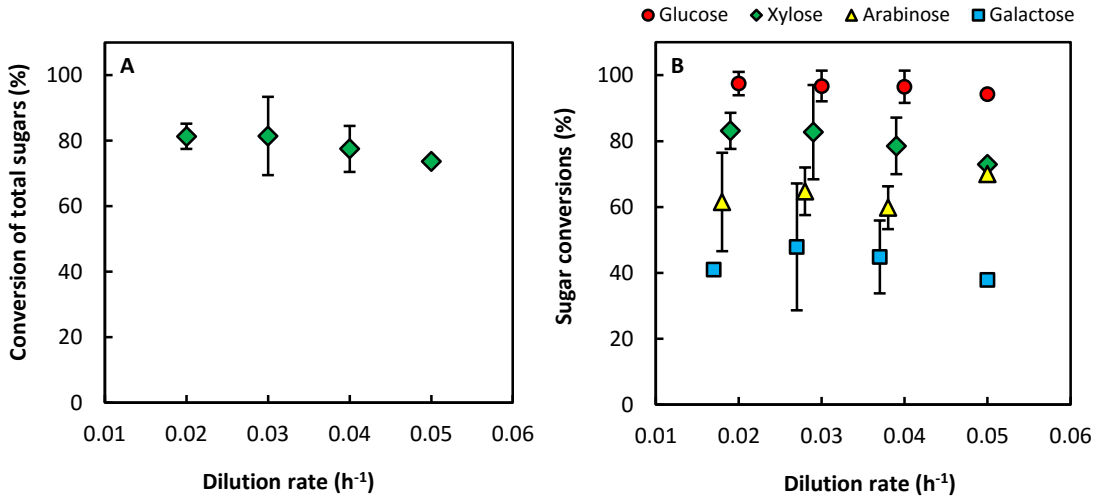

Figure 5.7. Conversion of carbohydrates in the DDAP-H fermentations as a function of dilution rate. (A) The conversion of total sugars, and **(B)** the individual conversion of each sugar. Error bars represent standard deviation and are hidden by the markers in cases where the deviation is negligible. No repeats were performed at D = 0.05 h^{-1}. Large deviations in arabinose and galactose data are due to reduced HPLC system sensitivity at low sugar concentrations

5.5 CONTINUOUS HYDROLYSATE (DDAP-H) FERMENTATIONS: MASS AND REDOX BALANCES

Similar to Chapter 3 and Chapter 4, to explore the consistency of the fermentation data, mass balances were performed on the data averages. Mass balance closures were between 74.0% and 83.9% (Figure 5.8A) suggesting that mass was unaccounted for in the form of either missing metabolites or as biomass since dry cell weights were not included. However, similar to the discussion in Chapter 3 (3.3), biomass, as dry cell weight measurements, was excluded from the mass balance calculation due to the presence of biofilm and because C_{SA} values were 33.0 g L^{-1} and 39.5 g L^{-1} throughout this study, meaning that the system was in a non-growth state. Therefore, the unaccounted mass is likely due to undetected metabolites, which may have been produced through alternative metabolic pathways. Nevertheless, the incomplete mass balances do not detract from the utility of the fermentation results and are in themselves a useful result, yet it is instructive to further explore this discrepancy and to this end, redox balances were performed on the results, similar to Chapters 3 and 4 (3.3).

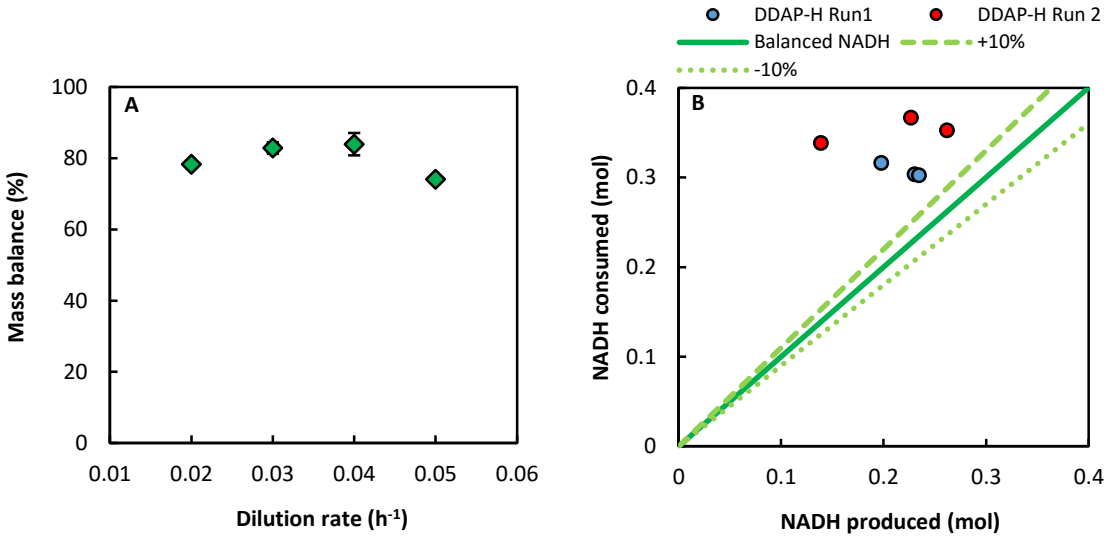

Figure 5.8. Mass and redox balance analyses of the DDAP-H fermentations. (A) Mass balances at each dilution rate and, **(B)** A parity plot of the NADH produced as a function of the NADH consumed for each steady state from DDAP-H runs 1 and 2. Error bars represent standard deviation and are hidden by the markers in cases where the deviation is negligible. No repeats were performed at D = 0.05 h^{-1}.

As discussed in Chapter 3 (3.3), the only route of SA synthesis in *A. succinogenes* is via the reductive branch of the TCA cycle since the organism lacks a complete TCA cycle, a glyoxylate shunt and an Entner-Doudoroff pathway [81]. Furthermore, the main reported end products during *A. succinogenes* fermentations are acetic acid, formic acid and ethanol [49], and as described in Chapter 3, pyruvic acid when fermenting xylose. However, no pyruvic acid or ethanol was detected in the DDAP-H fermentations. The redox balance was therefore restricted to the formation of succinic-, acetic- and formic acids. Elemental balancing and knowledge of metabolic pathways was used to determine overall equations, on a carbon mole basis, in converting substrate to product (Equations 2-6 to 2-8; repeated below on a general carbohydrate basis). Since the degree of reduction of each carbohydrate (i.e. glucose, xylose, galactose and arabinose) is the same (i.e. equal C:H:O ratios), the redox implications will be equivalent for each substrate and therefore the C-mole redox balances will be identical.

$$\textbf{SA}: CH_2O(\text{carbohydrtate}) + \frac{1}{3}NADH + \frac{1}{3}CO_2 \rightarrow \frac{4}{3}CH_{\frac{3}{2}}O(SA) + \frac{1}{3}H_2O \quad \textbf{5-1}$$

$$\textbf{PFL}: CH_2O(\text{carbohydrtate}) + \frac{1}{3}H_2O \rightarrow \frac{2}{3}CH_2O(AA) + \frac{1}{3}CH_2O_2(FA) + \frac{1}{3}NADH \quad \textbf{5-2}$$

$$\textbf{PDH}: CH_2O(\text{carbohydrtate}) + \frac{1}{3}H_2O \rightarrow \frac{2}{3}CH_2O(AA) + \frac{2}{3}NADH + \frac{1}{3}CO_2 \quad \textbf{5-3}$$

Equations 2-7 and 2-8 give the overall oxidative pathways in which NADH is produced, via either the pyruvate dehydrogenase (Equation 2-8) or the pyruvate formate-lyase (Equation 2-7) route. However, since no formic acid was observed during the DDAP-H fermentations, only Equation 2-8 featured in the NADH calculation. Equation 2-6 gives the overall reductive pathway in which there is a net consumption of NADH in producing SA. Using metabolite measurements, the corresponding NADH for each pathway can be calculated and the total should sum to zero in a redox balanced system. However, in this study, and similar to the results of Chapter 3 and Chapter 4, the total amount of NADH consumed distinctly exceeded the amount of NADH produced (Figure 5.8B), which dovetails with the high Y_{AASA} ratios (Figure 5.6C). The extent to which the consumed NADH exceeds the produced NADH clearly reflects that NADH generated in the production of the measured metabolites was insufficient. In essence, therefore, the system displayed an overall mass imbalance together with an NADH imbalance on the measured mass.

The mass deficit could be associated with NADH production where NADH is produced together with the potential missing metabolite(s), thereby accounting for both the excess NADH and the missing mass. Furthermore, as demonstrated in Chapter 4 (4.4), the additional reduction power can be generated in the OPPP, especially since the fermentations in the current chapter were also performed under biofilm conditions and displayed similar yields as before. However, as discussed in 4.4, OPPP flux would only satisfy the redox balance while leaving closure of the overall mass balance incomplete. Alternatively, and as mentioned in Chapter 4, if the OPPP produced NADH beyond that needed to close the NADH balance, and the additional NADH produced was oxidised by an external agent (e.g. yeast extract in the feed serving as an electron acceptor as mentioned in [53]), a concomitant loss of CO_2 would occur. In this scenario, the undetected metabolite would be CO_2.

When using non-detoxified hydrolysate as feedstock, it may be possible for the detoxification reactions to serve as NADH-sinks. As observed in the preliminary batch fermentations (5.2), *A. succinogenes* converts furfural to furfuryl alcohol and as seen below, furfural is completely consumed in the continuous DDAP-H fermentations. The conversion will increase the demand for NADH as it requires two NADH molecules [154] to proceed. If this NADH is supplied by the OPPP, mass would be lost as CO_2, thereby partially contributing to the incomplete mass balance closures. A similar process could occur in the conversion of HMF to HMF alcohol as this reaction requires two NADPH molecules [155], although HMF alcohol has not yet been established as the conversion product of HMF in *A. succinogenes* fermentations.

5.6 EFFECT OF INHIBITORS ON THE FERMENTATION PERFORMANCE

The concentrations of the primary suspected fermentation inhibitors, furfural and HMF, were found to decrease to, and remain at zero, during all fermentations. This finding is in agreement with the previous batch study where furfural was converted to furfuryl alcohol and consequently decreased to zero, together with HMF, during the course of the fermentation [148]. As suggested in a previous study [156], furfural conversion to furfuryl alcohol likely occurs by means of an aldehyde reductase since the aldehyde is reduced to its alcohol form. Also, the genome of *A. succinogenes* encodes an aldo/keto reductase (KEGG: Asuc_0311), which may be responsible for the reduction of furfural. Despite HMF and furfural remaining at zero, it was necessary to increase the dilution rate gradually to enable the culture to better tolerate the hydrolysate (*5.8 Dynamic behaviour of the hydrolysate (DDAP-H) fermentations: start-up and stability*) suggesting either the presence of other inhibitors in the feed, or that *A. succinogenes* metabolises these compounds at a regulated rate that increases with increasing dilution rate after adaptation. Similarly, in our comparative batch study [148], the mock hydrolysates that contained furfural and HMF distinctly outperformed the actual hydrolysates suggesting that there are inhibitors present in the hydrolysate besides HMF and furfural. Phenolic compounds resulting from hydrolysis pretreatment processes are also known to inhibit microbial growth [143]. As such, the concentrations of selected phenolic compounds in the feed were compared to those of the fermentation broth across all steady-states in the second DDAP-H fermentation (Table 5.4). Interestingly, an increase in the concentrations of the phenolics was observed between the feed and the fermentation broth, with the exception of 4-hydroxybenzaldehyde. Also, the increase in phenolics occurred at all dilution rates and to the same extent. An increase in phenolics could be a result of breakdown of lignin oligomers or aromatic-carbohydrate linkages, either through microbial action or through abiotic degradation. Related to microbial action, the genome of *A. succinogenes* includes a feruloyl-esterase enzyme (KEGG: Asuc_0433) which is able to catalyse the break-down of the complex feruloyl-polysaccharide thereby releasing ferulate (Expasy: EC 3.1.1.73). Because the enzyme contains a signal peptide (predicted by SignalP 4.1 [157]), it may be performing extracellular hydrolysis reactions, which could be the mechanism behind the increase in ferulic acid. In spite of this potential mechanism, it remains to be seen whether overall fermentation performance can be enhanced by detoxification of the hydrolysate prior to fermentation without considerably impacting the economics of the process.

Table 5.4. Concentrations of phenolic compounds present in the feed and outlet during the second DDAP-H fermentation. *ND* = not detected

Dilution rate (h^{-1})	(mg L^{-1})					
	4-hydroxy benzaldehyde	Caffeic acid	Syringic acid	p-Coumaric acid	Ferulic acid	Total phenolics
Feed medium	1.779	*ND*	*ND*	22.71	5.20	29.68
0.02	0.105	0.895	0.269	51.84	15.15	68.26
0.03	0.104	0.886	0.261	51.40	15.20	67.85
0.04	0.107	0.881	0.264	51.05	14.85	67.15
0.05	0.111	0.887	0.272	51.93	15.14	68.34

5.7 COMPARISON TO OTHER RELEVANT STUDIES ON SUCCINIC ACID PRODUCTION

The results achieved in this study compare well with previous SA production studies using *A. succinogenes* and a biomass feedstock. Particularly, the highest productivity achieved in this study (1.77 g L^{-1} h^{-1}) exceeds previous batch studies that utilised a lignocellulosic feedstock, a starch-derived feedstock, or a detoxified feed stream but was lower than the previous continuous xylose study (3.41 g L^{-1} h^{-1}; at D = 0.3 h^{-1}) (Table 5.5). As with the baseline xylose fermentation, the high productivities attained in the DDAP-H fermentations highlight the productivity benefits of operating continuously with immobilised cells. However, the maximum titre attained (39.6 g L^{-1}) was lower than previous studies which underscores a potential downside to operating continuously at appreciable productivities. The maximum yield on total sugars attained in the DDAP-H fermentations of 0.78 g g^{-1} compares well with the xylose baseline fermentation (0.77 g g^{-1}) and with previous studies, especially since the hydrolysate contained known fermentation inhibitors, and comprised a mix of sugars that are metabolised to varying degrees by *A. succinogenes* (Figure 4B). Furthermore, the maximum yield in this study exceeded that of the preliminary batch study [148]. Interestingly, the steady state, achieved at D = 0.05 h^{-1} in the second DDAP-H fermentation, outperformed that of the baseline xylose fermentation in terms of productivity (1.77 vs. 1.54 g L^{-1} h^{-1}), but showed similar values for titre (33.6 vs. 32.5 g L^{-1}) and yield (0.69 vs. 0.72 g g^{-1}). The greater productivity is most likely due to a higher cell density in the DDAP-H fermentation where the porosity of the PP fitting is expected to provide a greater surface area for cell attachment than the silicone arms used in the xylose fermentation. Also, the comparable performance could suggest that the lower initial, and gradual increase in, the dilution rates of the second DDAP-H fermentation (discussed below) together with increased exposure times of the cells to DDAP-H through cell retention, led to adaptation of the culture to the extent where it was able to perform similarly to one operating on a clean, xylose feed - since the comparison is only valid for one dilution rate (0.05 h^{-1}) which occurred

late in the DDAP-H run. With this in mind, prior detoxification of the DDAP-H could lead to performance similar to that of the xylose fermentation without the need for extended start-up phases. Essentially, the results achieved in this study are of substantial value to the development of a SA production processes that could be incorporated into a lignocellulosic biorefinery. However, all studies on lignocellulosic feedstock still fall well short of the performance obtained with pure glucose fermentations (Table 5.5). In addition to *A. succinogenes*, the ability of other microorganisms to produce SA from lignocellulosic biomass has been reviewed [86].

Table 5.5. Summary of the most relevant succinic acid production studies using *A. succinogenes* and a potentially scalable, renewable feedstock with pure sugar studies given for comparison. The highest SA productivity, concentration and yield for each study are shown.

Substrate (Feedstock)	Pretreatment method	Mode	q_{SA}[a] ($g\ L^{-1}\ h^{-1}$)	C_{SA}[b] ($g\ L^{-1}$)	Y_{sSA}[c] ($g\ g^{-1}$)	Reference
Corn stover (xylose, glucose, arabinose, galactose)	Pilot-scale: deacetylation followed by dilute sulfuric acid hydrolysis	Continuous	1.77	39.6	0.78	This Chapter
Xylose	-	Continuous	2.64	32.5	0.77	This Chapter
Xylose	-	Continuous	3.41	29.4	0.68	Chapter 3/[122]
Xylose (60 $g\ L^{-1}$)	-	Batch	0.94	38.4	0.70	Preliminary Batch Study/[148]
Corn stover	Pilot-scale: deacetylation followed by dilute sulfuric acid hydrolysis (DDAP-H)	Batch	0.30	42.8	0.74	
	Pilot-scale: dilute sulfuric acid hydrolysis (DAP-H)	Batch	0.12	17.0	0.52	
Mock DDAP-H (xylose, glucose, arabinose, galactose, inhibitors, low acetate)	-	Batch	0.61	43.8	0.68	
Mock DAP-H (xylose, glucose, arabinose, galactose, inhibitors, high acetate)	-	Batch	0.61	43.7	0.72	
Sugarcane bagasse (xylose)	Dilute sulfuric acid hydrolysis	Batch	1.01	22.5	0.43	[110]
Wheat (glucose)	Enzymatic hydrolysis	Batch	1.01	35.6	0.82	[158]
		Batch	1.57	64.2	0.81	[159]
		Batch	0.91	62.1	1.02	[111]
Corn fibre (glucose, xylose, arabinose)	Dilute sulfuric acid hydrolysis by autoclaving	Batch	0.98	35.4	0.73	[103]
		Batch	0.63	47.0	0.68	[160]
Corn stover (glucose, xylose, arabinose)	Dilute sulfuric acid hydrolysis followed by cellulose treatment	Batch	1.08	56.4	0.73	[161]
Sugarcane molasses (sucrose, glucose, fructose)	Sulfuric acid treatment of crude molasses	Batch	1.30	60.7	0.81	[162]
		Fed-batch	1.40	64.7	0.86	[162]
		Batch	0.97	57.9	0.69	[101]
		Fed-batch	1.07	64.3	0.76	[101]
Glucose†	-	Continuous	10.8	32.5	0.90	[13]
	-	Fed-batch	2.77	98.7	0.89	[14]

[a] succinic acid productivity; [b] succinic acid concentration; [c] yield of succinic acid on carbohydrate substrate(s); † comparative baseline study

5.8 DYNAMIC BEHAVIOUR OF THE HYDROLYSATE (DDAP-H) FERMENTATIONS: START-UP AND STABILITY

The initial operational strategy for the DDAP-H fermentations was to operate at a low dilution rate similar to the lowest rate used in the xylose baseline fermentation (0.05 h^{-1}) to allow the culture to adapt to the hydrolysate. Given stability of the system, the dilution rate would then be increased to accelerate biofilm formation. Once substantial and stable biofilm had been established, the dilution rate would be systematically changed to assess the performance of the system under steady state conditions across a range of dilution rates. The system was considered to be at steady state once the time-averaged NaOH flow rate remained within 5% of the average for at least 24 hours and minimal fluctuations (< 3%) in residual sugar and metabolite concentrations were observed after at least two samples over the same period.

In the first continuous DDAP-H fermentation (Figure 5.9A), once the initial start-up batch was nearing completion, the system was switched to continuous mode at a dilution rate of 0.025 h^{-1} (half of the lowest rate used in the xylose fermentation). The response was positive and a C_{SA} of 20 g L^{-1} was achieved. Given this, the dilution rate was increased to 0.05 h^{-1} before the system was able to reach steady state. However, the productivity of the system decreased significantly and ultimately approached zero. To restore the system, the reactor was switched to batch mode allowing the cells a period of revival. Batch operation showed an increase in C_{SA} after which the dilution rate was changed to 0.01 h^{-1} followed by an increase to 0.02 h^{-1} due to a promising increase in C_{SA}. The dilution rate was then increased to 0.03 h^{-1} which resulted in a progressive decrease in C_{SA}. Once again the system was switched to batch mode for recovery.

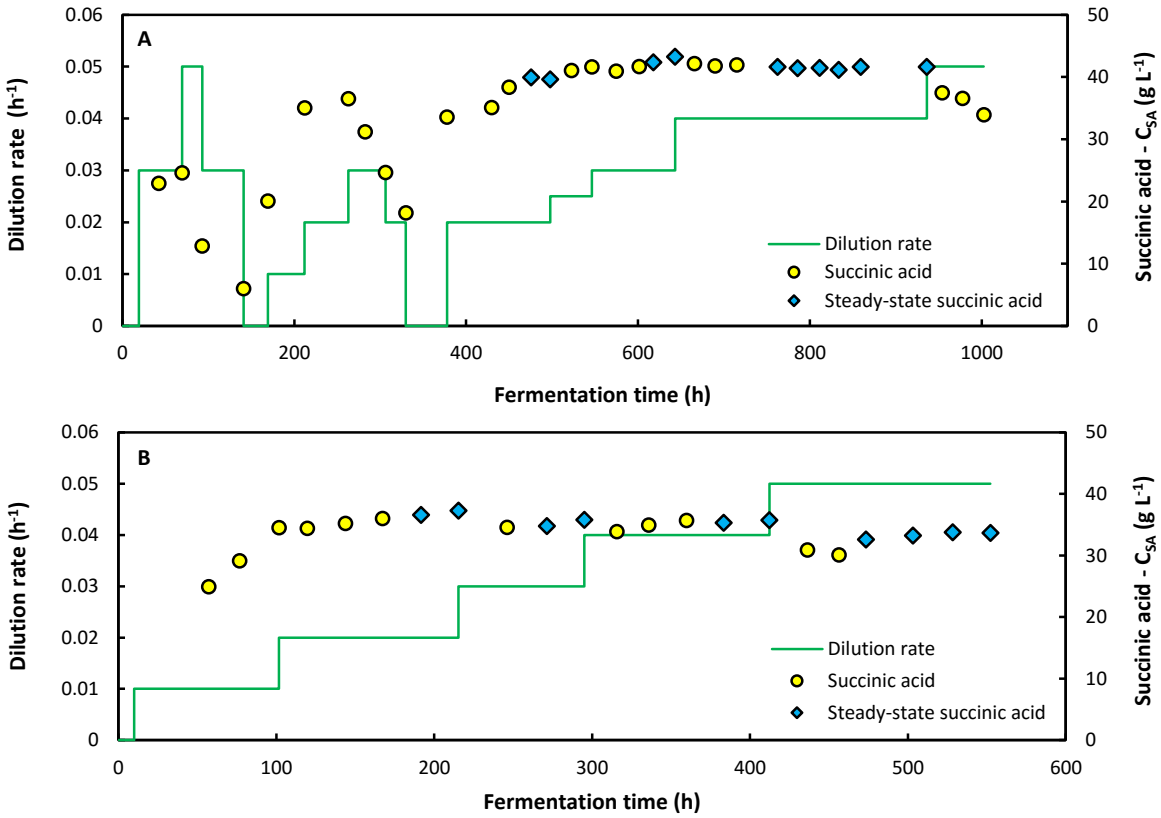

Figure 5.9. Dynamic behaviour of the DDAP-H fermentations. Time profiles of the dilution rate and succinic acid concentration for: **(A)** The first DDAP-H fermentation where too rapid an increase in the dilution rate led to washout, and **(B)** The second DDAP-H fermentation where the dilution rate was more gradually increased to facilitate adaptation of the culture to the hydrolysate.

The increase in D from 0.01 to 0.03 h^{-1} may have been too rapid for the culture to adapt, thereby causing washout or cell death. Therefore, once the system had recovered, the dilution rate was switched to 0.02 h^{-1} and held for 120 hours after which the first steady-state was achieved at a C_{SA} of 39.6 g L^{-1}. Subsequently, D was increased to 0.025 h^{-1} and then to 0.03 h^{-1}. As evidenced by Figure 5.9A, the more gradual increase in D resulted in an increase in C_{SA} up to a point where it plateaued over time and steady-states were obtained at Ds of 0.03 h^{-1} and 0.04 h^{-1}. After the switch in D from 0.03 h^{-1} to 0.04 h^{-1}, the system exhibited steady behaviour after approximately 70 hours. To further assess the stability of the system, the steady-state performance was examined at a dilution rate of 0.04 h^{-1} over a period of 120 hours, approaching five volume turnovers. Figure 5.10A illustrates good stability where the productivity and yield at a specific instant in the period remained within 4.3% and 3.8% of the average productivity and yield, respectively. Minimal deviation in the productivity implies a consistent SA production rate and titre, while minimal deviation in the yield implies constant metabolic flux distributions indicating that the microbial population was indeed at steady state. This further suggests that the active biomass content in the fermenter was constant during this interval. However, further increasing the dilution rate to 0.05 h^{-1} led to a significant decrease in

C_{SA} after which the fermentation was terminated. The first fermentation thus provided important insights into the response of *A. succinogenes* to the throughput rates of non-detoxified DDAP-H, and suggests that a gradual increase in D is vital in maintaining culture stability.

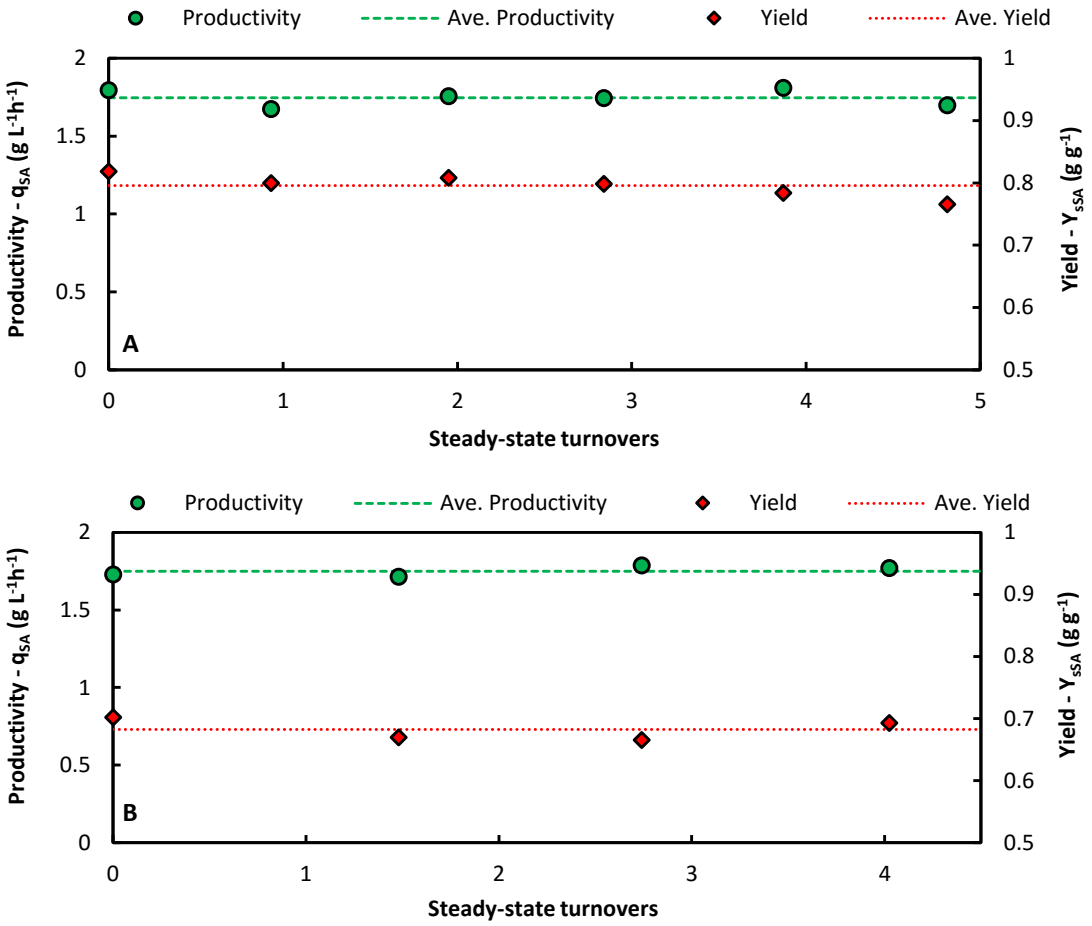

Figure 5.10. Steady-state stability of the DDAP-H fermentations. Time profiles of the succinic acid productivity and yield at steady-state for: **(A)** The first DDAP-H fermentation at D = 0.04 h^{-1} for almost five volume turnovers (120 h), where the slight decrease in yield and productivity towards the end of the time frame are due to biofilm shedding caused by minor pH control issues, and **(B)** The second DDAP-H fermentation at D = 0.05 h^{-1} for just over four volume turnovers (81 h). The points of each graph correspond to the consecutive steady-state points in Figure 5.9.

Based on the conclusions of the first DDAP-H fermentation, the strategy of the second DDAP-H fermentation was to operate at a low dilution rate for an extended period of time (approximately 100-hour holding times), followed by dilution rate increases in increments of 0.01 h^{-1}. Figure 5.9B shows that by operating at D = 0.01 h^{-1} after the initial batch phase for approximately 90 hours, then increasing D incrementally after holding times of approximately 100 hours, results in a steady increase in C_{SA} up to 36.6 g L^{-1}, followed by a stable value of 35.3 g L^{-1} on average. Therefore, by gradually increasing D, the culture was able to acclimatise sufficiently for stable operation at practical dilution rates and unlike in the first DDAP-H run, the system did not destabilise at 0.05 h^{-1}. Instead, the system showed good stability at an average C_{SA} of around 33.3 g L^{-1}, and similar to the

above analysis, the productivity and yield fluctuated minimally around the averages remaining within 2.1% and 2.9% respectively (Figure 5.10B). Furthermore, the biofilm appeared stable throughout the fermentation as no major shedding or sloughing events occurred and the effluent did not contain large clumps of biomass. It is plausible that the thickness of biofilm and biofilm build-up on the fitting were limited by shear effects through sufficient agitation, in addition to product inhibition.

Interestingly, the cell morphology was found to differ between batch (Figure 5.11A) and continuous modes (Figure 5.11B) where cells exhibited a more elongated, irregular shape during continuous operation as compared to batch. The irregular shape could be indicative of stress caused by the high acid titres or merely from washed out fragments of biofilm. As a comparison to Figure 5.2B, Figure 5.11C shows the agitator fitting after termination of the first DDAP-H run where biofilm attachment is clearly visible on the centre PP tube and the porous PP protruding arms. Overall, the second fermentation demonstrated that *A. succinogenes* is able to effectively convert non-detoxified DDAP-H into succinic acid, given a gradual increase in the dilution rate to allow the organism to adapt to the inhibitors in the hydrolysate, whilst showing good overall stability and sustainable steady-state conditions.

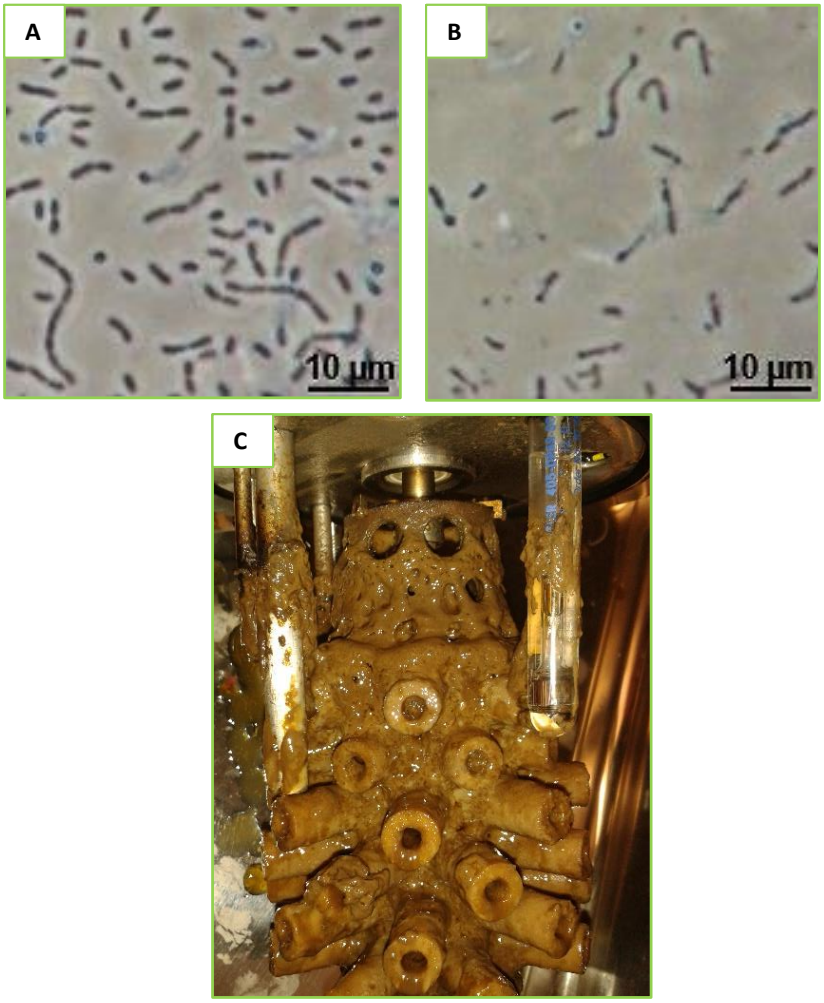

Figure 5.11. Microscope images and biofilm from the DDAP-H fermentations. Microscope images from the first DDAP-H fermentation: **(A)** During the batch start-up phase, and **(B)** After continuous operation at D = 0.02 h^{-1} for 64 hours (approx. 167 hours of fermentation time); **(C)** Biofilm attached to the agitator fitting and reactor internals as seen at the termination of the first DDAP-H fermentation.

5.9 CONCLUSIONS

Value-added chemicals produced in conjunction to biofuels are important in reducing the risks inherent in the overall economics of a lignocellulosic biorefinery. Production of such chemicals requires co-development with upstream and downstream processes including pretreatment and separation. It is therefore necessary to assess the performance of co-production fermentation processes using a process-relevant feed stream and with consideration of downstream requirements. In this chapter, a target value-added chemical - succinic acid - was produced continuously as the major end-product by immobilised *A. succinogenes* at competitive productivities (1.77 g L^{-1} h^{-1}), yields (0.78 g g^{-1}) and titres (39.6 g L^{-1}) on a non-detoxified, xylose-rich hydrolysate stream for the first time. The productivities attained in this study exceed those of similar studies whilst achieving similar yields and titres over prolonged periods of operation. High productivities

were possible due to high cell densities achieved through immobilisation of cells as a biofilm on a novel agitator fitting, and through continuous operation of the fermenter. Ultimately, effective conversion of a process-relevant, lignocellulose-derived hydrolysate stream at high succinate production rates, and titres favourable for downstream separation processes, is demonstrated. Therefore, this work illustrates that co-production of value-added chemicals is feasible by microbial conversion of biorefinery streams, and provides a baseline for similar studies in the future. It is recommended that a similar study be performed on detoxified hydrolysate (e.g. activated carbon) to determine whether improved performance is possible.

6 | CONCLUSIONS

This thesis demonstrates that xylose is a suitable feedstock for succinic acid (SA) production by wild-type *A. succinogenes*. Under continuous operation, xylose consumption rates are shown to be similar to those of glucose at dilution rates of 0.05, 0.10 and 0.30 h^{-1}, but lower yields (0.55 – 0.68 g g^{-1}) and SA productivities (1.5 – 3.4 g L^{-1} h^{-1}) are attained. SA titres of between 10.9 and 29.4 g L^{-1} are seen at SA-to-acetic acid ratios between 3.0 and 5.0 g g^{-1}. In addition, pyruvic acid formation is found to be substantially greater in xylose fermentations (1.2 – 1.9 g L^{-1}) as detected by means of a modified HPLC method. In agreement with glucose fermentations, increased SA yields on xylose are observed at increasing SA titres indicating increased flux to SA. Mass balance closures on xylose (80.6 to 85.3%) are found to be lower than those on glucose, and are incomplete for both substrates suggesting that undetected metabolites are present or alternative metabolic pathways are active. Furthermore, redox balances suggest that the central metabolic network, based on measurements of excreted metabolites and excluding the pentose phosphate pathway, is unable to produce the required reduction power (as NADH) to account for the measured SA concentrations.

Following this, the study provides evidence that the incomplete redox balance closures are linked to an active oxidative pentose phosphate pathway (OPPP) under non-growth conditions on both glucose and xylose. Assays of glucose-6-phsophate dehydrogenase coupled to a kinetic model show that flux into the OPPP, relative to total substrate uptake flux, increases with increasing succinic acid titre, corresponding to an increase in redox balance deviations. Furthermore, the experimentally determined flux relationships are supported by metabolic flux models that include the OPPP and use metabolite measurements as inputs. The OPPP is the likely source of the required reduction power as it generates NADPH which can be converted to NADH by transhydrogenase, thereby allowing greater flux to the reductive, SA pathway. In addition, the only by-product of the OPPP is CO_2 which cannot be detected by HPLC and, more importantly, there is a net consumption of CO_2 during SA production making OPPP-related CO_2 difficult to determine.

In addition to pure sugar feed streams, *A. succinogenes* biofilms are shown to effectively ferment a process-relevant biorefinery stream to SA in a custom, continuous reactor. *A. succinogenes* is able to achieve competitive yields (0.78 g g^{-1}), titres (39.6 g L^{-1}) and productivities (1.77 g $L^{-1}h^{-1}$) on non-

detoxified, deacetylated, dilute acid pretreated, corn stover hydrolysate at dilution rates of 0.02, 0.03, 0.04 and 0.05 h^{-1}. High productivities were possible due to high cell densities in the fermenter attained through biofilm attachment to a novel agitator fitting. Furthermore, the organism is able to deal with putative microbial inhibitors such as furfural and hydroxymethyfurfural (HMF) through conversion to less inhibitory compounds, likely the alcohol counterparts. However, continuous operation at reasonable productivities is only possible by starting at low dilution rates (0.01 h^{-1}) after batch operation, then gradually increasing the flow rate to allow the culture to adapt – even under complete conversion of furfural and HMF. Various lignin-derived, low molecular weight phenolic compounds are shown to be present in the feed and increase during fermentation suggesting a possible link to the observed inhibition and the need for an acclimatisation phase.

Overall this thesis demonstrates that biofilms of *A. succinogenes* have the potential to produce SA at enhanced yields and productivities on glucose, xylose and a scalable, process-relevant biorefinery stream. Furthermore, insight is provided into the unique metabolic behaviour of the organism under non-growth conditions where increased OPPP flux generates reduction power capable of sustaining increased flux to SA. In future work, this advantageous behaviour should be leveraged to develop a process capable of homosuccinate production with *A. succinogenes*, particularly employing a biorefinery stream as feedstock.

7 | REFERENCES

[1] T. Willke, K.-D. Vorlop, Industrial bioconversion of renewable resources as an alternative to conventional chemistry, Appl. Microbiol. Biotechnol. 66 (2004) 131–42. doi:10.1007/s00253-004-1733-0.

[2] A.M. Omer, Energy, environment and sustainable development, Renew. Sustain. Energy Rev. 12 (2008) 2265–2300. doi:10.1016/j.rser.2007.05.001.

[3] K. Hiller, P. Kehrer, Erfahrungskurven bei der Suche nach und Förderung von Erdöl, Erdöl, Erdgas, Kohle. 116 (n.d.) 427–430. http://cat.inist.fr/?aModele=afficheN&cpsidt=864642 (accessed December 29, 2015).

[4] N.A. Owen, O.R. Inderwildi, D.A. King, The status of conventional world oil reserves—Hype or cause for concern?, Energy Policy. 38 (2010) 4743–4749. doi:10.1016/j.enpol.2010.02.026.

[5] S. VijayaVenkataRaman, S. Iniyan, R. Goic, A review of climate change, mitigation and adaptation, Renew. Sustain. Energy Rev. 16 (2012) 878–897. doi:10.1016/j.rser.2011.09.009.

[6] Reverdia, Reverdia: Biorefinery Model, (2015). http://www.reverdia.com/technology/biorefinery-model/ (accessed July 24, 2015).

[7] POET-DSM, First commercial-scale cellulosic ethanol plant in the U.S. opens for business, (2014). http://poet-dsm.com/pr/first-commercial-scale-cellulosic-plant (accessed December 28, 2015).

[8] Myriant, Myriant: Succinic acid and Derivatives SBU, (2015). http://www.myriant.com/pdf/myriant-succinic-acid-customer-presentation-english.pdf (accessed July 24, 2015).

[9] L. Lynd, C. Wyman, T. Gerngross, Biocommodity Engineering., Biotechnol. Prog. 15 (1999) 777–793. doi:10.1021/bp990109e.

[10] J.J. Bozell, G.R. Petersen, Technology development for the production of biobased products from biorefinery carbohydrates—the US Department of Energy's "Top 10" revisited, Green Chem. 12 (2010) 539. doi:10.1039/b922014c.

[11] M. Patel, M. Cranck, V. Dornburg, B. Hermann, L. Roes, B. Husing, The BREW project - Medium and Long-term Opportunities and Risks of the Biotechnological Production of Bulk Chemicals from Renewable Resources, 2006.

[12] H. Song, S.Y. Lee, Production of succinic acid by bacterial fermentation, Enzyme Microb. Technol. 39 (2006) 352–361. doi:10.1016/j.enzmictec.2005.11.043.

[13] K. Maharaj, M.F.A. Bradfield, W. Nicol, Succinic acid-producing biofilms of *Actinobacillus succinogenes*: reproducibility, stability and productivity., Appl. Microbiol. Biotechnol. (2014). doi:10.1007/s00253-014-5779-3.

[14] Q. Yan, P. Zheng, J.-J. Dong, Z.-H. Sun, A fibrous bed bioreactor to improve the productivity of succinic acid by *Actinobacillus succinogenes*, J. Chem. Technol. Biotechnol. 89 (2014) 1760–1766. doi:10.1002/jctb.4257.

[15] M.F.A. Bradfield, W. Nicol, Continuous succinic acid production by *Actinobacillus succinogenes* in a biofilm reactor: Steady-state metabolic flux variation, Biochem. Eng. J. 85 (2014) 1–7. doi:10.1016/j.bej.2014.01.009.

[16] H.G. Brink, W. Nicol, Succinic acid production with *Actinobacillus succinogenes*: rate and yield analysis of chemostat and biofilm cultures., Microb. Cell Fact. 13 (2014) 111. doi:10.1186/s12934-014-0111-6.

[17] I. Meynial-Salles, S. Dorotyn, P. Soucaille, A new process for the continuous production of succinic acid from glucose at high yield, titer, and productivity, Biotechnol. Bioeng. 99 (2008) 129–35. doi:10.1002/bit.21521.

[18] S.Y. Lee, P. Cheon, H.N. Chang, Kinetic study of organic acid formations and growth of *Anaerobiospirillum succiniciproducens* during continuous cultures, J. Microbiol. Biotechnol. 19 (2009) 1379–1384. doi:10.4014/jmb.0905.05026.

[19] E. Scholten, T. Renz, J. Thomas, Continuous cultivation approach for fermentative succinic acid production from crude glycerol by *Basfia succiniciproducens* DD1., Biotechnol. Lett. 31 (2009) 1947–51. doi:10.1007/s10529-009-0104-4.

[20] P. Kuhnert, E. Scholten, S. Haefner, D. Mayor, J. Frey, *Basfia succiniciproducens* gen. nov., sp. nov., a new member of the family *Pasteurellaceae* isolated from bovine rumen, Int. J. Syst. Evol. Microbiol. 60 (2010) 44–50. doi:10.1099/ijs.0.011809-0.

[21] I. Oh, H. Lee, C. Park, S.Y. Lee, J. Lee, Succinic acid production by continuous fermentation process using *Mannheimia succiniciproducens* LPK7, J. Microbiol. Biotechnol. 18 (2008) 908–912. http://dspace.kaist.ac.kr/handle/10203/22624?viewType=local (accessed December 11, 2012).

[22] P.C. Lee, S.Y. Lee, S.H. Hong, H.N. Chang, Batch and continuous cultures of *Mannheimia succiniciproducens* MBEL55E for the production of succinic acid from whey and corn steep liquor., Bioprocess Biosyst. Eng. 26 (2003) 63–7. doi:10.1007/s00449-003-0341-1.

[23] P.C. Lee, S.Y. Lee, S.H. Hong, H.N. Chang, Isolation and characterization of a new succinic acid-producing bacterium, *Mannheimia succiniciproducens* MBEL55E, from bovine rumen, Appl. Microbiol.

Biotechnol. 58 (2002) 663–8. doi:10.1007/s00253-002-0935-6.

[24] G.N. Vemuri, M.A. Eiteman, E. Altman, Effects of growth mode and pyruvate carboxylase on succinic acid production by metabolically engineered strains of *Escherichia coli*, Appl. Environ. Microbiol. 68 (2002) 1715–1727. doi:10.1128/AEM.68.4.1715-1727.2002.

[25] C. Van Heerden, W. Nicol, Continuous and batch cultures of *Escherichia coli* KJ134 for succinic acid fermentation: metabolic flux distributions and production characteristics., Microb. Cell Fact. 12 (2013) 80. doi:10.1186/1475-2859-12-80.

[26] K. Jantama, M.J. Haupt, S. a Svoronos, X. Zhang, J.C. Moore, K.T. Shanmugam, L.O. Ingram, Combining metabolic engineering and metabolic evolution to develop nonrecombinant strains of *Escherichia coli* C that produce succinate and malate., Biotechnol. Bioeng. 99 (2008) 1140–53. doi:10.1002/bit.21694.

[27] G.J. Balzer, C. Thakker, G.N. Bennett, K.-Y. San, Metabolic engineering of *Escherichia coli* to minimize byproduct formate and improving succinate productivity through increasing NADH availability by heterologous expression of NAD(+)-dependent formate dehydrogenase., Metab. Eng. 20 (2013) 1–8. doi:10.1016/j.ymben.2013.07.005.

[28] M.L.A. Jansen, W.M. van Gulik, Towards large scale fermentative production of succinic acid., Curr. Opin. Biotechnol. 30C (2014) 190–197. doi:10.1016/j.copbio.2014.07.003.

[29] S.K.C. Lin, C. Du, A. Koutinas, R. Wang, C. Webb, Substrate and product inhibition kinetics in succinic acid production by *Actinobacillus succinogenes*, Biochem. Eng. J. 41 (2008) 128–135. doi:10.1016/j.bej.2008.03.013.

[30] M. Guettler, D. Rumler, M. Jain, *Actinobacillus succinogenes* sp. nov., a novel succinic-acid-producing strain from the bovine rumen, Int. J. Syst. Bacteriol. 49 (1999) 207–216. http://ijs.sgmjournals.org/content/49/1/207.short (accessed December 9, 2012).

[31] I.B. Gunnarsson, M. Alvarado-Morales, I. Angelidaki, Utilization of CO_2 fixating bacterium *Actinobacillus succinogenes* 130Z for simultaneous biogas upgrading and biosuccinic acid production, Environ. Sci. Technol. 48 (2014) 12464–8. doi:10.1021/es504000h.

[32] J. Villadsen, J. Nielsen, G. Lidén, Bioreaction Engineering Principles, Third Edit, Springer US, Boston, MA, 2011. doi:10.1007/978-1-4419-9688-6.

[33] S.E. Urbance, A.L. Pometto, A.A. Dispirito, A. Demirci, Medium evaluation and plastic composite support ingredient selection for biofilm formation and succinic acid production by *Actinobacillus succinogenes*, Food Biotechnol. 17 (2003) 53–65. doi:10.1081/FBT-120019984.

[34] M. Guettler, M. Jain, B. Soni, Process for making succinic acid, microorganisms for use in the process and methods of obtaining the microorganisms, US005723322A, 1998.

[35] R.I. Corona-González, A. Bories, V. González-Álvarez, C. Pelayo-Ortiz, Kinetic study of succinic acid

production by *Actinobacillus succinogenes* ZT-130, Process Biochem. 43 (2008) 1047–1053. doi:10.1016/j.procbio.2008.05.011.

[36] M. Il Kim, N.-J. Kim, L. Shang, Y.K. Chang, S.Y. Lee, H.N. Chang, Continuous production of succinic acid using an external membrane cell recycle system, J. Microbiol. Biotechnol. 19 (2009) 1369–1373. doi:10.4014/jmb.0903.03034.

[37] S.E. Urbance, A.L. Pometto, A.A. Dispirito, Y. Denli, Evaluation of succinic acid continuous and repeat-batch biofilm fermentation by *Actinobacillus succinogenes* using plastic composite support bioreactors, Appl. Microbiol. Biotechnol. 65 (2004) 664–70. doi:10.1007/s00253-004-1634-2.

[38] C. Van Heerden, W. Nicol, Continuous succinic acid fermentation by *Actinobacillus succinogenes*, Biochem. Eng. J. 73 (2013) 5–11. doi:10.1016/j.bej.2013.01.015.

[39] Q. Yan, P. Zheng, S.-T. Tao, J.-J. Dong, Fermentation process for continuous production of succinic acid in a fibrous bed bioreactor, Biochem. Eng. J. 91 (2014) 92–98. doi:10.1016/j.bej.2014.08.002.

[40] M. FitzPatrick, P. Champagne, M.F. Cunningham, R. a Whitney, A biorefinery processing perspective: treatment of lignocellulosic materials for the production of value-added products., Bioresour. Technol. 101 (2010) 8915–22. doi:10.1016/j.biortech.2010.06.125.

[41] J.B. McKinlay, M. Laivenieks, B.D. Schindler, A. a McKinlay, S. Siddaramappa, J.F. Challacombe, S.R. Lowry, A. Clum, A.L. Lapidus, K.B. Burkhart, V. Harkins, C. Vieille, A genomic perspective on the potential of *Actinobacillus succinogenes* for industrial succinate production., BMC Genomics. 11 (2010) 680. doi:10.1186/1471-2164-11-680.

[42] P. Zheng, K. Zhang, Q. Yan, Y. Xu, Z. Sun, Enhanced succinic acid production by *Actinobacillus succinogenes* after genome shuffling., J. Ind. Microbiol. Biotechnol. 40 (2013) 831–40. doi:10.1007/s10295-013-1283-5.

[43] M. Guettler, M. Jain, D. Rumler, Method for making succinic acid, bacterial variants for use in the process, and methods for obatining variants, 5,573,931, 1996.

[44] M. Guettler, R. Hanchar, S. Kleff, S. Jadhav, Recombinant microorganisms for producing organic acids, EP2904104 A1, 2015. http://www.google.com/patents/EP2904104A1?cl=en.

[45] G. Stephanopoulos, Metabolic fluxes and metabolic engineering., Metab. Eng. 1 (1999) 1–11. doi:10.1006/mben.1998.0101.

[46] M. Sauer, D. Porro, D. Mattanovich, P. Branduardi, Microbial production of organic acids: expanding the markets., Trends Biotechnol. 26 (2008) 100–8. doi:10.1016/j.tibtech.2007.11.006.

[47] J.H. Clark, F.E.I. Deswarte, T.J. Farmer, The integration of green chemistry into future biorefineries, Biofuels, Bioprod. Biorefining. 3 (2009) 72–90. doi:10.1002/bbb.119.

[48] T. Werpy, G. Petersen, Top value added chemicals from biomass, Volume 1. Results of screening for potential candidates from sugars and synthesis gas, 2004.

[49] A. Aikin, C.R. Aikin, A dictionary of chemistry and mineralogy. Volume 1, Printed for John and Arthur Arch, Cornhill; and William Phillips, London, 1807.

[50] J.G. Zeikus, M.K. Jain, P. Elankovan, Biotechnology of succinic acid production and markets for derived industrial products, Appl. Microbiol. Biotechnol. 51 (1999) 545–552. doi:10.1007/s002530051431.

[51] Weastra s.r.o, WP 8.1. Determination of market potential for selected platform chemicals: Itaconic acid, Succinic acid, 2,5-Furandicarboxylic acid, 2011. http://www.bioconsept.eu/wp-content/uploads/BioConSepT_Market-potential-for-selected-platform-chemicals_report1.pdf.

[52] M. Howe-Grant, J. Kroschwitz, eds., Kirk-Othmer Encyclopedia of Chemical Technology, Fourth, John Wiley & Sons, New York, 1991.

[53] I. Bechthold, K. Bretz, S. Kabasci, R. Kopitzky, A. Springer, Succinic Acid: A new platform chemical for biobased polymers from renewable resources, Chem. Eng. Technol. 31 (2008) 647–654. doi:10.1002/ceat.200800063.

[54] Succinity, Succinity: Technology, (2015). http://www.succinity.com/biobased-succinic-acid/technology (accessed July 24, 2015).

[55] Y. Cao, R. Zhang, C. Sun, T. Cheng, Y. Liu, M. Xian, Fermentative succinate production: an emerging technology to replace the traditional petrochemical processes, Biomed Res. Int. 2013 (2013) 723412. doi:10.1155/2013/723412.

[56] C.A. Roa Engel, A.J.J. Straathof, T.W. Zijlmans, W.M. van Gulik, L.A.M. van der Wielen, Fumaric acid production by fermentation, Appl. Microbiol. Biotechnol. 78 (2008) 379–389. doi:10.1007/s00253-007-1341-x.

[57] M. Jansen, M. Van de Graaf, R. Verwaal, Dicarboxylic acid production process, US 2012/0040422 A1, 2012. http://www.google.com/patents/US20120040422.

[58] S. Okino, R. Noburyu, M. Suda, T. Jojima, M. Inui, H. Yukawa, An efficient succinic acid production process in a metabolically engineered *Corynebacterium glutamicum* strain, Appl. Microbiol. Biotechnol. 81 (2008) 459–64. doi:10.1007/s00253-008-1668-y.

[59] Y.-J. Wee, J.-S. Yun, K.-H. Kang, H.-W. Ryu, Continuous production of succinic acid by a fumarate-reducing bacterium immobilized in a hollow-fiber bioreactor., Appl. Biochem. Biotechnol. 98-100 (2002) 1093–104. http://www.ncbi.nlm.nih.gov/pubmed/12018233.

[60] A. Krige, W. Nicol, Continuous succinic acid fermentation by *Escherichia coli* KJ122 with cell recycle, Process Biochem. 50 (2015) 2004–2011. doi:10.1016/j.procbio.2015.09.023.

[61] A.M. Raab, G. Gebhardt, N. Bolotina, D. Weuster-Botz, C. Lang, Metabolic engineering of *Saccharomyces cerevisiae* for the biotechnological production of succinic acid., Metab. Eng. 12 (2010) 518–25. doi:10.1016/j.ymben.2010.08.005.

[62] P. Zheng, J.-J. Dong, Z.-H. Sun, Y. Ni, L. Fang, Fermentative production of succinic acid from straw hydrolysate by *Actinobacillus succinogenes*, Bioresour. Technol. 100 (2009) 2425–9. doi:10.1016/j.biortech.2008.11.043.

[63] P.C. Lee, W.G. Lee, S. Kwon, S.Y. Lee, H.N. Chang, Batch and continuous cultivation of *Anaerobiospirillum succiniciproducens* for the production of succinic acid from whey, Appl. Microbiol. Biotechnol. 54 (2000) 23–7. http://www.ncbi.nlm.nih.gov/pubmed/10952000.

[64] J. Ma, F. Li, R. Liu, L. Liang, Y. Ji, C. Wei, M. Jiang, H. Jia, P. Ouyang, Succinic acid production from sucrose and molasses by metabolically engineered *E. coli* using a cell surface display system, Biochem. Eng. J. 91 (2014) 240–249. doi:10.1016/j.bej.2014.08.014.

[65] D.B. Hodge, C. Andersson, K. a. Berglund, U. Rova, Detoxification requirements for bioconversion of softwood dilute acid hydrolyzates to succinic acid, Enzyme Microb. Technol. 44 (2009) 309–316. doi:10.1016/j.enzmictec.2008.11.007.

[66] P.J. Weimer, Effects of dilution rate and pH on the ruminal cellulolytic bacterium *Fibrobacter succinogenes* S85 in cellulose-fed continuous culture., Arch. Microbiol. 160 (1993) 288–94. http://www.ncbi.nlm.nih.gov/pubmed/8239881.

[67] D.Y. Kim, S.C. Yim, P.C. Lee, W.G. Lee, S.Y. Lee, H.N. Chang, Batch and continuous fermentation of succinic acid from wood hydrolysate by *Mannheimia succiniciproducens* MBEL55E, Enzyme Microb. Technol. 35 (2004) 648–653. doi:10.1016/j.enzmictec.2004.08.018.

[68] H. Song, T.Y. Kim, B.-K. Choi, S.J. Choi, L.K. Nielsen, H.N. Chang, S.Y. Lee, Development of chemically defined medium for *Mannheimia succiniciproducens* based on its genome sequence, Appl. Microbiol. Biotechnol. 79 (2008) 263–272. doi:10.1007/s00253-008-1425-2.

[69] S.H. Hong, J.S. Kim, S.Y. Lee, Y.H. In, S.S. Choi, J.-K. Rih, C.H. Kim, H. Jeong, C.G. Hur, J.J. Kim, The genome sequence of the capnophilic rumen bacterium *Mannheimia succiniciproducens*, Nat. Biotechnol. 22 (2004) 1275–1281. doi:10.1038/nbt1010.

[70] W. Tee, T.M. Korman, M.J. Waters, a Macphee, a Jenney, L. Joyce, M.L. Dyall-Smith, Three cases of *Anaerobiospirillum succiniciproducens* bacteremia confirmed by 16S rRNA gene sequencing., J. Clin. Microbiol. 36 (1998) 1209–13. http://www.pubmedcentral.nih.gov/articlerender.fcgi?artid=104801&tool=pmcentrez&rendertype=abstract.

[71] S.-K. Moon, Y.-J. Wee, J.-S. Yun, H.-W. Ryu, Production of fumaric acid using rice bran and subsequent conversion to succinic acid through a two-step process, in: Proc. Twenty-Fifth Symp. Biotechnol. Fuels

Chem. Held May 4–7, 2003, Breckenridge, CO, Humana Press, Totowa, NJ, 2004: pp. 843–855. doi:10.1007/978-1-59259-837-3_69.

[72] A.M. Sánchez, G.N. Bennett, K.-Y. San, Novel pathway engineering design of the anaerobic central metabolic pathway in *Escherichia coli* to increase succinate yield and productivity, Metab. Eng. 7 (2005) 229–39. doi:10.1016/j.ymben.2005.03.001.

[73] L.H. Christensen, C.M. Henriksen, J. Nielsen, J. Villadsen, M. Egel-Mitani, Continuous cultivation of *Penicillium chrysogenum*. Growth on glucose and penicillin production, J. Biotechnol. 42 (1995) 95–107. doi:10.1016/0168-1656(95)00056-V.

[74] M.J. Van der Werf, M. V Guettler, M.K. Jain, J.G. Zeikus, Environmental and physiological factors affecting the succinate product ratio during carbohydrate fermentation by *Actinobacillus* sp. 130Z, Arch. Microbiol. 167 (1997) 332–42. http://www.ncbi.nlm.nih.gov/pubmed/9148774.

[75] Y. Arikawa, T. Kuroyanagi, M. Shimosaka, H. Muratsubaki, K. Enomoto, R. Kodaira, M. Okazaki, Effect of gene disruptions of the TCA cycle on production of succinic acid in *Saccharomyces cerevisiae*, J. Biosci. Bioeng. 87 (1999) 28–36. doi:10.1016/S1389-1723(99)80004-8.

[76] Y. Xi, K. Chen, J. Li, X. Fang, X. Zheng, S. Sui, M. Jiang, P. Wei, Optimization of culture conditions in CO_2 fixation for succinic acid production using *Actinobacillus succinogenes*, J. Ind. Microbiol. Biotechnol. 38 (2011) 1605–12. doi:10.1007/s10295-011-0952-5.

[77] J.B. McKinlay, Y. Shachar-Hill, J.G. Zeikus, C. Vieille, Determining *Actinobacillus succinogenes* metabolic pathways and fluxes by NMR and GC-MS analyses of ^{13}C-labeled metabolic product isotopomers, Metab. Eng. 9 (2007) 177–92. doi:10.1016/j.ymben.2006.10.006.

[78] BRENDA, Information on EC 4.1.1.49 - phosphoenolpyruvate carboxykinase (ATP) and Organism(s) *Escherichia coli*, (2015). http://www.brenda-enzymes.info/enzyme.php?ecno=4.1.1.49&Suchword=&organism%5B%5D=Escherichia+coli&show_tm=0 (accessed November 8, 2015).

[79] P. Kim, M. Laivenieks, C. Vieille, J.G. Zeikus, Effect of overexpression of *Actinobacillus succinogenes* phosphoenolpyruvate carboxykinase on succinate production in *Escherichia coli*, Appl. Environ. Microbiol. 70 (2004) 1238–1241. doi:10.1128/AEM.70.2.1238-1241.2004.

[80] Q. Li, D. Wang, Z. Song, W. Zhou, Y. Wu, J. Xing, Z. Su, Dual-phase fermentation enables *Actinobacillus succinogenes* 130ZT to be a potential role for high-level lactate production from the bioresource., Bioresour. Technol. 101 (2010) 7665–7. doi:10.1016/j.biortech.2010.04.058.

[81] J.B. McKinlay, J.G. Zeikus, C. Vieille, Insights into *Actinobacillus succinogenes* fermentative metabolism in a chemically defined growth medium, Appl. Environ. Microbiol. 71 (2005) 6651–6. doi:10.1128/AEM.71.11.6651-6656.2005.

[82] Y. Xi, K. Chen, R. Xu, J. Zhang, X. Bai, M. Jiang, P. Wei, J. Chen, Effect of biotin and a similar compound on succinic acid fermentation by *Actinobacillus succinogenes* in a chemically defined medium, Biochem. Eng. J. 69 (2012) 87–92. doi:10.1016/j.bej.2012.08.016.

[83] R. Davis, L. Tao, E.C.D. Tan, M.J. Biddy, G.T. Beckham, C. Scarlata, J. Jacobson, K. Cafferty, J. Ross, J. Lukas, D. Knorr, P. Schoen, Process Design and Economics for the Conversion of Lignocellulosic Biomass to Hydrocarbons: Dilute-Acid and Enzymatic Deconstruction of Biomass to Sugars and Biological Conversion of Sugars to Hydrocarbons, Golden, CO (United States), 2013. doi:10.2172/1107470.

[84] S. Kwon, P.C. Lee, E.G. Lee, Y. Keun Chang, N. Chang, Production of lactic acid by *Lactobacillus rhamnosus* with vitamin-supplemented soybean hydrolysate, Enzyme Microb. Technol. 26 (2000) 209–215. doi:10.1016/S0141-0229(99)00134-9.

[85] D.H. Park, J.G. Zeikus, Utilization of electrically reduced neutral red by *Actinobacillus succinogenes*: physiological function of neutral red in membrane-driven fumarate reduction and energy conservation., J. Bacteriol. 181 (1999) 2403–10. http://www.pubmedcentral.nih.gov/articlerender.fcgi?artid=93664&tool=pmcentrez&rendertype=abstract.

[86] J. Akhtar, A. Idris, R. Abd Aziz, Recent advances in production of succinic acid from lignocellulosic biomass, Appl. Microbiol. Biotechnol. 98 (2014) 987–1000. doi:10.1007/s00253-013-5319-6.

[87] Y.-P. Liu, P. Zheng, Z. Sun, Y. Ni, J.-J. Dong, P. Wei, Strategies of pH control and glucose-fed batch fermentation for production of succinic acid by *Actinobacillus succinogenes* CGMCC1593, J. Chem. Technol. Biotechnol. 83 (2008) 722–729. doi:10.1002/jctb.1862.

[88] J. Zeikus, C. Vieille, J. McKinlay, Minimal growth medium for *Actinobacillus succinogenes*, WO 2007/035589 A1, 2007.

[89] L.-W. Zhu, C.-C. Wang, R.-S. Liu, H.-M. Li, D.-J. Wan, Y.-J. Tang, *Actinobacillus succinogenes* ATCC 55618 fermentation medium optimization for the production of succinic acid by response surface methodology., J. Biomed. Biotechnol. 2012 (2012) 626137. doi:10.1155/2012/626137.

[90] C.-C. Wang, L.-W. Zhu, H.-M. Li, Y.-J. Tang, Performance analyses of a neutralizing agent combination strategy for the production of succinic acid by *Actinobacillus succinogenes* ATCC 55618., Bioprocess Biosyst. Eng. 35 (2012) 659–64. doi:10.1007/s00449-011-0644-6.

[91] R.I. Corona-González, R. Miramontes-Murillo, E. Arriola-Guevara, G. Guatemala-Morales, G. Toriz, C. Pelayo-Ortiz, Immobilization of *Actinobacillus succinogenes* by adhesion or entrapment for the production of succinic acid, Bioresour. Technol. 164C (2014) 113–118. doi:10.1016/j.biortech.2014.04.081.

[92] W. Zou, L.-W. Zhu, H.-M. Li, Y.-J. Tang, Significance of CO_2 donor on the production of succinic acid by *Actinobacillus succinogenes* ATCC 55618, Microb. Cell Fact. 10 (2011) 87. doi:10.1186/1475-2859-10-

87.

[93] P. Kim, M. Laivenieks, J. McKinlay, C. Vieille, J.G. Zeikus, Construction of a shuttle vector for the overexpression of recombinant proteins in *Actinobacillus succinogenes*, Plasmid. 51 (2004) 108–115. doi:10.1016/j.plasmid.2003.11.003.

[94] R. V. Joshi, B.D. Schindler, N.R. McPherson, K. Tiwari, C. Vieille, Development of a markerless knockout method for *Actinobacillus succinogenes*, Appl. Environ. Microbiol. 80 (2014) 3053–3061. doi:10.1128/AEM.00492-14.

[95] K.-K. Cheng, G.-Y. Wang, J. Zeng, J.-A. Zhang, Improved succinate production by metabolic engineering., Biomed Res. Int. 2013 (2013) 538790. doi:10.1155/2013/538790.

[96] M. Jiang, R. Xu, Y. Xi, J. Zhang, W. Dai, Y. Wan, K. Chen, P. Wei, Succinic acid production from cellobiose by *Actinobacillus succinogenes*, Bioresour. Technol. 135 (2013) 469–74. doi:10.1016/j.biortech.2012.10.019.

[97] Y.-P. Liu, P. Zheng, Z.-H. Sun, Y. Ni, J.-J. Dong, L.-L. Zhu, Economical succinic acid production from cane molasses by *Actinobacillus succinogenes*, Bioresour. Technol. 99 (2008) 1736–42. doi:10.1016/j.biortech.2007.03.044.

[98] M. Carvalho, M. Matos, C. Roca, M. a M. Reis, Succinic acid production from glycerol by *Actinobacillus succinogenes* using dimethylsulfoxide as electron acceptor, N. Biotechnol. 31 (2014) 133–139. doi:10.1016/j.nbt.2013.06.006.

[99] M. Jiang, W. Dai, Y. Xi, M. Wu, X. Kong, J. Ma, M. Zhang, K. Chen, P. Wei, Succinic acid production from sucrose by *Actinobacillus succinogenes* NJ113, Bioresour. Technol. 153 (2014) 327–332. doi:10.1016/j.biortech.2013.11.062.

[100] C.C.J. Leung, A.S.Y. Cheung, A.Y. Zhang, K.F. Lam, C.S.K. Lin, Utilisation of waste bread for fermentative succinic acid production, Biochem. Eng. J. 65 (2012) 10–15. doi:10.1016/j.bej.2012.03.010.

[101] N. Shen, Q. Wang, Y. Qin, J. Zhu, Q. Zhu, H. Mi, Y. Wei, R. Huang, Optimization of succinic acid production from cane molasses by *Actinobacillus succinogenes* GXAS137 using response surface methodology (RSM), Food Sci. Biotechnol. 23 (2014) 1911–1919. doi:10.1007/s10068-014-0261-7.

[102] C. Wan, Y. Li, A. Shahbazi, S. Xiu, Succinic Acid Production from cheese whey using *Actinobacillus succinogenes* 130 Z, Appl. Biochem. Biotechnol. 145 (2008) 111–119. doi:10.1007/s12010-007-8031-0.

[103] K. Chen, M. Jiang, P. Wei, J. Yao, H. Wu, Succinic acid production from acid hydrolysate of corn fiber by *Actinobacillus succinogenes*, Appl. Biochem. Biotechnol. 160 (2010) 477–85. doi:10.1007/s12010-008-8367-0.

[104] Q. Li, M. Yang, D. Wang, W. Li, Y. Wu, Y. Zhang, J. Xing, Z. Su, Efficient conversion of crop stalk wastes into succinic acid production by *Actinobacillus succinogenes*, Bioresour. Technol. 101 (2010) 3292–4.

doi:10.1016/j.biortech.2009.12.064.

[105] J. Yu, Z. Li, Q. Ye, Y. Yang, S. Chen, Development of succinic acid production from corncob hydrolysate by *Actinobacillus succinogenes*, J. Ind. Microbiol. Biotechnol. 37 (2010) 1033–40. doi:10.1007/s10295-010-0750-5.

[106] Q. Li, J. Lei, R. Zhang, J. Li, J. Xing, F. Gao, F. Gong, X. Yan, D. Wang, Z. Su, G. Ma, Efficient decolorization and deproteinization using uniform polymer microspheres in the succinic acid biorefinery from bio-waste cotton (*Gossypium hirsutum* L.) stalks, Bioresour. Technol. 135 (2013) 604–609. doi:10.1016/j.biortech.2012.06.101.

[107] M. Alvarado-Morales, I.B. Gunnarsson, I. a. Fotidis, E. Vasilakou, G. Lyberatos, I. Angelidaki, *Laminaria digitata* as a potential carbon source for succinic acid and bioenergy production in a biorefinery perspective, Algal Res. 9 (2015) 126–132. doi:10.1016/j.algal.2015.03.008.

[108] K. Chen, H. Zhang, Y. Miao, P. Wei, J. Chen, Simultaneous saccharification and fermentation of acid-pretreated rapeseed meal for succinic acid production using *Actinobacillus succinogenes*, Enzyme Microb. Technol. 48 (2011) 339–44. doi:10.1016/j.enzmictec.2010.12.009.

[109] K.-Q. Chen, Enhanced succinic acid production from sake lees hydrolysate by dilute sulfuric acid pretreatment and biotin supplementation, J. Sustain. Bioenergy Syst. 02 (2012) 19–25. doi:10.4236/jsbs.2012.22003.

[110] E.R. Borges, N. Pereira, Succinic acid production from sugarcane bagasse hemicellulose hydrolysate by *Actinobacillus succinogenes*, J. Ind. Microbiol. Biotechnol. 38 (2011) 1001–11. doi:10.1007/s10295-010-0874-7.

[111] M.P. Dorado, S.K.C. Lin, A. Koutinas, C. Du, R. Wang, C. Webb, Cereal-based biorefinery development: utilisation of wheat milling by-products for the production of succinic acid., J. Biotechnol. 143 (2009) 51–9. doi:10.1016/j.jbiotec.2009.06.009.

[112] M.S. Croughan, K.B. Konstantinov, C. Cooney, The future of industrial bioprocessing: Batch or continuous?, Biotechnol. Bioeng. 112 (2015) 648–651. doi:10.1002/bit.25529.

[113] M.R. Kunduru, A. Pometto, Continuous ethanol production by *Zymomonas mobilis* and *Saccharomyces cerevisiae* in biofilm reactors, J. Ind. Microbiol. 16 (1996) 249–256. doi:10.1007/BF01570029.

[114] L.M.D. Goncalves, M.T.O. Barreto, A.M.B.R. Xavier, M.J.T. Carrondo, J. Klein, Inert supports for lactic acid fermentation - a technological assessment, Appl. Microbiol. Biotechnol. 38 (1992). doi:10.1007/BF00170077.

[115] D. Kumar, G.S. Murthy, Impact of pretreatment and downstream processing technologies on economics and energy in cellulosic ethanol production, Biotechnol. Biofuels. 4 (2011) 27. doi:10.1186/1754-6834-4-27.

[116] B. Rosche, X.Z. Li, B. Hauer, A. Schmid, K. Buehler, Microbial biofilms: a concept for industrial catalysis?, Trends Biotechnol. 27 (2009) 636–43. doi:10.1016/j.tibtech.2009.08.001.

[117] K.G. Ho, A.L.I. Pometto, P.N. Hinz, J.S. Dickson, A. Demirci, Ingredient Selection for Plastic Composite Supports for L-(1)-Lactic Acid Biofilm Fermentation by *Lactobacillus casei* subsp. *rhamnosus*, Appl. Environ. Microbiol. 63 (1997) 2516–2523. http://aem.asm.org/content/63/7/2516.short.

[118] K.J. Kauffman, P. Prakash, J.S. Edwards, Advances in flux balance analysis, Curr. Opin. Biotechnol. 14 (2003) 491–496. doi:10.1016/j.copbio.2003.08.001.

[119] C.A. Shaw-Reid, Branchpoint Flux Analysis in the L-Lysine Pathway of *Corynebacterium glutamicum*, Massachusetts Institute of Technology, 1997.

[120] F. Cherubini, The biorefinery concept: Using biomass instead of oil for producing energy and chemicals, Energy Convers. Manag. 51 (2010) 1412–1421. doi:10.1016/j.enconman.2010.01.015.

[121] X. Zhao, L. Zhang, D. Liu, Biomass recalcitrance. Part I: The chemical compositions and physical structures affecting the enzymatic hydrolysis of lignocellulose, Biofuels, Bioprod. Biorefining. 6 (2012) 465–482. doi:10.1002/bbb.1331.

[122] M.F.A. Bradfield, W. Nicol, Continuous succinic acid production from xylose by *Actinobacillus succinogenes*, Bioprocess Biosyst. Eng. 39 (2016) 233–244. doi:10.1007/s00449-015-1507-3.

[123] M.F.A. Bradfield, Continuous production of succinic acid by *Actinobacillus succinogenes*: Steady state metabolic flux variation, University of Pretoria, 2013. http://repository.up.ac.za/handle/2263/40826. Masters dissertation.

[124] K.-C. Cheng, A. Demirci, J.M. Catchmark, Advances in biofilm reactors for production of value-added products, Appl. Microbiol. Biotechnol. 87 (2010) 445–56. doi:10.1007/s00253-010-2622-3.

[125] Y. Xi, W. Dai, R. Xu, J. Zhang, K. Chen, M. Jiang, P. Wei, P. Ouyang, Ultrasonic pretreatment and acid hydrolysis of sugarcane bagasse for succinic acid production using *Actinobacillus succinogenes*, Bioprocess Biosyst. Eng. 36 (2013) 1779–85. doi:10.1007/s00449-013-0953-z.

[126] L. Liang, R. Liu, F. Li, M. Wu, K. Chen, J. Ma, M. Jiang, P. Wei, P. Ouyang, Repetitive succinic acid production from lignocellulose hydrolysates by enhancement of ATP supply in metabolically engineered *Escherichia coli*, Bioresour. Technol. 143 (2013) 405–412. doi:10.1016/j.biortech.2013.06.031.

[127] N. Qureshi, B. a Annous, T.C. Ezeji, P. Karcher, I.S. Maddox, Biofilm reactors for industrial bioconversion processes: employing potential of enhanced reaction rates., Microb. Cell Fact. 4 (2005) 24. doi:10.1186/1475-2859-4-24.

[128] J.B. McKinlay, C. Vieille, ^{13}C-metabolic flux analysis of *Actinobacillus succinogenes* fermentative metabolism at different $NaHCO_3$ and H_2 concentrations, Metab. Eng. 10 (2008) 55–68.

doi:10.1016/j.ymben.2007.08.004.

[129] S. Lu, M. a Eiteman, E. Altman, Effect of CO_2 on succinate production in dual-phase *Escherichia coli* fermentations., J. Biotechnol. 143 (2009) 213–23. doi:10.1016/j.jbiotec.2009.07.012.

[130] D. Runquist, B. Hahn-Hägerdal, M. Bettiga, Increased expression of the oxidative pentose phosphate pathway and gluconeogenesis in anaerobically growing xylose-utilizing *Saccharomyces cerevisiae*., Microb. Cell Fact. 8 (2009) 49. doi:10.1186/1475-2859-8-49.

[131] C.F.B. Witteveen, R. Busink, P. van de Vondervoort, C. Dijkema, K. Swart, J. Visser, L-Arabinose and D-xylose catabolism in *Aspergillus niger*, J. Gen. Microbiol. 135 (1989) 2163–2171. http://mic.sgmjournals.org/content/journal/micro/10.1099/00221287-135-8-2163?crawler=true&mimetype=application/pdf.

[132] B.D. Schindler, R. V Joshi, C. Vieille, Respiratory glycerol metabolism of *Actinobacillus succinogenes* 130Z for succinate production, J. Ind. Microbiol. Biotechnol. 41 (2014) 1339–1352. doi:10.1007/s10295-014-1480-x.

[133] A.K. Gombert, J. Nielsen, Mathematical modelling of metabolism, Curr. Opin. Biotechnol. 11 (2000) 180–186. doi:10.1016/S0958-1669(00)00079-3.

[134] E.A. Noltmann, C.J. Gubler, S.A. Kuby, Glucose 6-Phosphate Dehydrogenase (Zwischenferment), J. Biol. Chem. 236 (1961) 1225–1230. http://www.jbc.org/content/236/5/1225.full.pdf.

[135] J.E.D. Dyson, E. a Noltmann, The effect of pH and temperature on the kinetic parameters of phosphoglucose isomerase, J. Biol. Chem. 243 (1968) 1401–1414.

[136] A. Varma, B.O. Palsson, Metabolic Flux Balancing: Basic Concepts, Scientific and Practical Use, Bio/Technology. 12 (1994) 994–998. doi:10.1038/nbt1094-994.

[137] M.F.A. Bradfield, A. Mohagheghi, D. Salvachúa, H. Smith, B.A. Black, N. Dowe, G.T. Beckham, W. Nicol, Continuous succinic acid production by *Actinobacillus succinogenes* on xylose-enriched hydrolysate, Biotechnol. Biofuels. 8 (2015) 181. doi:10.1186/s13068-015-0363-3.

[138] R.C. Stanton, Glucose-6-phosphate dehydrogenase, NADPH, and cell survival., IUBMB Life. 64 (2012) 362–9. doi:10.1002/iub.1017.

[139] W.T. Lee, H.R. Levy, Lysine-21 of *Leuconostoc mesenteroides* glucose-6-phosphate dehydrogenase participates in substrate binding through charge-charge interaction., Protein Sci. 1 (1992) 329–334. http://www.ncbi.nlm.nih.gov/pmc/articles/PMC2142207/.

[140] R.K. Scopes, V. Testolin, A. Stoter, K. Griffiths-Smith, E.M. Algar, Simultaneous purification and characterization of glucokinase, fructokinase and glucose-6-phosphate dehydrogenase from *Zymomonas mobilis*, Biochem. J. 228 (1985) 627–634. doi:10.1042/bj2280627.

[141] B.D. Bennett, E.H. Kimball, M. Gao, R. Osterhout, S.J. Van Dien, J.D. Rabinowitz, Absolute metabolite concentrations and implied enzyme active site occupancy in *Escherichia coli*, Nat Chem Biol. 5 (2009) 593–599. doi:10.1038/nchembio.186.

[142] M. Rühl, D. Le Coq, S. Aymerich, U. Sauer, ^{13}C-flux analysis reveals NADPH-balancing transhydrogenation cycles in stationary phase of nitrogen-starving *Bacillus subtilis*, J. Biol. Chem. 287 (2012) 27959–70. doi:10.1074/jbc.M112.366492.

[143] E. Palmqvist, B. Hahn-Hägerdal, Fermentation of lignocellulosic hydrolysates. I: Inhibition and detoxification, Bioresour. Technol. 74 (2000) 17–24. doi:10.1016/S0960-8524(99)00160-1.

[144] X. Chen, J. Shekiro, R. Elander, M. Tucker, Improved xylan hydrolysis of corn stover by deacetylation with high solids dilute acid pretreatment, Ind. Eng. Chem. Res. 51 (2012) 70–76. doi:10.1021/ie201493g.

[145] X. Chen, J. Shekiro, M.A. Franden, W. Wang, M. Zhang, E. Kuhn, D.K. Johnson, M.P. Tucker, The impacts of deacetylation prior to dilute acid pretreatment on the bioethanol process, Biotechnol. Biofuels. 5 (2012) 8. doi:10.1186/1754-6834-5-8.

[146] D. a. Sievers, J.J. Lischeske, M.J. Biddy, J.J. Stickel, A low-cost solid–liquid separation process for enzymatically hydrolyzed corn stover slurries, Bioresour. Technol. 187 (2015) 37–42. doi:10.1016/j.biortech.2015.03.087.

[147] J.J. Bozell, J.E. Holladay, D. Johnson, J.F. White, Top Value-Added Chemicals from Biomass Volume II — Results of Screening for Potential Candidates from Biorefinery Lignin, 2007. http://www.pnl.gov/main/publications/external/technical_reports/PNNL-16983.pdf.

[148] D. Salvachúa, A. Mohagheghi, H. Smith, M.F.A. Bradfield, W. Nicol, B.A. Black, M.J. Biddy, N. Dowe, G.T. Beckham, Succinic acid production on xylose-enriched biorefinery streams by *Actinobacillus succinogenes* in batch fermentation, Biotechnol. Biofuels. 9 (2016) 28. doi:10.1186/s13068-016-0425-1.

[149] J. Shekiro Iii, E.M. Kuhn, N.J. Nagle, M.P. Tucker, R.T. Elander, D.J. Schell, Characterization of pilot-scale dilute acid pretreatment performance using deacetylated corn stover, Biotechnol. Biofuels. 7 (2014) 23. doi:10.1186/1754-6834-7-23.

[150] N.D. Weiss, J.D. Farmer, D.J. Schell, Impact of corn stover composition on hemicellulose conversion during dilute acid pretreatment and enzymatic cellulose digestibility of the pretreated solids, Bioresour. Technol. 101 (2010) 674–678. doi:10.1016/j.biortech.2009.08.082.

[151] N.D. Weiss, N.J. Nagle, M.P. Tucker, R.T. Elander, High xylose yields from dilute acid pretreatment of corn stover under process-relevant conditions, Appl. Biochem. Biotechnol. 155 (2009) 418–428. doi:10.1007/s12010-008-8490-y.

[152] D. Schell, J. Farmer, Dilute-sulfuric acid pretreatment of corn stover in pilot-scale reactor, Appl. Biochem. Biotechnol. 105 (2003) 69–85. http://link.springer.com/chapter/10.1007/978-1-4612-0057-4_6 (accessed December 20, 2014).

[153] Q. Li, D. Wang, Y. Wu, M. Yang, W. Li, J. Xing, Z. Su, Kinetic evaluation of products inhibition to succinic acid producers *Escherichia coli* NZN111, AFP111, BL21, and *Actinobacillus succinogenes* 130Z T., J. Microbiol. 48 (2010) 290–6. doi:10.1007/s12275-010-9262-2.

[154] A. Mandalika, L. Qin, T.K. Sato, T. Runge, Integrated biorefinery model based on production of furans using open-ended high yield processes, Green Chem. 16 (2014) 2480–2489. doi:10.1039/C3GC42424C.

[155] H. Ran, J. Zhang, Q. Gao, Z. Lin, J. Bao, Analysis of biodegradation performance of furfural and 5-hydroxymethylfurfural by *Amorphotheca resinae* ZN1, Biotechnol. Biofuels. 7 (2014) 51. doi:10.1186/1754-6834-7-51.

[156] H. Ran, J. Zhang, Q. Gao, Z. Lin, J. Bao, Analysis of biodegradation performance of furfural and 5-hydroxymethylfurfural by *Amorphotheca resinae* ZN1., Biotechnol. Biofuels. 7 (2014) 51. doi:10.1186/1754-6834-7-51.

[157] T.N. Petersen, S. Brunak, G. von Heijne, H. Nielsen, SignalP 4.0: discriminating signal peptides from transmembrane regions, Nat Meth. 8 (2011) 785–786. http://dx.doi.org/10.1038/nmeth.1701.

[158] C. Du, S.K.C. Lin, A. Koutinas, R. Wang, C. Webb, Succinic acid production from wheat using a biorefining strategy, Appl. Microbiol. Biotechnol. 76 (2007) 1263–70. doi:10.1007/s00253-007-1113-7.

[159] C. Du, S.K.C. Lin, A. Koutinas, R. Wang, P. Dorado, C. Webb, A wheat biorefining strategy based on solid-state fermentation for fermentative production of succinic acid, Bioresour. Technol. 99 (2008) 8310–5. doi:10.1016/j.biortech.2008.03.019.

[160] K.-Q. Chen, J. Li, J.-F. Ma, M. Jiang, P. Wei, Z.-M. Liu, H.-J. Ying, Succinic acid production by *Actinobacillus succinogenes* using hydrolysates of spent yeast cells and corn fiber, Bioresour. Technol. 102 (2011) 1704–8. doi:10.1016/j.biortech.2010.08.011.

[161] J. Li, X.-Y. Zheng, X.-J. Fang, S.-W. Liu, K.-Q. Chen, M. Jiang, P. Wei, P.-K. Ouyang, A complete industrial system for economical succinic acid production by *Actinobacillus succinogenes*, Bioresour. Technol. 102 (2011) 6147–52. doi:10.1016/j.biortech.2011.02.093.

[162] N. Shen, Y. Qin, Q. Wang, S. Liao, J. Zhu, Q. Zhu, H. Mi, B. Adhikari, Y. Wei, R. Huang, Production of succinic acid from sugarcane molasses supplemented with a mixture of corn steep liquor powder and peanut meal as nitrogen sources by *Actinobacillus succinogenes*, Lett. Appl. Microbiol. 60 (2015) 544–551. doi:10.1111/lam.12399.

APPENDIX A: MATLAB PROGRAMME FOR KINETIC FITS

A Matlab programme was used for fitting the assay data to a kinetic model. The program comprised a main routine within which subroutines were nested. The subroutines dealt with the following operations:

1. Data extraction from Excel spreadsheets
2. Least squares, non-linear optimisation to minimise error in fitting kinetic parameters. Matlab function used: *lsqnonlin*
3. Computation of the error between modelled and experimental data
4. Solving the system of differential equations representing reaction rates. Matlab function used: *ode45*

CODE

*****

```
% MAIN SCRIPT

% Kinetic fit programme - Main script linking to sub-routines

clear all; clc;

SampleDate = '%YYYYMMDD%'; %For individual steady-state fits
Substrate='Glucose'; %'Xylose'
DilutionRate='01';
sets=5; %i.e. number of assay conditions
steadyS=5; %number of steady-states (allows for flexibity in fitting
various steady-states

%Use DataRead for individual steady-state fits
%[tExp, absExp, n, c0, v2max] =
DataRead(SampleDate,Substrate,DilutionRate);

%Use DataRead2 for fits on all data sets from substrate
[tExp, absExp, n, c0, v2max] = DataRead2(Substrate);

eps = 6.22; %Extinction coefficient [/mM/cm] {C = A/eps/L; L=1 cm}
cExp = absExp/eps; %mM

c0 = [c0(:,1) zeros(n,1) c0(:,3) cExp(1,:)' c0(:,2)]; %[G6P Ru5P Nadp+
Nadph F6P]

k(1)=0.433; %fixing A<->C kinetics
k(2)=0.202;
keq=0.312;
k1=k(1);
k2=k(2);

v1=2.9; %Guess - high
```

```
v3=0.00037; %Guess - low
k3=0.26; %Km(G6P) for G6PDH reaction [mM]

b=ones(1,steadyS-1); %Initialise proportional rate vector
coeff_lb = 0.01; %Scaling lower bound
coeff_ub = 10; %Scaling upper bound
c_lb = ones(1,(steadyS-1))*coeff_lb;
c_ub = ones(1,(steadyS-1))*coeff_ub;

xguess = [v3   k3      v1    b];
lb =     [1e-8 0.01    0.001 c_lb]; % Lower constraint
ub =     [10   0.99    3     c_ub]; % Upper constraint

tEnd = tExp(end); %last time point to evaluate
dt = tExp(2)-tExp(1); %Time between assays readings

options2 = optimset('TolFun',1e-10,'TolX',1e-10, 'MaxFunEvals',2000,
'MaxIter',2000);

%Optimisation subroutine
xout = lsqnonlin(@(x) modelMM(x,dt, tEnd, cExp, keq, c0, n, k,
sets,steadyS), xguess,lb,ub, options2)

xout(3)/xout(1)
tspan = 0:15:tEnd;
A=0;
parity_model=[]; %Combine sets for overall fit parity plot
parity_exp = [];

%Generate figures of fits
for i=1:n
    A=A+1;
    setNum = ceil(i/sets); %i.e.steady-state
    [t, cout] = ode45(@(t, c) dsysdtB(t, c, xout, keq,k, setNum,steadyS),
tspan, c0(i,:));
    figure(ceil(i/sets))
    subplot(sets,2,A)
    plot(t, cout(:,4), tExp, cExp(:,i),'x')
    subplot(sets,2,A+1)
    plot(t, cout(:,1),'k', t, cout(:,2),'b', t, cout(:,3),'y', t,
cout(:,4),'m')%, t,cout(:,5))
    parity_model = [parity_model cout(:,4)'];
    parity_exp = [parity_exp cExp(:,i)'];
    if A==(2*sets-1) %single figure per data set
        A=0;
    else
        A=A+1;
    end
end
```

*****

```
%DATA EXTRACTION FROM EXCEL (SINGLE)

function [tExp, absExp, n, c0, v2max] =
DataRead(SampleDate,Substrate,DilutionRate)
%Read absorbance data and intial conditions from spreadsheet
%Used for separate steady-states

ParentFolder = '%C:\RootDirectory%';
```

```
FileName= [ParentFolder '\' SampleDate '\' SampleDate '-' Substrate '-D'
DilutionRate '.xlsx']; %Unique to location
num = xlsread(FileName, 'Combined');
tExp = num(:,1);

absExp = num(:,2:end);
dataSets = size(absExp);
n=dataSets(2);

num2 = xlsread(FileName, 'InitialConditions');
c0 =num2
num3 = xlsread(FileName, 'v2max');
v2max = num3

%DATA EXTRACTION (ALL)

function [tExp, absExp, n, c0, v2max] = DataRead2(Substrate)
%Read absorbance data and intial conditions from spreadsheet
%Used for entire data sets per substrate

ParentFolder =
'C:\Users\Michael\Dropbox\PhD\Experiments\Exp5PPPFlux\Paradigm';
FileName= [ParentFolder '\KineticProfiles-' Substrate '.xlsx']
num = xlsread(FileName, 'All');
tExp = num(:,1);

absExp = num(:,2:end);
dataSets = size(absExp);
n=dataSets(2)

num2 = xlsread(FileName, 'InitialConditions');
c0 =num2
num3 = xlsread(FileName, 'v2max');
v2max = num3
                                    *****

% SOLVE SYSTEM OF ODES AND GENERATE ERROR FOR OPTIMISATION

function err = modelMM(x, dt, tEnd, cExp, keq, c0, n, k, sets, steady)
%Integrate rate ODEs and generate error vector
%n=number of data sets to optimise
%Compute MAPE to gauge overall fit quality

tspan = 0:dt:tEnd;
errV=[];
sumMAPE=[];
count=0;
for i = 1:n
  setNum = ceil(i/sets);
  [t, cout] = ode45(@(t, c) dsysdtB(t, c, x, keq, k, setNum, steady),
tspan, c0(i,:)); %solve for each set of initial conditions (unique to each
assay)
  cModel = cout(:,4);
  errSet = cExp(:,i) - cModel; %calculate error vector for data set
  errV = [errV errSet']; %append error vector with new errors
  perErr = abs(abs(cExp(:,i))-abs(cModel))./abs(cExp(:,i))*100;
  sumMAPE = [sumMAPE perErr'];
  count=count+length(cModel);
end
```

```
MAPE = sum(sumMAPE)/count %compute Mean Absolute Percentage Error
err=errV;
```

*****

%DIFFERENTIAL EQUATIONS AND RATE DEFINITIONS

```
function dc = dsysdtB(t,c,x,keq,k,setNum,steady)
%Solves system of differential rate equations

v3=x(1);
k3=x(2);
v1=x(3);
k1=k(1);
k2=k(2);

diff=steady-2;
v2=v1*k2/keq/k1;
b = [1 x(end-diff:end)];

%Reversible Michaelis-Menten PGI reaction
rac = @(c) (v1*c(1)/k1 - v2*c(2)/k2)/(1+c(1)/k1+c(2)/k2);

%Michaelis-Menten G6PDH reaction
rab = @(c) b(setNum)*v3*c(1)/(k3 + c(1));

dc = zeros(5,1);
dc(1) = -rab(c(4)) - rac([c(1) c(5)]);     %dG6P/dt
dc(2) = rab(c(1));                         %dRu5P/dt
dc(3) = -2*rab(c(1));                      %dNADP+dt
dc(4) = 2*rab(c(1));                       %dNADPHdt
dc(5) = rac([c(1) c(5)]);                  %dF6Pdt
```

*****